

## Direct Renin Inhibitors as a New Therapy for Hypertension

Randy L. Webb,<sup>†</sup> Nikolaus Schiering,<sup>‡</sup> Richard Sedrani,<sup>‡</sup> and Jürgen Maibaum<sup>\*‡</sup>

<sup>†</sup>Novartis Pharmaceuticals Corp., Institutes for BioMedical Research, East Hanover, New Jersey, and <sup>‡</sup>Novartis Pharma AG, Institutes for BioMedical Research, Novartis Campus, CH-4056 Basel, Switzerland

Received December 21, 2009

### Introduction

The history of the renin angiotensin system (RAS<sup>a</sup>) traces its roots to the seminal experiments of Tigerstedt and Bergman describing a pressor response in the rabbit following injection of a rabbit kidney homogenate.<sup>1</sup> These studies were the first to describe the hypertensive effect of renin and laid the foundation for future investigations into the RAS pathway. Several crucial studies followed over the next 50 years that further elaborated additional key components of the RAS, including the identification of angiotensin II (AngII) as the principal substance mediating the activity of this system (Figure 1).<sup>2</sup> Angiotensinogen, the endogenous renin substrate, was first described in an elegant series of experiments in which the serial components of the system were clearly delineated.<sup>3</sup> Skeggs went on to explain how therapeutic benefit could be achieved by interfering with this system at several distinct points: by blocking the receptor for AngII, by inhibiting angiotensin converting enzyme (ACE) as the enzymatic step required for generation of AngII, or by preventing the formation of AngI through direct inhibition of renin. Interestingly, these investigators realized early on that “Since renin is the initial and rate-limiting substance in the renin–hypertensin system, it would seem that this last approach would be the most likely to succeed.”

It has been shown consistently that blockade of the RAS, either with an ACE inhibitor (ACEi) or with an AngII AT1 receptor blocker (ARB) reduces blood pressure (BP). However, a powerful counter-regulatory mechanism is activated during RAS blockade and is in part responsible for the “flat” dose–response relationship observed with the use of these inhibitors.<sup>4</sup> Under normal physiologic conditions, AngII inhibits renin release through stimulation of the AT1 receptor. Therapeutic interventions that either reduce AngII (ACEi) or

attenuate AT1 signaling (ARB) ultimately result in enhanced release of renin. Consequently, the historical depiction of this system as a linear cascade is an inappropriate representation of the pathway. The RAS is now better portrayed as a physiological circuit encompassing a negative feedback “loop” whereby renin levels are controlled by the amount of AngII present in plasma and tissues (Figure 1).<sup>5</sup> This renders renin a highly attractive target from a therapeutic standpoint, as it would provide the only tactic to reduce plasma renin activity and thus offers a novel approach for the management of hypertension. While a compensatory rise in renin occurs as a result of RAS blockade with an ACEi, ARB, or a renin inhibitor, renin is rendered ineffective only by renin inhibition. Renin inhibitors bind to the active site of renin, a member of the aspartic protease family with high specificity for its endogenous substrate angiotensinogen, and are now commonly referred to as “direct renin inhibitors” (DRI), as opposed to drugs interfering with other components of the RAS, like ACE inhibitors, ARBs, or  $\beta$ -adrenoceptor antagonists.<sup>6</sup> Despite many treatment options available to the clinician, hypertension remains an important public health issue. Hypertension affected more than 65 million Americans and more than 25% of adults worldwide and is a key risk factor for myocardial infarction, stroke, and heart and renal failure.<sup>7</sup> Its prevalence is expected to increase by 60% to >1.5 billion people worldwide by 2025.<sup>8</sup>

Academic institutions and major pharmaceutical companies have committed substantial resources over the past 50 years in an effort to discover the best therapeutic tactic for modulating the RAS. Initial therapeutic success was achieved with the introduction of ACEi<sup>9</sup> and then with the identification of ARBs a decade later.<sup>10</sup> While it was widely recognized that direct renin inhibition held great therapeutic potential, the design of small nonpeptidic molecules that effectively interact with the catalytic domain of renin and that demonstrate oral efficacy in humans remained elusive for more than 2 decades.<sup>4</sup> Compound **1** (aliskiren, CGP60536B, SPP100; Figure 2) represents a new generation of orally highly effective DRIs of a unique structural class designed by molecular modeling and X-ray crystallography.<sup>11–13</sup> This drug was introduced in the United States as Tekturna and in Europe as Rasilez in 2007<sup>14</sup> and hence became the first new therapy for the treatment of hypertension in more than 10 years.

Since the late 1990s, a resurgence of interest in DRIs in the industry became increasingly evident and was driven by several major advancements.<sup>15</sup> Emerging new insights at the molecular level related to human renin–inhibitor active site

\*To whom correspondence should be addressed. Phone: +41-61-6965560. Fax: +41-61-6967155. E-mail: juergen\_klaus.maibaum@novartis.com.

<sup>a</sup>Abbreviations: ADME, absorption, distribution, metabolism, and excretion; ACE(i), angiotensin converting enzyme (inhibitor); Ang, angiotensin; ARB, angiotensin II receptor blocker; BACE,  $\beta$ -site of  $\beta$ -amyloid precursor protein cleaving enzyme; BP, blood pressure; CYP, cytochrome P450; DRI, direct renin inhibitor(s); dTGM, double-transgenic mouse; dTGR, double-transgenic rat; GRAB, group replacement assisted binding; H-bond, hydrogen bond; HTS, high-throughput screening; ITC, isothermal titration calorimetry; PK, pharmacokinetics; PRA, plasma renin activity; PRC, plasma renin concentration; (P)RR, (pro)renin receptor; RAS, renin angiotensin system; rh-renin, recombinant human renin; SAR, structure–activity relationship; SHR, spontaneously hypertensive rat; TS, transition state; TSA, transition-state analogue.

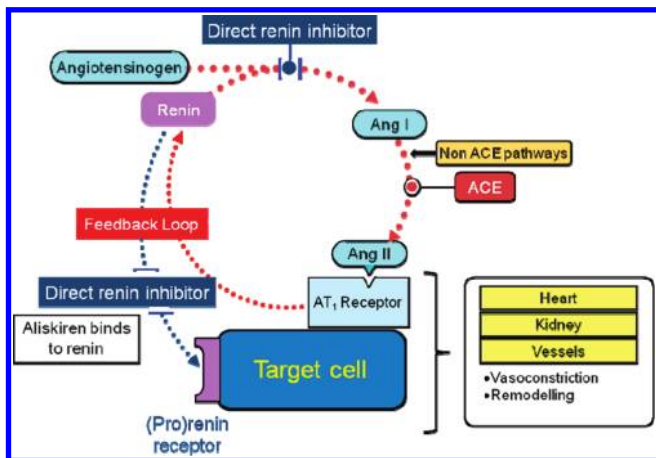


Figure 1. Renin–angiotensin system (RAS).<sup>5</sup>

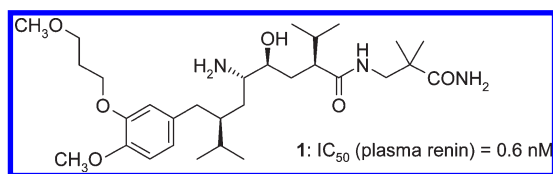


Figure 2. Compound **1** (aliskiren), the first marketed direct renin inhibitor (DRI).

interactions have paved new avenues for designing distinct chemotype inhibitors. The introduction of transgenic rodent models provided the capability to assess biological actions in small animals and thus reduced reliance on the use of non-human primates.<sup>16</sup> Also, the advanced clinical testing of **1** offered promise that this long sought after therapeutic approach might finally become a reality. Most importantly, extensive clinical trial results are now available and demonstrate its benefit.<sup>5</sup> Previous DRIs had been evaluated in limited clinical testing with short-term administration.

The objective of this review is to highlight key events and recent advances in the evolution of non-peptide peptidomimetic DRIs.<sup>17</sup> Special emphasis will be placed on the successful structure-based strategies that enabled the discovery of several novel classes of DRIs.<sup>18,19</sup> The potential limitations associated with these inhibitors and opportunities for future directions of renin inhibitor design will be discussed from a chemical and biological perspective. Lessons learned will also be discussed in an effort to provide a unique perspective on the development of **1**. With its introduction, it is now very important to distinguish this mechanism of action from indirect means of inhibiting renin. In this regard, ongoing clinical trials designed to demonstrate a clear benefit, beyond an effect on blood pressure, by reduction in morbidity and mortality are of paramount importance.

### Medicinal Chemistry of DRIs: A Historical View

The search for clinically efficacious DRIs with druglike properties has a remarkable and long history. It has required tremendous investments in research and development in industry and has spanned more than 3 decades.<sup>20–23</sup> The first potent inhibitor of renin in plasma, reported as early as 1980, was completely peptidic in nature.<sup>20</sup> This decapeptide substrate analogue, labeled “RIP” (for renin inhibitor peptide), allowed the first in vivo pharmacology studies of a DRI in monkeys. The design of orally efficacious non-peptide DRIs

remained a formidable task with incremental progress made by the early 1990s, when several peptide-based peptidomimetic DRIs (**2–6**, Figure 3) had entered into clinical trials as investigational drugs.<sup>21b,22,23b</sup>

Structure-based drug design (SBDD) involving X-ray crystallography and computer-assisted molecular modeling emerged as one of the most preeminent paradigms in drug discovery<sup>24a,b</sup> in the 1980s, and the successful design of highly potent and selective DRIs represents one hallmark example. Numerous X-ray crystal structures of native aspartic proteases and enzyme–inhibitor complexes in combination with elegant mechanistic studies have provided detailed insight into fundamental aspects of the three-dimensional architecture and conformational dynamics of this class of endoproteases, as well as into the general acid–general base mechanism of enzyme-catalyzed peptide bond hydrolysis.<sup>20,25–29</sup> This information, together with computational modeling methods, has been of invaluable importance for developing a rational design approach toward potent DRIs, initially by the use of renin homology models.<sup>30</sup> Notably, the X-ray structure of human apo-renin was reported only in 1989,<sup>31</sup> and the first renin–inhibitor complexes became available shortly thereafter.<sup>30,32</sup>

Since the early reports describing angiotensinogen substrate-derived peptides as low affinity inhibitors of renin in the mid-1970s, the design of highly potent and selective DRIs as potentially useful drug candidates has witnessed a remarkable transition through various stages of structure-guided medicinal chemistry approaches. On the basis of the increasing knowledge about the three-dimensional structure and the enzymatic mechanism of substrate cleavage, several generations of DRIs have evolved over the years. These range from modified peptide inhibitors as target-validating pharmacology tools followed by more druglike second generation peptidic inhibitors to the more recent discovery of diverse classes of non-peptide DRIs.

The incorporation of mimetics of the putative transition-state of the enzyme-catalyzed amide bond hydrolysis as non-hydrolyzable replacements of the scissile cleavage site represents a general inhibitor design principle originating in the postulates by Pauling and Wolfenden.<sup>20,33</sup> The application of this approach to N-terminal angiotensinogen substrate-derived peptide sequences has been instrumental in generating potent and proteolytically stable inhibitors of renin. Key structural features of these transition-state analogues (TSAs) are hydroxyl or (pro)hydroxyl groups that interact via hydrogen bonding with the catalytic Asp<sub>32</sub> and Asp<sub>215</sub> carboxylates by extrusion of the enzyme-bound cosubstrate water of the catalytic center in native renin. The entropically favored water displacement by the TSA hydroxyl and further evidence would suggest that these analogues function at least in part as “collected-substrate” inhibitors rather than as tetrahedral intermediates of enzyme-catalyzed peptide cleavage.<sup>25,27,29</sup> Most prominent early representatives are the nonproteinogenic amino acid statine, identified from the pepstatin family of natural product aspartic protease inhibitors,<sup>34</sup> and the hydroxyethylene (HE) dipeptide isostere first introduced by Szelke et al. (Chart 1B and Chart 1A, respectively).<sup>20</sup> Key strategies of extensive structural modifications of first generation DRIs included the elimination of their peptidic nature, optimization of critical binding interactions to the renin specificity pockets spanning S<sub>3</sub>/S<sub>4</sub> to S<sub>2</sub>' of the extended enzyme cleft, and variation of the central TSA moiety. These concepts aimed to accomplish a minimal molecular size sufficient for strong binding affinity.

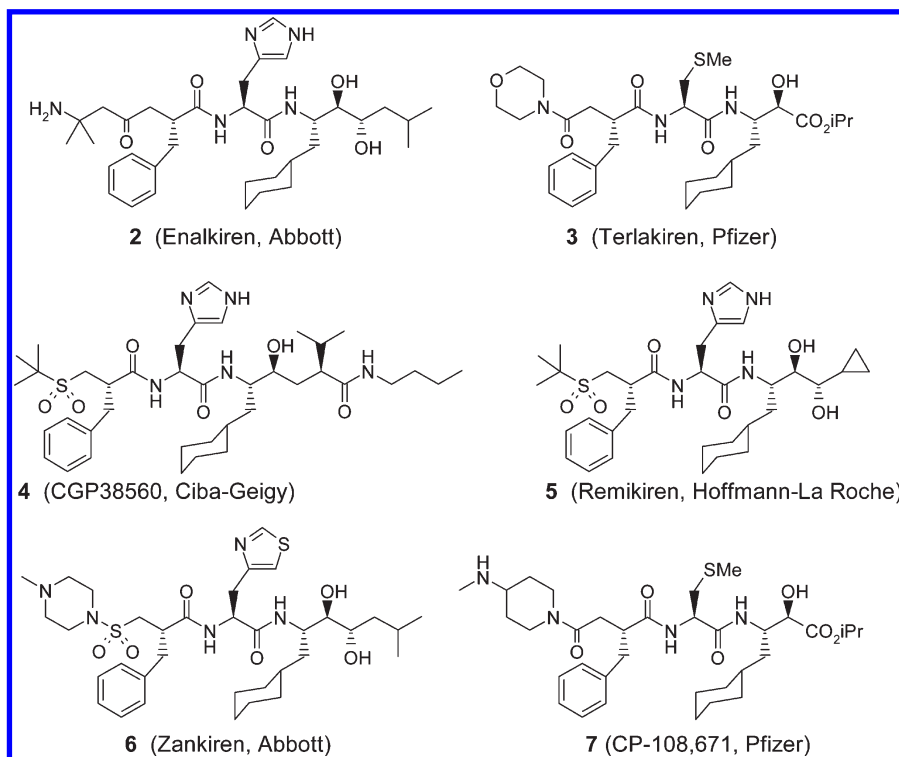
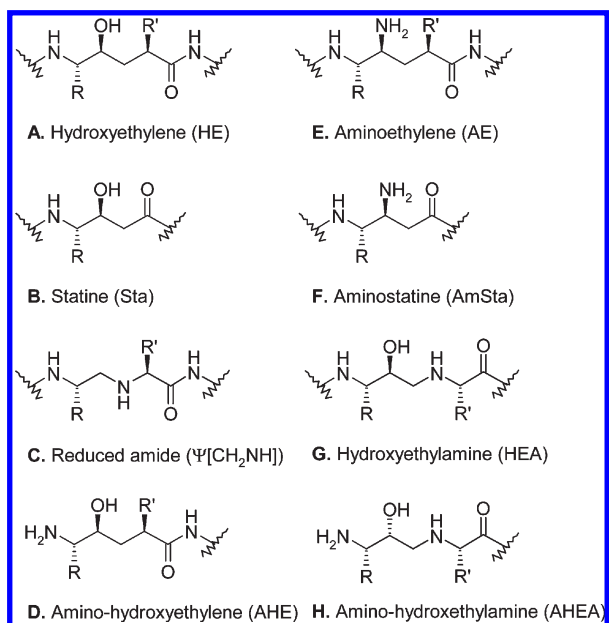


**Figure 3.** Second generation peptide-based peptidomimetic DRIs.

**Chart 1.** Aspartic Protease TSAs and Basic Amine TS Surrogates (Preferred Absolute Configurations Shown)



The vast majority of these potent peptide-derived peptidomimetics had limited druglike properties and hence multiple drawbacks, such as poor intestinal absorption and high liver first-pass metabolic inactivation resulting in low oral bioavailability, as well as high cost of goods due to synthetic complexity and high clinically effective doses. Excellent review articles<sup>21–23</sup> and historical cases, including the discovery of **7** (CP-108,671) exhibiting uniformly high oral bioavailability in dog and marmoset,<sup>35</sup> provide a comprehensive overview on these design efforts, the characterization of second generation DRIs, and their failure in clinical development.

### A New Era of Non-Peptide DRI Design

Several key developments during recent years have contributed to a rapid and fascinating evolution of medicinal chemistry approaches aimed at the design of promising new classes of DRIs. Both the druggable topographical space at the enzyme protein level and, in part as a direct consequence, the chemical diversity space at the ligand level have dramatically expanded. This has evidently opened ample avenues toward the discovery of new structural classes of potent and selective non-peptide peptidomimetic DRIs. The early notion that the large contiguous  $S_3$ – $S_1$  pocket constitutes a key hydrophobic “hot spot” for ligand binding has been successfully employed for a topological inhibitor design concept. Ligand binding sites in the renin active site have been identified, which are distinct from the substrate specificity pockets or even fundamentally different from the extended  $\beta$ -strand substrate binding topography resulting from major conformational movements adjacent to the catalytic center.<sup>29,36</sup> Most notably, the classical dipeptide TSA concept, the dominating theme of inhibitor design over many years, has vanished. Novel privileged basic amine scaffolds that act as TS surrogates by a combination of electrostatic and H-bonding interactions to the catalytic aspartates have been uncovered and provide versatile templates for decoration with recognition site pharmacophores.

These major scientific advances are best illustrated by the discoveries of the orally active topological peptidomimetic **1** (Figure 2), an aminohydroxyethylene dipeptide isostere (AHE, Chart 1D) of a unique chemical class described by Ciba-Geigy (now Novartis),<sup>11–13</sup> and the new type of 3,4-disubstituted piperidine-derived DRIs reported by Hoffmann-La Roche.<sup>36</sup> The DRI **1** resulted from an entirely structure-based design concept using a renin homology model, by addressing the  $S_3/S_3^{SP}$ – $S_1$  active site topography in an unprecedented way (Figure 4). In contrast, the novel structural principle of



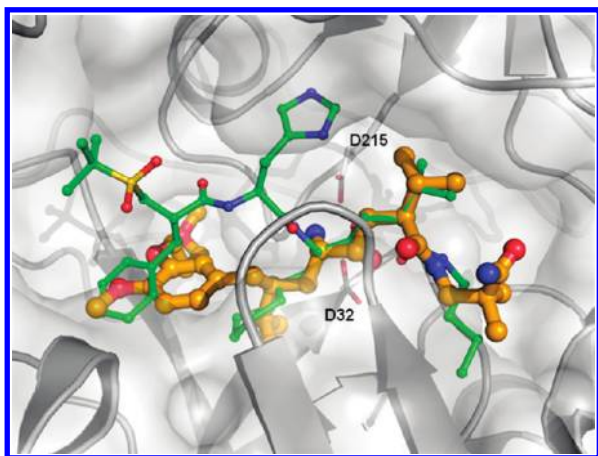


**Figure 4.** Structure of rh-renin in complex with inhibitor **1** (orange). Renin is shown in gray (ribbon diagram and surface) with the side chains of the catalytic aspartates Asp<sub>32</sub> and Asp<sub>215</sub> with gray carbon atoms (flap residues Ser<sub>76</sub> and Thr<sub>77</sub> were omitted from the surface calculation). The peptide-based peptidomimetic **4** (CGP38560) is shown superimposed (green).

4-arylpiperidine peptidomimetics emerged from high-throughput screening (HTS), followed by hit-to-lead elaboration based on crystallographic elucidation of renin–inhibitor complex structures. These inhibitors target a fundamentally different conformational topography of the renin active site. Both critical accomplishments and the positive outcome of late stage clinical trials with **1**<sup>5</sup> have triggered intense efforts to identify “best-in-class” DRIs and have provided several new clinical development candidates.<sup>15</sup> The structural diversity of non-peptide DRIs is anticipated to further expand in the future with the application of evolving state-of-the-art drug discovery concepts.

Major advances in renin inhibitor design will first be reviewed in the following sections by focusing, on one hand, on the identification of core scaffolds binding to the catalytic aspartates and, on the other hand, on specific approaches taken to address the individual binding pockets of the active site, i.e., the S<sub>3</sub>–S<sub>1</sub> “superpocket”, the S<sub>3</sub><sup>SP</sup> and other non-substrate binding pockets, as well as the S<sub>2</sub> and S<sub>1</sub>′–S<sub>2</sub>′ sites. Subsequently, considerations regarding the optimization of ADME and safety properties of different novel chemotype DRIs and their preclinical pharmacology will be addressed, and finally aspects of the clinical pharmacology of **1** are reviewed.

### Novel Lead Discovery Approaches

The discovery and optimization of DRIs have for many years relied mainly on rational substrate-based design by targeting the extended β-strand binding active site topography. Since the mid-1990s, HTS of large historical corporate collections, often containing more than 1 million compounds, has been used as one of the standard methods for identifying starting points for medicinal chemistry against a drug target of interest. In the case of aspartic proteases, as well as for other protease families, HTS has been perceived to suffer from low success rates in the identification of hits having a good potential for further optimization.<sup>13,37</sup> This is certainly related to the fact that the active sites of these enzymes are designed to recognize peptide sequences in an extended conformation and therefore are generally characterized by rather large van der Waals volumes. Remarkably, several pharmaceutical companies have been successful in their search for new chemotype

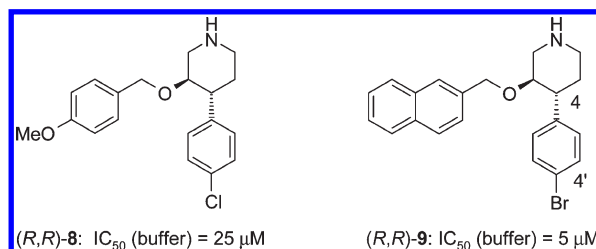


**Figure 5.** 4-Phenylpiperidine DRIs discovered by high-throughput screening (HTS).

scaffolds inhibiting renin, by performing large-scale HTS campaigns based on biochemical assays.<sup>36,38</sup> More recently, alternative technologies based mainly on biophysical methods (nuclear magnetic resonance (NMR), surface plasmon resonance, X-ray crystallography, mass spectrometry) and used in large part for fragment-based screening, as well as in silico computational approaches, were also successfully applied to identify novel active site binding motifs for aspartic proteases, including renin<sup>38d,39</sup> and BACE-1.<sup>40</sup>

In 1999, researchers at Hoffmann-La Roche described the discovery by HTS of the first non-peptide small molecule DRI.<sup>36a</sup> The original hit, *rac*-**8** (IC<sub>50</sub> = 50 μM), showed only weak affinity against the purified enzyme, with the *R,R*-enantiomer accounting for the activity (Figure 5).<sup>36b</sup> The low resolution X-ray structures obtained for *R,R*-**8** and its close analogue *R,R*-**9** revealed the piperidine nitrogen atom to be positioned between the catalytic aspartates, with the naphthyl occupying the S<sub>3</sub>–S<sub>1</sub> subsite. This finding has guided the initial structure–activity relationship (SAR) exploration using combinatorial chemistry.<sup>36a–c</sup> As will be detailed later, modifications at the 4′-position afforded prototype leads with dramatically improved in vitro potencies. Their X-ray crystal structures in complex with recombinant human (rh) renin revealed features very distinct from the binding mode of peptide-derived TSA inhibitors. The terminology of “group replacement assisted binding” (GRAB) peptidomimetics was introduced to account for the topographical and dynamic aspects of these renin–inhibitor interactions.<sup>29</sup> The attractiveness of this remarkable class of DRIs has subsequently fueled drug discovery programs at several other pharmaceutical companies.

A HTS conducted at Pfizer led to the discovery of the 5-phenyl substituted 6-ethyl-2,4-diaminopyrimidine **10** as a weak inhibitor of rh-renin (Figure 6).<sup>38a</sup> Variation of the benzylic moiety employing parallel chemistry led to **11** with 7-fold improved activity. The X-ray cocrystal structure of the renin–**11** complex revealed an active site conformation in which the flap (residues Thr<sub>72</sub>–Ser<sub>81</sub>) is closed. Notably, the 2,4-diaminopyrimidine was identified as a novel planar center scaffold forming H-bonds with the two catalytic aspartates, while also providing constrained, favorable trajectories for both the 6-ethyl group binding into the S<sub>1</sub> pocket and for the difluorobenzylaminophenyl moiety extending into the S<sub>3</sub> and partly into the S<sub>4</sub> subsites (vide infra). This series was further optimized by conformational rigidification of the benzylic portion and introduction of a P<sub>3</sub><sup>SP</sup> side chain (**12**, Figure 6), with additional modifications of the bicyclic (S<sub>3</sub>–S<sub>1</sub>)-motif leading to inhibitors exhibiting high in vitro potency and oral bioavailability (**34**–**37**, Figure 19).<sup>38b</sup>

Fragment-based drug discovery (FBDD) has become an approach of increasing importance over the past years in pharmaceutical research.<sup>24b,c</sup> The group at Pfizer has reported on an in silico docking approach using GOLD, combined with

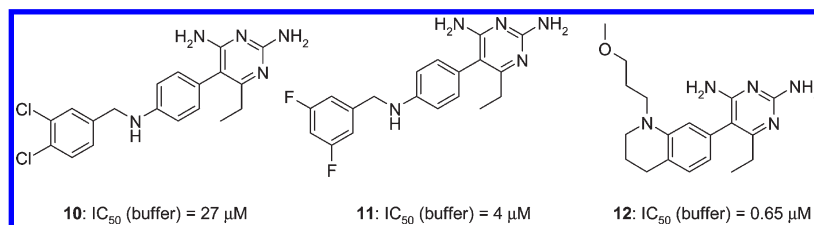


**Figure 6.** 2,4-Diaminopyrimidine-based DRIs originating from HTS.

a NMR auxiliary binding screen of a fragment library, to target specifically the renin  $S_2$  pocket as part of the lead optimization efforts in the 6-ethyl-2,4-diaminopyrimidine series.<sup>38c,d</sup> The identified single fragment hit was shown by saturated transfer difference NMR via interligand NOEs in the presence of renin to be an active site coligand of the C4 aminomethyl analogue of compound **12** (Figure 6). Fragment-linking via a two-carbon spacer and cocrystallization of the resulting inhibitor confirmed the tethered fragment to be positioned in the  $S_2$  pocket. Further elaboration using X-ray crystallographic data in combination with isothermal titration calorimetry (ITC) analyses resulted in significant potency improvement (cf. section “ $S_2$  Specificity Pocket”).<sup>38c</sup> This example highlights the potential of fragment-based approaches for mapping the renin active site. Future applications may uncover new promising lead templates and possibly so far unrecognized binding hot spots for renin.

Various *in silico* screening approaches have emerged recently and found application for renin hit discovery, as either alternative or complementary methods to the screening of physically available compound libraries. Researchers at Vitae Pharmaceuticals disclosed a novel class of DRIs, identified by a *de novo* structure-based design approach<sup>39</sup> using their computational tool Contour and starting from the X-ray structure of the peptidic inhibitor **4** bound to renin.<sup>32</sup> Interestingly, defined criteria for inhibitor design were to target exclusively the  $S_3$ – $S_1$  and  $S_3^{sp}$  pockets while leaving the  $S_2$ ,  $S_4$ , and the prime-site pockets unoccupied. Furthermore, incorporation of a solubilizing basic amine that could interact with the catalytic aspartates was envisaged. Potent DRIs exhibiting reasonable pharmacokinetic (PK) properties and *in vivo* efficacy were identified as a result of design and synthesis iterations and further optimization of prototype leads.<sup>39</sup> The experimental X-ray structure of a renin–inhibitor complex was reportedly in close agreement with the predicted design model. It is noteworthy that *de novo in silico* design approaches targeting alternative, potentially pre-existing conformational ensembles of the renin active site<sup>29</sup> remain an extremely challenging task.

The tremendous progress in high sensitivity assay technologies and emerging powerful new enabling methodologies not only are providing new opportunities to enlarge the chemical space but also allow early validation of very low-affinity small molecule hits as active site binders. Furthermore, computational modeling approaches in combination with timely structural elucidation of an increasing number of renin–ligand complexes by X-ray crystallography have become even more indispensable for an efficient iterative drug discovery process. These approaches encompass hit finding and validation, hit selection, and progression toward enhanced inhibitory potency, all the way through to lead optimization and identification of preclinical candidates. This is most evident for the development of novel class DRIs in view of the multiple pre-existing conformational topographies of the renin active site.<sup>29,36</sup>

The impressive power of new screening technologies and advanced approaches in modern drug discovery is similarly reflected by the rapid development of nonpeptidic inhibitors of  $\beta$ -secretase (BACE-1, memapsin 2), a type-I membrane associated human aspartic proteases. BACE-1 is implicated in the proteolytic cleavage of  $\beta$ -amyloid precursor protein (APP) and subsequent formation of amyloid plaques and has attracted attention as a target for the treatment of Alzheimer’s disease.<sup>40</sup> Since the first report of the potent octapeptide HE isostere inhibitor L- $\alpha$ -glutamyl-L-valyl-L-asparaginyl-(2*R*,4*S*,5*S*)-5-amino-4-hydroxy-2,7-dimethyloctanoyl-L-alanyl-L- $\alpha$ -glutamyl-L-phenylalanine (OM99-2) and its X-ray crystal structure in complex with the protease domain of  $\beta$ -secretase,<sup>41</sup> it took only a few years to bring forth a number of distinct classes of potent non-peptide inhibitors, incorporating either classical TSAs or alternative TS surrogates.<sup>40</sup> While tremendous advancements were made toward the design of BACE-1 inhibitors leading to significant reductions of  $A\beta_{40-42}$  levels in animal models,<sup>42</sup> major hurdles such as brain penetration still need to be overcome with more promising development candidates.<sup>40a</sup>

The structural divergence of peptidomimetic inhibitors of renin and BACE-1 is striking and has limited a target enzyme family approach<sup>43</sup> beyond the application of some fundamental enzyme mechanism-related design principles. Non-peptide BACE-1 inhibitors show high selectivity toward renin,<sup>40</sup> and vice versa, non-peptide DRIs have been reported to be inactive against BACE-1.<sup>13,39</sup> This can be rationalized by both the distinct substrate specificity and the active site architecture of the two enzymes. Relationships between renin and BACE-1 inhibitors with respect to enzyme–inhibitor interactions will be briefly cross-referenced in cases where this could be particularly instructive to emphasize the impact on specific inhibitor design.

### ( $S_3$ – $S_1$ )-Topographical Hot Spot

The first X-ray crystal structure reported for rh-renin revealed the  $S_3$  and  $S_1$  recognition sites to form a large and contiguous space without an apparent division between the two pockets.<sup>31</sup> A similar spacious and open topography of the  $S_3$ – $S_1$  site had been observed previously for several fungal aspartic proteases with and without bound peptide TSA inhibitors.<sup>25,28,30,44,45</sup> Furthermore, these enzyme–ligand complexes revealed the substrate-based inhibitors to bind in an extended  $\beta$ -strand conformation with the hydrophobic  $P_3$  and  $P_1$  residues being tightly constrained and positioned close to each other. Both  $P_3$  and  $P_1$  residues are shielded from solvent space by the flap  $\beta$ -hairpin in its “closed conformation”. This  $S_3$ – $S_1$  binding topography was subsequently confirmed by the X-ray structures of peptide peptidomimetic DRIs, such as **4** (Figure 4).<sup>30,32</sup>

Different structure-based concepts have been investigated independently by several research groups based on the notion that the renin  $S_3$  and  $S_1$  pockets form a spacious hydrophobic

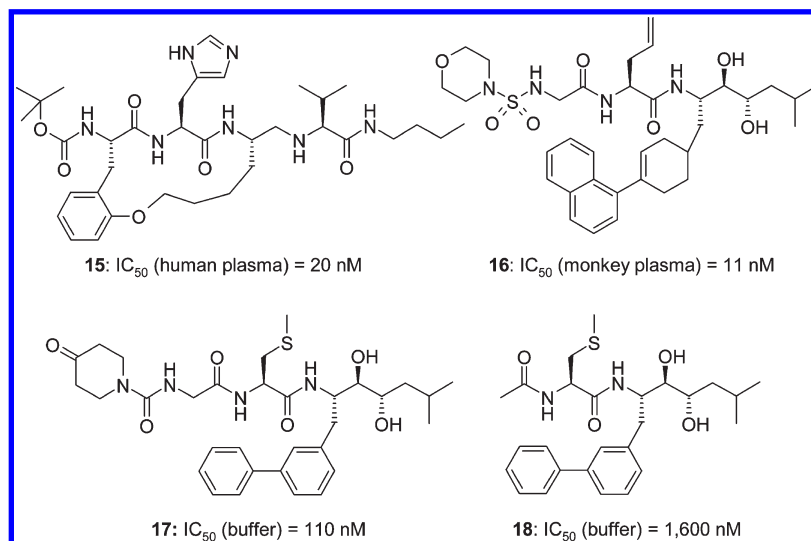


**Figure 7.** Peptide-based macrocyclic and ( $S_3$ – $S_1$ )-topological DRIs.

cavity. The formation of large-surface van der Waals contacts to the hydrophobic amino acids lining the  $S_3$ – $S_1$  cavity was considered to be energetically favorable as a driving force for binding affinity. Design efforts therefore were aimed at maximizing the hydrophobic interactions to this key binding site by covalently linking the  $P_3$  and  $P_1$  side chains and ultimately at identifying novel structural classes of small-molecule DRIs with enhanced oral efficacy.<sup>13,46–48</sup> Conformational constraints have been introduced in peptide-based peptidomimetics by cross-linking alternate side chains to enhance potency and selectivity by locking the inhibitor in the bound conformation and in addition to potentially improve the PK properties of the more flexible acyclic congeners.<sup>13,23a,23b,46</sup> The macrocyclic inhibitor **15** bearing a  $\psi$ [CH<sub>2</sub>NH]-reduced amide isostere (Figure 7) was 5 times more potent in vitro compared to the acyclic  $P_1$  cyclohexylalanine-based analogue.<sup>46</sup> While macrocyclization between the  $P_3$  and  $P_1$  side chains of peptidomimetic DRIs has found only limited application, in contrast to substantial efforts made for the design of  $P_3$ – $P_1$ -linked BACE-1 macrocyclic inhibitors,<sup>40</sup> the spatial proximity of other recognition sites has attracted more interest and provided potent macrocyclic TSA inhibitors of renin.<sup>23a,b</sup>

Dihydroxyethylene isostere peptidomimetics with topographically modified  $P_1$ ( $\rightarrow P_3$ ) side chains (**16**, Figure 7) have been explored by extending the  $P_1$  cyclohexyl directly toward the  $S_3$  binding pocket and by removing the linkage of  $P_3$  to the peptide backbone. The  $P_3$  glycine derivative **16** was found to be a potent inhibitor of monkey plasma renin.<sup>47</sup> Further truncation of the N-terminal backbone of these inhibitors was believed to be difficult to achieve without reducing the binding affinity.<sup>47a</sup> A similar design concept based on the X-ray structure of a tetrapeptide TSA in complex with rh-renin afforded inhibitors spanning the  $S_3$ – $S_1$  pocket, such as **17**, that were up to > 200-fold more potent than the respective  $P_1$  phenyl analogues lacking  $S_3$  interactions.<sup>48</sup> X-ray crystallography revealed the meta-biphenyl moiety of **17** to intrude into  $S_3$ – $S_1$  without completely filling this cavity, suggesting that additional lipophilic substituents could lead to more potent analogues. Removal of the  $P_4$  residue produced analogues with a 14-fold drop in potency (cf. **18**, Figure 7).<sup>48</sup>

Novartis has reported the structure-based design of several unique structural series of non-peptide aminohydroxyethylene (AHE, Chart 1D) isosteres spanning the  $S_3$ – $S_2'$  recognition

sites and lacking the  $P_4$ – $P_2$  peptide backbone of previous inhibitors (**19**–**22**, Figure 8). These efforts have culminated in the discovery of **1**, a remarkably potent and highly selective first-in-class oral DRI.<sup>11–13,49</sup> The stepwise evolution of the design concept was primarily driven by the  $S_3$ – $S_1$  topography derived from the predicted active site conformation of **4** using a renin homology model. Weakly active AHE isostere fragments were grown directly into the large contiguous  $S_3$ – $S_1$  site, considered as a hydrophobic hot spot<sup>50</sup> for ligand binding, by extending at the  $P_1$  position.<sup>13</sup> Most intriguingly, these novel classes of DRIs were discovered by X-ray crystallography to bind into a small and rigid cavity that extends from  $S_3$  toward the enzyme core perpendicular to the binding cleft and is not utilized by known substrate-based inhibitors.<sup>51</sup> The interaction to this nonsubstrate  $S_3^{SP}$  subpocket is essential for strong renin inhibition by these topological TSA inhibitors.

The X-ray structure of **1** in complex to rh-renin is depicted in Figure 4.<sup>12,51</sup> The ligand is bound in an extended conformation spanning the  $S_3$ – $S_2'$  recognition sites, leaving the  $S_4$  and  $S_2$  pockets unoccupied. Its  $P_1$  isopropyl residue is more deeply positioned in the  $S_1$  site compared to the  $P_1$  cyclohexyl of the peptide-based inhibitor **4**, while the hydrophobic space-filling phenyl residue positions the methoxy group into the  $S_3$  pocket. Remarkably, the ether oxygen is involved in a H-bond interaction with the hydroxyl of Thr<sub>12</sub> mediated by  $S_3$  bound water molecules. The extended flexible methoxypropoxy side chain penetrates deeply into the newly discovered  $S_3^{SP}$  cavity of renin (vide infra). The AHE isostere portion (Chart 1) forms reversible noncovalent tight binding interactions to both Asp<sub>35</sub> and Asp<sub>215</sub> via H-bonding and possibly electrostatic interactions. The structurally diverse ( $P_3$ – $P_1$ )-pharmacophores of **19** and **21**–**22** also fully occupy the  $S_3$ – $S_1$  cavity, forming close van der Waals contacts to the large surface, as shown by the X-ray complex structures of related analogues.<sup>51</sup>

Inhibitor **1** and related AHE isosteres **19**–**22** represent landmark examples of a successful ( $S_3$ – $S_1$ )-topography design concept supported by computer-aided molecular modeling and X-ray crystallography. Notably, the design of tetrapeptide-based aminohydroxyethylene (AHEA, Chart 1H) isosteres spanning the  $S_1$ – $S_3'$  sites and lacking the  $P_4$ – $P_2$  peptide portion was reported as early as 1989 and was similarly based on an endothiapepsin-derived renin homology model.<sup>52,53</sup> Inhibitor **23** (BW586C, Figure 9) bearing a tethered



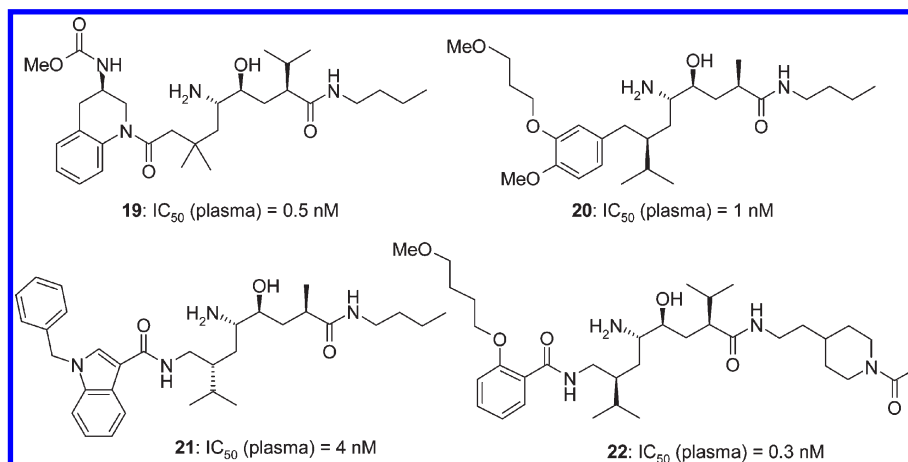


**Figure 8.** Nonpeptide ( $S_3$ – $S_1$ )-topological peptidomimetic TSAs.

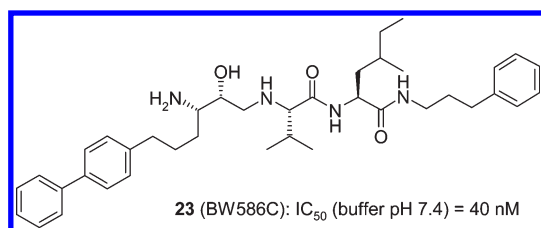


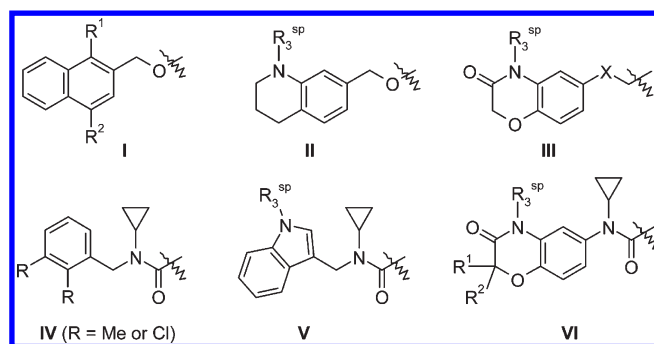
**Figure 9.** ( $S_3$ – $S_1$ )-Topological tripeptide-based amino alcohol DRI.

$P_1$  biphenyl moiety was remarkably potent *in vitro*. SAR data for related amino alcohols with preferred (*2R*)(*3S*)-configuration indicated a significant potency increase when the  $P_1$  residue was more lipophilic and extended.<sup>52,53</sup> An X-ray structure of **23** in complex with rh-renin, or any other aspartic protease, that could confirm the predicted occupancy of the  $S_3$ – $S_1$  cavity has not been reported.

Inhibitor **1** showed remarkable *in vitro* potency under more physiological conditions.<sup>11,12</sup> The methoxypropoxy side chain binding to  $S_3^{SP}$  turned out to be optimal for this inhibitor class, leading to high inhibitory affinity for plasma renin.<sup>12,49</sup> Significant increases in the  $IC_{50}$  of up to several orders of magnitude have been observed for analogues of **1** and other ( $S_3$ – $S_1$ )-topological inhibitors<sup>13</sup> in the presence of plasma (“plasma shift”). Such plasma shifts have also been reported for peptide-derived<sup>21a,54</sup> and non-peptide DRIs from various structural classes.<sup>36,39,55</sup> The drop in potency toward plasma renin has been attributed to low solubility and high lipophilicity and/or high unspecific binding to plasma proteins reducing the free fraction in blood.<sup>55</sup> However, other yet to be uncovered factors may also contribute to this phenomenon.<sup>21a,49,56</sup> The relevance of *in vitro* plasma  $IC_{50}$  values as predictive descriptors for BP lowering potency of a given DRI *in vivo* has been under debate,<sup>55</sup> in particular in view of the emerging evidence for the importance of local renin inhibition in the kidney and other tissues.<sup>57</sup> Notably, an increase in plasma renin concentration (PRC) has been generally accepted as an important clinical surrogate marker for RAS blockade and inhibition of plasma renin activity (PRA) for the effectiveness of drug treatment using a DRI.<sup>4</sup>

Novel ( $S_3$ – $S_1$ )-topological binding motifs have been identified from weakly active HTS hits (**8** and **10**, Figures 4 and 5),<sup>36a,38a</sup> and structure-based design has subsequently generated an array of privileged ( $P_3$ – $P_1$ )-pharmacophores (**I**–**VI**, Chart 2). These structural moieties have in common that they

**Chart 2.** Topological ( $P_3$ – $P_1$ )-Pharmacophores Used in Combination with Five- and Six-Membered Center Basic TS Surrogate Scaffolds of Non-Peptide DRIs (See Figures 5, 6, and 11)



have been linked to a basic center scaffold such as a piperidine or related mono- or bicyclic ring analogues (Figures 22 and 23)<sup>36,55,58</sup> and 2,4-diaminopyrimidines (**12**, Figure 6)<sup>38</sup> occupying the pivotal position between Asp<sub>32</sub> and Asp<sub>215</sub> by forming electrostatically enforced H-bonds (*vide infra*). These templates provide trajectories different from the  $P_1$ -tethering vector of AHE isosteres for extensions into the  $S_3$ – $S_1$  cavity. Optionally substituted naphthalene or tetrahydroquinoline as equipotent replacement (**I** and **II**, Chart 2), when bridged by a 3-methyleneoxy group to the 4-phenyl-piperidine scaffold, resulted in potent inhibitors classified as GRAB peptidomimetics<sup>29</sup> (cf. section “GRAB Peptidomimetic Class of DRIs”). The naphthalene occupies the  $S_3$ – $S_1$  site forming an edge-to-face interaction with the Phe<sub>117</sub> residue.<sup>38a,c</sup> The position of the oxymethylene spacer and the proximal edge of the naphthyl partially overlap with the binding position of the  $P_1$  isopropyl of **1**.

The nitrogen atom of the tetrahydroquinoline heterocycle provides an attachment point for side chains that can penetrate into the nonsubstrate  $S_3^{SP}$  cavity in a similar fashion as previously discovered for AHE isostere inhibitors **1** (Figure 2) and **19**–**22** (Figure 8). The 1,4-benzoxazin-3-one motif (**III**, Chart 2) was identified as a less hydrophobic tetrahydroquinoline replacement, being well accommodated by the  $S_3$ – $S_1$  site and providing an equally efficient trajectory for tethered  $P_3^{SP}$  residues.<sup>58c</sup> When attached to a 2-ketopiperazine center scaffold by a two-atom (thio)ether linkage, high affinity DRIs were obtained (*vide infra*). Subsequently, the 1,4-benzoxazinone pharmacophore and modifications thereof have attracted major interest by other groups.<sup>15</sup>

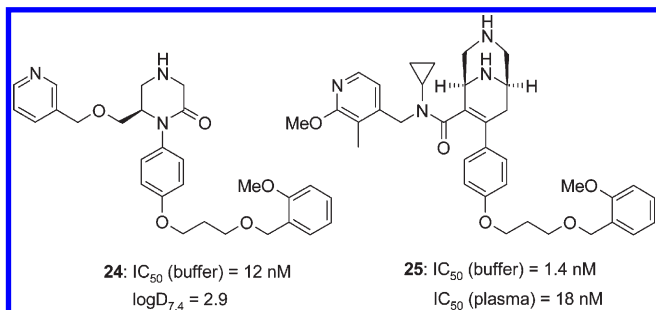


**Figure 10.** Renin inhibitor (P<sub>3</sub>–P<sub>1</sub>)-pharmacophores incorporating basic residues.

The 5-aryl-2,4-diaminopyrimidine (Figure 6)<sup>38</sup> constitutes a remarkable scaffold that functions as a basic TS surrogate by interacting with the catalytic dyad and in addition is part of a conformationally constrained (P<sub>3</sub>–P<sub>1</sub>)-pharmacophore. The X-ray structures of renin-bound **12** and related analogues revealed the C6 ethyl group to be positioned in the S<sub>1</sub> pocket closely overlapping with the P<sub>1</sub> isopropyl of **1**.<sup>38</sup> The 1,4-benzoxazinone of **34** (cf. Figure 19) extends into the S<sub>3</sub> pocket, with small alkyl groups at its (*S*)-configured C2 position fitting into a small indentation of the S<sub>3</sub> site, superimposing with the P<sub>3</sub> methoxy of **1**. The C2 phenyl of **35** is positioned within the hydrophobic but solvent exposed S<sub>4</sub> pocket, resulting in enhanced van der Waals contacts and hence increased binding affinities (**34** vs **35**).<sup>38b</sup> The C3 carbonyl favors a rigid conformation of the bicyclic moiety that directs the C2 phenyl toward S<sub>4</sub> and furthermore is involved in enzyme-water mediated H-bond interactions. Notably, a geminal disubstitution at C2 blocks this metabolic weak point prone to oxidative hydroxylation.

Researchers at Actelion were first to report the design of *N*-benzylated tertiary amides (**IV**, Chart 2) as a new pharmacophore tightly filling the hydrophobic S<sub>3</sub>–S<sub>1</sub> pocket when attached to a 7-aryl substituted 3,9-diazabicyclo[3.3.1]nonene template (Figure 10) and related monocyclic core scaffolds.<sup>55</sup> These findings resulted from a structure-based design effort to identify GRAB peptidomimetics with superior pharmacokinetic properties. The nature of the bicyclic scaffold with its vinylic double bond at the 6,7-position required a replacement of the ether linkage of previous (P<sub>3</sub>–P<sub>1</sub>)-pharmacophores (for example, compare **25**, Figure 10, with **30** and **31**, Figure 16)<sup>36,58</sup> by a chemically stable functional spacer group. A parallel chemistry approach uncovered 2,3-disubstituted benzylamides with a *N*-cyclopropyl group to be optimal for in vitro potency, particularly in the presence of plasma.<sup>55</sup> The X-ray structure of **52** (ACT-077825/MK-8141, Figure 11 and Figure 23)<sup>55</sup> in complex with rh-renin revealed the *N*-cyclopropyl to be positioned in a small subpocket of the open-flap conformational topography of renin. Remarkably, the cyclopropyl binding position closely superimposes with that of the P<sub>1</sub> isopropyl residue of **1** in complex with the β-strand binding active site conformation (Figure 11). Also, the 2,3-disubstituted phenyl of **52** overlays with the P<sub>3</sub> phenyl group of **1** with close to perfect overlap of the 3-methyl and the 4-methoxy groups, respectively. Introduction of tethered H-bond acceptor groups to the C5 phenyl position of **52**, or related analogues, to target the S<sub>3</sub><sup>SP</sup> pocket has also been investigated to optimize for potency.<sup>15</sup>

The tertiary benzylamide P<sub>3</sub>–P<sub>1</sub> motif has been further investigated in combination with 3,4-disubstituted piperidines and related basic monocyclic center scaffolds by several other

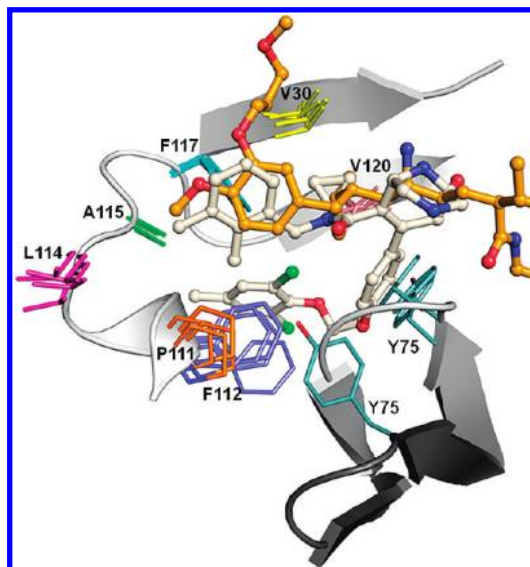


**Figure 11.** Conformational rigidity of the large contiguous S<sub>3</sub>–S<sub>1</sub> binding site of renin, as illustrated by the overlay of several X-ray crystal structures of enzyme-bound inhibitors from distinct compound classes. Shown are the hydrophobic side chains lining the boundaries of S<sub>3</sub> (Thr<sub>12</sub>, Gln<sub>13</sub>, Pro<sub>111</sub>, Phe<sub>112</sub>, Leu<sub>114</sub>, Ala<sub>115</sub>, Phe<sub>117</sub>, Ser<sub>219</sub>) and S<sub>1</sub> (Val<sub>30</sub>, Asp<sub>32</sub>, Tyr<sub>75</sub>, Thr<sub>77</sub>, Phe<sub>112</sub>, Phe<sub>117</sub>, Val<sub>120</sub>, Asp<sub>215</sub>; the residues shown in the figure are underlined), as observed for **1** (orange), the GRAB peptidomimetic **52** (gray), the 2,4-diaminopyrimidine **34**, and the *N*-ureapiperidine **38**. Inhibitors **34** and **38** were omitted for clarity. A partial ribbon diagram is shown for the complex with **1** (gray) and in addition for the flap β-hairpin as observed for **52** (dark gray). Phe<sub>112</sub> in the complex with **52** (flap pocket binder) is shifted significantly with respect to the other complexes. Large movements are observed only for the flap β-hairpin (e.g., 5.1 Å for the Cα of Tyr<sub>75</sub> in the complex with **1** vs **52**).

groups.<sup>15</sup> These include analogues bearing extended side chains with terminal functional groups capable of forming a H-bond to Tyr<sub>14</sub> of the S<sub>3</sub><sup>SP</sup> subpocket (vide infra), such as *N*-tethered indoles (**V**, Chart 2).<sup>15</sup> Novartis has disclosed *N*-cyclopropyl-*N*-1,4-benzoxazinone carboxamides (**VI**) attached to a 3,5-disubstituted piperidine center scaffold leading to a new class of DRIs.<sup>59</sup>

The design of less hydrophobic (P<sub>3</sub>–P<sub>1</sub>)-pharmacophores has been explored by incorporation of basic amines or aromatic heterocycles into different chemotype DRIs.<sup>36c,55a,56,58a,d</sup> Analogues of **1** bearing a basic P<sub>1</sub> tertiary amine motif were reported to be potent toward plasma renin in vitro.<sup>56</sup> The group at Speedel has claimed P<sub>3</sub><sup>SP</sup>-substituted pyridine analogues of **1** exhibiting high potency in vitro, albeit no detailed information on their potential was disclosed.<sup>60</sup> In the 2-ketopiperazine series of GRAB peptidomimetics, replacement of bicyclic P<sub>3</sub> motifs by simplified benzyl and pyridinyl ethers has been investigated using a Topliss approach.<sup>58d</sup> Notably, the 3-pyridinyl derivative **24** (Figure 10) was the only regioisomer shown to be active against rh-renin. The critical position of the pyridyl nitrogen atom was rationalized by H-bonding to Ser<sub>219</sub> suggested by modeling. Inhibitor **24** had a more favorable profile with respect to solubility, cell permeability, and affinity to CYP3A4 in comparison to its phenyl congener.<sup>58d</sup> More hydrophilic 4-pyridinyl substituted P<sub>3</sub> tertiary amides were well tolerated when combined with the 3,9-diazabicyclo[3.3.1]nonene scaffold.<sup>55a</sup> Inhibitor **25** exhibited only a 10-fold plasma IC<sub>50</sub> shift, while a 50-fold drop in plasma renin potency was observed for its 3-methoxy-2-methylphenyl analogue (buffer rh-renin IC<sub>50</sub> = 0.62 nM). While increasing evidence has emerged for the



feasibility to design less hydrophobic  $S_3$ – $S_1$  binding motifs, it remains to be seen whether this strategy will lead to the design of novel DRIs with more promising characteristics.

The  $S_3$ – $S_1$  binding topography of renin recognized by structurally diverse classes of non-peptide peptidomimetics emulating the extended  $\beta$ -strand binding conformation of the active site is remarkably conserved and very similar to the topography recognized by substrate-based DRIs. The hydrophobic amino acids lining the  $S_3$  and  $S_1$  pockets are located on four different sections of the protein chain ( $\beta$ -3, flap region,  $\alpha$  h<sub>N2</sub>,  $\beta$ -8). Their peptide backbone and side chains reveal only minor conformational differences in the X-ray crystal structures of various renin–inhibitor complexes (Figure 11). The carboxy-terminal boundary of the  $S_1$  pocket is occupied by the aromatic ring of Tyr<sub>75</sub>, which separates the  $S_1$  from the  $S_2'$  pocket when the  $\beta$ -hairpin is in a closed conformation.

4-Phenylpiperidine GRAB peptidomimetics stabilize a renin active site conformation that is substantially different from the extended  $\beta$ -strand binding conformation observed for classical peptide-like inhibitors.<sup>29,36,55,58</sup> The distinct topography results from major movements of the  $\beta$ -hairpin, in particular of the backbone and side chains of Tyr<sub>75</sub>, Leu<sub>73</sub>, and Trp<sub>39</sub>. This places the inhibitor C4 phenyl into the space vacated by the Tyr<sub>75</sub> aromatic ring, thereby reconstituting the carboxy-terminal boundary of the  $S_1$  pocket (vide infra). Most notably, these rearrangements have little impact on the conformation of the residues defining the boundaries of the  $S_3$  pocket and major portions of  $S_1$  (Figure 11). Moderate shifts, for example, of the Phe<sub>112</sub> side chain deeper toward the bottom of the  $S_3$  site (by  $\sim 1.5$  Å) and of Val<sub>120</sub> have been observed in some cases.<sup>36</sup> In the X-ray complexes with GRAB peptidomimetics, the renin flap region is in a more “open” conformation than observed for DRIs targeting the substrate-binding active site topography. The largest backbone displacement of  $\sim 6$  Å away from the ligand position is noted for the C $\alpha$  of Thr<sub>77</sub> at the tip of the flap  $\beta$ -turn (Tyr<sub>75</sub>–Ser<sub>76</sub>–Thr<sub>77</sub>–Gly<sub>78</sub>). However, the Tyr<sub>75</sub> phenyl side chain, rotated outward from its buried former position, is now directed toward the active site cleft, thereby closing the spatial gap to the enzyme-bound inhibitors (Figures 11 and 12).

The X-ray crystal structures of the topological peptidomimetics **28** and **29** (Figure 14) and a close analogue of **22** (Figure 8),<sup>13,51</sup> bearing a carbonyl group bridging the P<sub>1</sub> and P<sub>3</sub> residues, revealed a H-bond interaction to the Thr<sub>77</sub> hydroxyl at the tip of the flap region in its closed conformation. In vitro SAR data suggested this Thr<sub>77</sub> flap–inhibitor interaction to provide an important contribution to binding affinity.<sup>13</sup> In the case of peptide-derived inhibitors, the hydroxyl of Thr<sub>77</sub> forms H-bonds to the nitrogen of the P<sub>2</sub>/P<sub>3</sub> carboxamide and to the P<sub>2</sub> carbonyl.<sup>30,32</sup> In the renin-bound complex of several GRAB peptidomimetics, the reoriented Tyr<sub>75</sub> phenylhydroxyl overlaid within a remarkably close  $\sim 1$ – $2$  Å distance with the hydroxyl side chain of Thr<sub>77</sub> in the closed substrate-derived flap conformation observed for **4**, **28**, and **29** (Figure 12). This may suggest a potential role of the Tyr<sub>75</sub> hydroxyl for the future design of novel GRAB peptidomimetic DRIs.

The hydrophobic and contiguous  $S_3$ – $S_1$  recognition pocket of renin is now well established as a key hot spot for high affinity ligand binding. All potent DRIs reported to date closely interact with this spacious topography of the target enzyme. The hydrophobic solvent exposed  $S_4$  and the non-substrate  $S_3^{SP}$  cavity are directly accessible from  $S_3$  and have been successfully exploited for novel inhibitor design. Also,

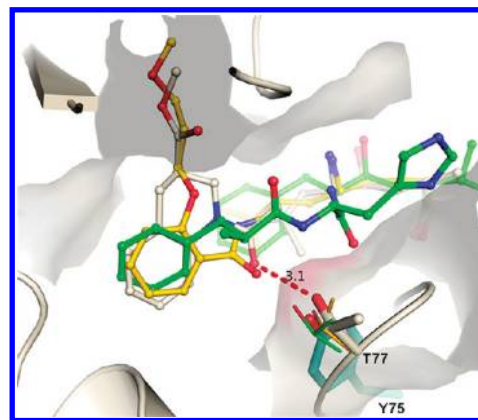


**Figure 12.** Hydrogen-bond interactions of the ( $S_3$ – $S_1$ )-topological peptidomimetic **28** (gray) and a close analogue of **22** (yellow, PDB code 2v12),<sup>51</sup> as well as peptidic inhibitor **4** (green), with Thr<sub>77</sub> of the flap  $\beta$ -turn. Portions of the enzyme chain in the complex with **28** are shown as a ribbon diagram in gray, and the Thr<sub>77</sub> side chains in the different complexes are shown with the color coding of the respective inhibitors. Flap domains are in closed conformations. The hydroxyl of the flap Tyr<sub>75</sub> (cyan) in complex with the GRAB peptidomimetic **32** (inhibitor not shown) is in a similar position as the Thr<sub>77</sub> hydroxyl ( $0.9$  Å distance) in complex with **28**. The H-bond between the carbonyl of **28** and the Thr<sub>77</sub> hydroxyl is indicated.

both the  $S_3$ – $S_1$  subsite and the Trp<sub>39</sub> “deep flap pocket” form a large open cleft in the renin conformational topography stabilized by GRAB peptidomimetics, as will be discussed in more detail in a later section devoted to this class of DRIs. This large accessible surface area may allow generation of unprecedented structural motifs binding to these, or possibly alternative, conformations, which could be combined with known center scaffolds interacting with the catalytic dyad. Conversely, it appears conceivable that the identification of new TS surrogates may offer distinct trajectories for novel ( $P_3$ – $P_1$ )-pharmacophores with high ligand binding efficacy. Very likely, the  $S_3$ – $S_1$ -topography of renin will remain a major target for future design of diverse non-peptide DRIs with possibly enhanced druglike characteristics.

### Nonsubstrate $S_3^{SP}$ Binding Pocket

Several investigators have independently discovered the presence of a distinct narrow cavity in native renin, extending from the  $S_3$  site perpendicular to the active site cleft toward the center of the enzyme.<sup>13,61–63</sup> This pocket, now generally termed  $S_3^{SP}$ , is occupied by ordered water molecules and is not involved in substrate or peptide-based inhibitor binding. To our knowledge, Hanson et al.<sup>61</sup> were first to postulate this cavity as a potential auxiliary binding site based on computational energy surface analysis of a renin–peptide inhibitor complex and SAR data. The X-ray structure of **26** (SC-51106, Figure 13)<sup>61</sup> in complex with deglycosylated rh-renin demonstrated the  $\beta$ -(*S*)-methyl of the hydrocinnamoyl portion to occupy  $S_3^{SP}$  by replacing one enzyme-bound water. Lefker et al.<sup>63</sup> have reported the design of **27** (CP-305,202, Figure 13) and showed by X-ray that the flexible 3-pyridylpropoxy side chain was binding into the  $S_3^{SP}$  cavity.

Researchers at Ciba-Geigy/Novartis have described the design of topological AHE dipeptide isosteres bearing distinct hydrophobic ( $P_3$ – $P_1$ )-pharmacophores.<sup>12,13,49</sup> The potent inhibitors **20** (Figure 8) and **28** and **29** (Figure 14) were discovered by X-ray crystallography to interact with the non-substrate  $S_3^{SP}$  pocket of renin. A key element of the evolving

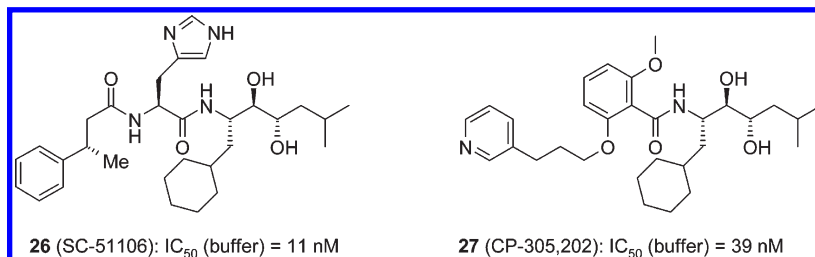


**Figure 13.** Early examples of DRIs binding to the  $S_3^{SP}$  subpocket of renin.

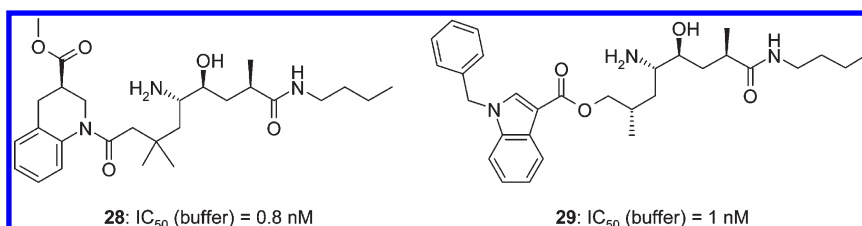


**Figure 14.** ( $S_3$ - $S_1$ )-topological peptidomimetics binding to the nonsubstrate  $S_3^{SP}$  pocket.

design concept at Novartis has been to target H-bond interactions to Ser<sub>219</sub> of renin.<sup>13</sup> This position is highly conserved as either serine or threonine in all aspartic proteases. Interactions with this residue had been recognized by in vitro SAR data and X-ray crystallography of multiple enzyme–inhibitor complexes to be important for the alignment of substrate-based peptidomimetics within the active site,<sup>44</sup> including renin and BACE-1 inhibitors.<sup>40b</sup> Hence, substitution of hydrophobic ( $P_3$ - $P_1$ )-scaffolds of weakly active leads with suitable H-bond acceptors/donors was considered to mimic the conserved H-bond of the main chain  $P_3/P_2$  carboxamide known to be essential for the tight binding of peptide-based inhibitors. The carboxylic ester **28** (Figure 15), a precursor analogue of **19**, was indeed shown by X-ray to interact with both the NH and OH of Ser<sub>219</sub> (vide infra). Inhibitor **1**, but not the  $P_2'$  analogue **20**, forms a water-mediated H-bond between the proximal ether oxygen of the  $P_3^{SP}$  side chain and the Ser<sub>219</sub> hydroxyl, which however is not critical for binding.<sup>12,13,49</sup>

The carboxylic ester of the tetrahydroquinoline analogue **28** is filling the  $S_3^{SP}$  cavity only partially with the methyl group being suboptimal in length and in addition forms a direct H-bond to Ser<sub>219</sub> at the entrance of this site. In contrast, both the hydrophobic *N*-benzyl residue of the indole derivative **29** and the more polar flexible methoxypropoxy side chain of **20** penetrate deeply inside and fully occupy the  $S_3^{SP}$  pocket. Moreover, the terminal methoxy group of **20**, and likewise of **1**, is involved in H-bonding to the NH of Tyr<sub>14</sub> at the bottom of the channel (Figure 15).<sup>12,49,51</sup> Most notably, these unprecedented binding interactions to the nonsubstrate  $S_3^{SP}$  site had not been predicted by molecular modeling. Further SAR efforts resulted in the identification of the preclinical candidates **19** and **22** (Figure 8) which exhibited high potency in vivo.<sup>13</sup>

The three-dimensional architecture of the renin  $S_3^{SP}$  subsite and its electrostatic surface properties are now well-defined by multiple enzyme–inhibitor X-ray crystal structures (Figure 15). This cavity constitutes a narrow channel extending from the  $P_3$  pocket by about 10 Å in depth, flanked by residues located on five different segments of the enzyme. The hydrophilic nature of the channel is reflected by its capability to bind up to three water molecules in native renin and to accommodate inhibitors with a range of polar residues, including basic aliphatic amines.<sup>36</sup>

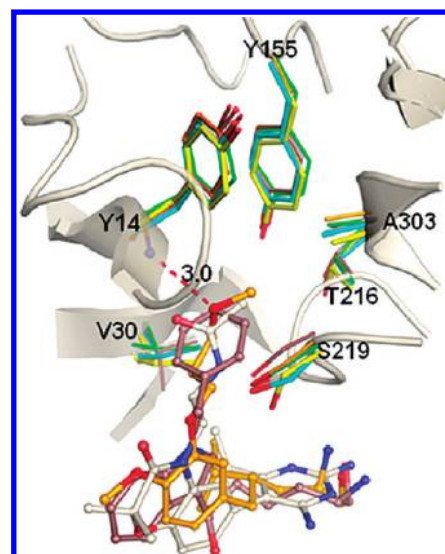


**Figure 15.** Illustration of the conformational rigidity of the renin  $S_3^{SP}$  pocket. Shown are the superimposed X-ray structures of rhrenin in complex with **1** (orange) (protein ribbon diagram in gray), *N*-benzylindole **29** (brown), and the *N*-ethylacetamide-substituted 2,4-diaminopyrimidine **34** (gray). Of the key side chains lining the boundaries of  $S_3^{SP}$  (Thr<sub>12</sub>, Gln<sub>13</sub>, Tyr<sub>14</sub>, Val<sub>30</sub>, Tyr<sub>155</sub>, Thr<sub>216</sub>, Gly<sub>217</sub>, Ser<sub>219</sub>, and Ala<sub>303</sub>) those underlined are shown with the color codes used for the inhibitors. In addition, the corresponding side chains are shown for the renin complexes with inhibitor **4** (green), the *N*-hydroxypropyl analogue of 2-ketopiperazine **48** (PDB code 2fs4, cyan), and native renin (yellow).<sup>31</sup> The H-bond of the methoxypropoxy side chain of **1** to the backbone amide nitrogen of Tyr<sub>14</sub> is highlighted.

Several lipophilic side chains lining the cavity boundaries explain the propensity of  $S_3^{SP}$  to accommodate equally well hydrophobic aliphatic and aryl ligands. Filling the  $S_3^{SP}$  pocket while displacing one or more bound water molecules and extruding them into bulk solvent is considered to be favorable because of entropic and enthalpic energy gains.<sup>51</sup>

Targeting binding interactions to the nonsubstrate  $S_3^{SP}$  pocket has significantly enlarged the arsenal for designing potent and selective DRIs and has been a key element in lead optimization of several new classes of non-peptide peptidomimetics including piperidines (**30** and **31**, Figure 16),<sup>36</sup> 2,4-diaminopyrimidines

(**34**–**37**, Figure 19),<sup>38b</sup> *N*-ureapiperidine-based reduced amide isosteres (**38**–**41**, Figure 20),<sup>39</sup> and 2-ketopiperazines (**46**–**50**, Figure 22).<sup>58</sup> Substituting distinct (P<sub>3</sub>–P<sub>1</sub>)-pharmacophores of various non-peptide peptidomimetics with optimized S<sub>3</sub><sup>SP</sup>-binding residues has generated DRIs with a ≥50-fold increased potency,<sup>13,19,39,58c</sup> illustrating the importance of S<sub>3</sub><sup>SP</sup>–ligand interactions for tight binding. Terminal alkyl ethers, acetamides, and alkyl carbamates were, in general, found to be optimal for in vitro potency toward rh-renin and more importantly often provided inhibitors with small in vitro plasma IC<sub>50</sub> shifts (vide supra).<sup>36,39,49</sup> Conversely, combinations with hydrophobic P<sub>3</sub><sup>SP</sup> motifs resulted in a significant loss of potency in the presence of plasma, even within inhibitor classes that generally demonstrated low lipophilicity and high solubility, as represented by **19**–**22** (Figure 8).<sup>13,49</sup> The specific structure–activity relationship for P<sub>3</sub><sup>SP</sup> side chain modifications may be depending, to some extent, on the class of DRIs.<sup>36,38b,39</sup>

Introducing more hydrophilic P<sub>3</sub><sup>SP</sup> side chains has also been explored as a strategy to modulate physicochemical and ADME properties of various classes of DRIs.<sup>36,38,58</sup> The group at Hoffmann-La Roche was the first to investigate this approach as part of the optimization of their highly lipophilic (log *P* > 5) GRAB peptidomimetic series (**30** and **31**, Figure 16).<sup>36</sup> The tetrahydroquinoline moiety of **30** (RO-65-2349) provides an ideal vector for hydrophilic extensions toward S<sub>3</sub><sup>SP</sup>, as was suggested by the X-ray structure of **32** (Figure 18) bound to rh-renin.<sup>36b,d</sup> The less lipophilic and more soluble **31** (RO-66-1168), bearing a polar *N*-acetylaminoethyl residue, showed picomolar IC<sub>50</sub> against rh-renin and most notably a 50-fold increase in potency against plasma renin. This compound demonstrated potent BP lowering efficacy in vivo but had poor PK properties in rat.<sup>36d</sup>

The group at Pfizer has subsequently used a similar concept to enhance the in vitro potency of related 2-ketopiperazine GRAB peptidomimetics and to address their strong affinities for CYP3A4.<sup>58</sup> Various linear side chain functionalities were investigated to probe the requirements for efficient S<sub>3</sub><sup>SP</sup> binding interactions. These modifications resulted in subnanomolar inhibitors of rh-renin (cf. **46** vs **47**–**50**, Figure 22), albeit no IC<sub>50</sub> values for plasma renin were reported. While a terminal hydroxyl, and particularly a carboxylic acid residue, reduced the affinity for CYP450 enzymes, these modifications were not well-tolerated in this series leading to modest in vitro potencies.<sup>58c</sup> The acidic carboxylate of these inhibitors does not interact with the S<sub>3</sub><sup>SP</sup> cavity but rather is solvent exposed, as was shown by X-ray analysis (PDB code 2g26) of a 2-ketopiperazine analogue bearing a (1*H*-indol-1-yl)acetate moiety.<sup>58f</sup>

Extensive efforts were conducted at Pfizer to optimize the 2,4-diaminopyrimidine class of DRIs via modification of the P<sub>3</sub><sup>SP</sup> side chain with the aim to modulate the physicochemical profile, CYP450 affinity, metabolic clearance, Caco-2 permeability, and in vivo PK.<sup>38</sup> Inhibitors **34**–**37** (Figure 19) illustrate key examples for an expanded exploration of S<sub>3</sub><sup>SP</sup> binding motifs in combination with variations of the 1,4-benzoxazinone scaffold targeting the S<sub>4</sub> pocket. The persisting challenge to accomplish a proper balance between inhibitory potency and desirable ADME properties within this series will be further discussed in later sections.

The buried human renin S<sub>3</sub><sup>SP</sup> cavity is characterized by high rigidity and hence a conserved van der Waals volume. Multiple X-ray crystal structures of apo-renin and renin-bound non-peptide inhibitors from different classes and bearing a diversity range of hydrophobic vs more polar S<sub>3</sub><sup>SP</sup> binding motifs revealed only minor conformational movements for

the amino acid side chains forming the boundaries of this pocket (Figure 15). Linear small side chains extending by about four to six atoms in length are preferred for optimal interactions with S<sub>3</sub><sup>SP</sup>, in line with its well-defined elongated shape. Terminal H-bond acceptors form a favorable binding interaction with the NH of Tyr<sub>14</sub>, by extruding the ordered water of apo-renin, as illustrated in Figure 15 for **1** and the 2,4-diaminopyrimidine **34**.<sup>38b</sup> The formation of a S<sub>3</sub><sup>SP</sup> bound water-mediated H-bond to Thr<sub>216</sub> has been observed for the *N*-hydroxypropyl analogue of 2-ketopiperazine **48** (Figure 22).<sup>58c</sup> An additional H-bonding opportunity involving Gly<sub>217</sub> at the entrance of the S<sub>3</sub><sup>SP</sup> site has been identified for a terminal methyl carbamate residue.<sup>39</sup> The lack of conformational flexibility of the S<sub>3</sub><sup>SP</sup> cavity explains why sterically more demanding ligands are less tolerated, limiting the scope for structural modifications. Notably, the S<sub>3</sub><sup>SP</sup> channel is present in other human aspartic proteases,<sup>64</sup> which in principle could have implications for the selectivity of DRIs (vide infra).

The discovery of the nonsubstrate S<sub>3</sub><sup>SP</sup> cavity of renin as a targetable ligand binding site has contributed considerably to the recent advancements toward identifying several attractive new DRI chemotypes. The preferred P<sub>3</sub><sup>SP</sup> pharmacophores reported to date, however, contain features such as a relatively high number of rotatable bonds and H-bond acceptors/donors that could limit oral absorption and in vivo metabolic stability or enhance the drug–drug interaction (DDI) potential. This is most evident when they are combined with unfavorable characteristics predominating in the basic pharmacophore of an inhibitor class. On the other hand, the design of potent non-peptide DRIs that are not dependent on interactions with S<sub>3</sub><sup>SP</sup> has been successful. The most prominent example, the GRAB peptidomimetic **52** (Figure 23),<sup>55a</sup> had advanced to clinical trials. Future work will show whether novel class DRIs lacking a P<sub>3</sub><sup>SP</sup> pharmacophore could offer advantages with respect to PK, in vivo efficacy, safety, and tolerability.

### Basic Amine Transition-State Surrogates

The conceptual idea of modifying the dipeptide cleavage site of a peptide substrate sequence and of introducing a basic amino group at this position was reported as early as 1972 by Szelke et al. for the design of DRIs.<sup>20,65</sup> Replacing the scissile Leu-Val dipeptide of a minimal substrate sequence derived from angiotensinogen by a nonhydrolyzable reduced peptide bond isostere ( $\psi$ [CH<sub>2</sub>NH], Chart 1C) generated the potent decapeptide L-prolyl-L-histidyl-L-prolyl-L-phenylalanyl-L-histidyl-L-leucyl- $\psi$ (CH<sub>2</sub>-NH)-L-valyl-L-isoleucyl-L-histidyl-L-lysine (H-142),<sup>66</sup> one of the first DRIs that underwent investigational clinical studies and that was shown to reduce BP and circulating AngI and AngII levels in humans.<sup>67</sup> The geometry of the reduced amide methylene was considered to be a mimic of the tetrahedral transition state for the proposed mechanism of peptide bond hydrolysis.<sup>68</sup> X-ray crystal structures of this and other peptidic inhibitors in complex with fungal aspartic proteases revealed the likely protonated nitrogen atom of the reduced amide to be in H-bond distance to only Asp<sub>215</sub> of the catalytic dyad.<sup>28,44,45</sup>

Hydroxyl-containing dipeptide isosteres such as statine (Sta, Chart 1B)<sup>69</sup> of the pepstatin family of natural aspartic protease inhibitors<sup>34</sup> and the hydroxyethylene isostere (HE, Chart 1A)<sup>20</sup> have subsequently attracted the most attention and emerged as the key paradigm of aspartic protease inhibitor design. These TSAs, considered to resemble the



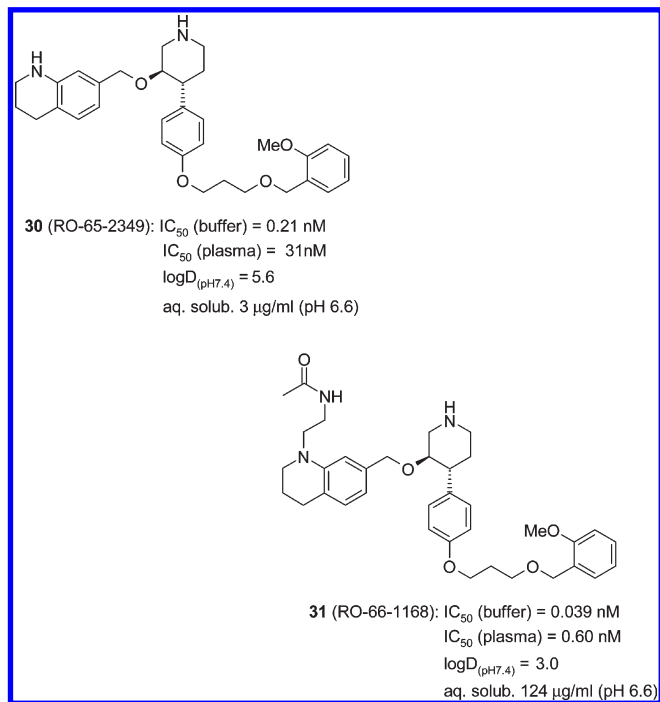


**Figure 16.** 3,4-Piperidine GRAB peptidomimetics:  $P_3^{SP}$  side chain approach.

geometry of the tetrahedral intermediate of enzyme-catalyzed amide bond hydrolysis, are engaged in a close H-bond network between the isostere hydroxyl and the active site Asp<sub>35</sub> and Asp<sub>215</sub> carboxylates. The binding position of the hydroxyl group is very similar to the site occupied by the extruded enzyme-bound “substrate” water molecule of native renin, suggesting at least in part a collected-substrate mechanism of inhibition.<sup>25,27,29</sup> A rich collection of highly effective acyclic hydroxyl-containing TSAs has evolved, and these have found wide application in the design of highly potent peptide-derived peptidomimetic DRIs (2–7, Figure 3).<sup>20–23</sup>

Relatively few attempts were made initially to design basic amine-based TSAs as a concept to overcome the limitations associated with peptide-derived peptidomimetic inhibitors. Several modified TSAs in which the hydroxyl is replaced by an isosteric NH<sub>2</sub> have been investigated anticipating favorable electrostatic interactions between a positively charged ammonium group and the Asp<sub>32</sub>/Asp<sub>215</sub> carboxylates. Incorporation of the aminoethylene (AE) motif (Chart 1E) into angiotensinogen-based peptide sequences has generated potent inhibitors of human renin and notably the first in vivo active inhibitors of rat renin.<sup>70</sup> The AE isostere approach was recently revisited for the design of soluble non-peptide isonicotinamide-derived BACE-1 inhibitors with good intracellular potency.<sup>71</sup> The cocrystal structure of an enzyme-bound analogue<sup>71</sup> has demonstrated the NH<sub>2</sub> to be in a binding position identical to that for the hydroxyl of an octapeptide BACE-1 inhibitor bearing a central hydroxyethylene dipeptide isostere and forming H-bonds to both catalytic aspartates.<sup>41</sup> Peptide-derived analogues containing aminostatine (AmSta, Chart 1F)<sup>72,73</sup> displayed potencies toward rh-renin similar to that of their Sta congeners and superior inhibition of rat renin.<sup>72</sup> Potent 1,2,4-triazolo[4,3-*a*]pyrazine-based inhibitors bearing a P<sub>1</sub> cyclohexyl-modified AmSta have been reported to reduce BP in Na-depleted marmosets when given parenterally.<sup>73</sup> For both Sta and AmSta, the 3(*S*)-configuration was preferred for binding, albeit the

relative potency difference for the (*S*)- vs (*R*)-AmSta isostere was not very pronounced depending on the inhibitor framework. The lack of superior inhibitory affinity for AmSta vs Sta analogues was rationalized by unfavorable partial desolvation energy required for the ammonium group upon binding to the active site.<sup>72c</sup>

The hydroxyethylene (HEA, Chart 1G) isostere has been envisaged to retain the favorable interactions of the tetrahedral carbon bearing the hydroxyl group and to mimic the dipeptide nitrogen atom during substrate hydrolysis. Initially, octapeptide HEA inhibitors of high potency against human renin have been reported.<sup>74</sup> Tripeptide-based ( $P_3$ – $P_1$ )-spanning amino alcohols with a terminal NH<sub>2</sub> at the prime site showed only weak inhibitory affinities.<sup>75</sup> On the other hand, truncation of the nonprime site has generated moderately active  $P_1$ – $P_3'$  tetrapeptides with primary or secondary amines at the P<sub>1</sub> position (AHEA, Chart 1H).<sup>52,53</sup> Interestingly, the reversed (*R*)-configuration is preferred for the AHEA hydroxyl. The cocrystal structure of a (*S*)-AHEA containing inhibitor bound to endothiapepsin has revealed the terminal amine to be in weak contact with Gly<sub>217</sub> and the hydroxyl group to interact with both aspartates. By use of a human renin homology model, optimization of the occupancy of the S<sub>1</sub> pocket was achieved by extending the hydrophobic P<sub>1</sub> residue to afford the potent inhibitor **23** (Figure 9).<sup>52,53</sup>

Incorporation of the HEA dipeptide isostere has been very successful for development of several marketed antiviral HIV-1 protease inhibitors<sup>76</sup> and more recently for the design of BACE-1 inhibitors.<sup>40</sup> Furthermore, tertiary carbinamines have been designed as TS surrogates by simplification of the HEA motif to a primary amine, which in combination with a bioisosteric replacement of the P<sub>1</sub> carboxamide has culminated in a CNS penetrating BACE-1 inhibitor orally active in rhesus monkeys.<sup>42</sup>

The aminohydroxyethylene (AHE, Chart 1D) isostere of **1** and **19**–**22** constitutes an interesting variant of a basic amine central motif. Binding interactions to the catalytic dyad were found to be partially distinct from the H-bond pattern of classical hydroxyethylene (HE) isosteres. When incorporated into peptide-derived peptidomimetics, the HE hydroxyl is positioned symmetrically between Asp<sub>32</sub> and Asp<sub>215</sub> within the plane formed by the two carboxylates. In contrast, the X-ray structures of renin-bound **1** (Figures 4 and 17) and the tetrahydroquinoline analogue **28** revealed the NH<sub>2</sub> to be within binding distance of both the Gly<sub>217</sub> carbonyl and the Asp<sub>215</sub> carboxylate, possibly forming an electrostatic interaction.<sup>51</sup> The AHE isostere hydroxyl formed H-bonds to both aspartates, albeit its binding distance was closer to Asp<sub>32</sub>. The hydroxyl of **20**, an analogue of **1** with modifications at P<sub>1'</sub> and P<sub>2'</sub>, was engaged in a H-bond exclusively to Asp<sub>32</sub>, while the NH<sub>2</sub> was within binding distance to the carbonyl of Gly<sub>217</sub> but not to the aspartates.<sup>49</sup> These markedly altered H-bond patterns of the AHE moiety resulted from a positional shift of the ligands within the enzyme cleft and conformational adaptations of the isostere backbones. In addition, a slight movement of the Asp<sub>215</sub> side chain was observed for **28**.<sup>51</sup> It is conceivable that novel amino alcohol motifs, possibly as part of a cyclic framework, will be designed in the future, leading to novel non-peptide DRIs.

The 4-phenylpiperidine scaffold was discovered by HTS as a novel druglike basic amine TS surrogate, first reported in 1999 by Hoffmann-La Roche.<sup>36</sup> X-ray crystallography of the potent prototype leads **32** and **33** (Figure 18), derived from the weakly active hit (*rac*)-**8** (Figure 5), demonstrated the

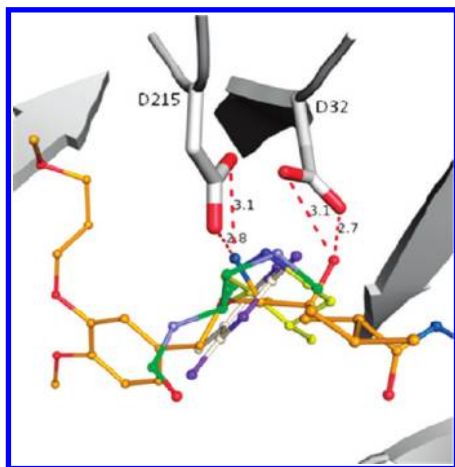


**Figure 17.** Overlay of different chemotype basic amine TS surrogate DRIs interacting with Asp<sub>32</sub> and Asp<sub>215</sub> of the catalytic center. Inhibitors shown are **1** (orange), the GRAB peptidomimetic **33** (yellow), the 2,4-diaminopyrimidine **34** (gray), and the  $\psi$ [CH<sub>2</sub>NH]-reduced isostere **38** (green). For the rh-renin–**1** complex, residues Asp<sub>32</sub>/Asp<sub>215</sub> and a partial ribbon diagram are shown. To better distinguish the inhibitors, portions of their structures were omitted and nitrogen atoms were colored using different shades of blue.

piperidine nitrogen atom to symmetrically occupy the pivotal position between the catalytic Asp<sub>32</sub> and Asp<sub>215</sub> of renin, similar to the hydroxyl group of classical dipeptide TS isosteres (Figure 17).<sup>36a,b</sup> The endocyclic nitrogen is most likely protonated, thus forming two enthalpically favorable electrostatically enforced H-bonds to both aspartates. In retrospect, it is remarkable that this intriguing new principle of efficiently blocking the catalytic site of an aspartic protease had not been uncovered earlier by de novo design considerations.<sup>29</sup> More strikingly, inhibitors **32** and **33** revealed a noncanonical ligand binding mode to a previously not observed conformational active site topography that is fundamentally different from the renin conformation targeted by substrate-derived peptidomimetics (vide infra). The C4 phenyl and substituents extending at its para-position are accommodated by a newly formed large hydrophobic binding site under the flap  $\beta$ -hairpin.<sup>29,36</sup> Furthermore, compared to the peptide-derived framework, the piperidine template provides a very distinct trajectory for topological extensions into the hydrophobic S<sub>3</sub>–S<sub>1</sub> “superpocket”, such as the naphthalene of **32** and **33** tethered at the C3 position.

From a conceptual perspective, piperidine and ring-size congeners have been postulated to constitute enzyme family directed privileged TS surrogates<sup>36a,43</sup> for the design of more druglike inhibitors of human and nonmammalian aspartic proteases. Indeed, novel non-peptide inhibitors based on mono- or bicyclic secondary amine center scaffolds have been described for the antimalarial target plasmepsin-II and -IV,<sup>77</sup> pepsin,<sup>29,78</sup> cathepsin D,<sup>79</sup> and the viral HIV-1 protease.<sup>79</sup> Intriguingly, the successful application of the piperidine core motif for the design of potent BACE-1 inhibitors has not been documented to the best of our knowledge.

Cyclic basic amine TS surrogates constitute highly versatile modules to attach structurally diverse peripheral pharmacophores that could reach into the enzyme specificity pockets flanking the core catalytic center or possibly target other yet uncovered ligand binding topographies of renin. Various piperidine-based inhibitors with distinct substitution patterns, including *trans*-2,5-, *cis*-3,5- and *trans*-3,5-disubstituted piperidines, and structurally diversified ring substitutions have

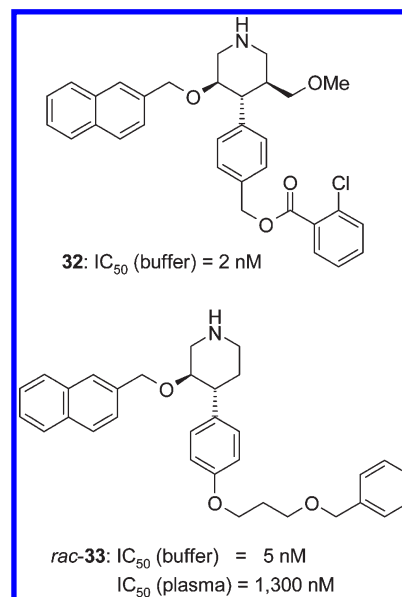


**Figure 18.** Early prototype 4-phenylpiperidine TS surrogate DRIs.

been disclosed in the patent literature.<sup>15</sup> Related 3,4-*trans*-disubstituted pyrrolidines have also been explored by several groups and were claimed to be potent DRIs.<sup>15</sup> This is indicative of the intense interest in the design of such cyclic amine scaffolds and may suggest that the potential of diversely decorating such TS surrogates has not been fully exploited yet. Some evidence, based on the resemblance of common structural features, is emerging indicating that the design of such inhibitors with a binding pose allowing access to the prime site of renin is likely feasible.<sup>15,36</sup>

Predicting the binding interactions of unprecedented inhibitor chemotypes designed by de novo computational modeling relying on the enzyme structure–knowledge base and ligand structure commonalities remains challenging.<sup>13,40b,79</sup> Potent pyrrolidine-based HIV-1 protease inhibitors have been designed by decorating the 3,4-positions with side chains known from substrate-based inhibitors to optimally fill the S<sub>2</sub>–S<sub>2</sub>' recognition sites.<sup>79</sup> X-ray crystallography confirmed the pyrrolidine nitrogen of a prototype analogue to be positioned in binding distance to the catalytic dyad of the enzyme; however, the inhibitor adopted an unexpected binding pose which was distinct from the model on which the design was based. It was characterized by replacement of the structural flap water, a distinct H-bond pattern and altered occupation of the enzyme subsites, as well as a distortion of the geometry of the flap region.<sup>36a,79</sup> Hence, novel TS surrogates may potentially address previously unobserved energetically favored active site conformations, including deviations in the position and geometry of the catalytic aspartates.<sup>40b,51,80</sup>

The 2,4-diaminopyrimidine TS surrogate, discovered at Pfizer from an HTS hit (**10**, Figure 6), forms multiple H-bond interactions within the catalytic center of rh-renin, as shown by the X-ray crystal structures for several analogues of this inhibitor class (e.g., for **11**, **34**, and **36**; Figure 19).<sup>19,38</sup> The pyrimidine NH<sub>2</sub> at C2 is in binding distance to both catalytic Asp<sub>32</sub> and Asp<sub>215</sub>, and the N1 nitrogen interacts with the Asp<sub>32</sub> carboxylate. Interactions of the pyrimidine NH<sub>2</sub> at C4 with Thr<sub>77</sub> and Ser<sub>76</sub> of the  $\beta$ -hairpin and of the N3 nitrogen with an enzyme-bound water contribute to the strong network of H-bonds and a significant gain in binding enthalpy as determined by ITC.<sup>38c</sup> The 2,4-diaminopyrimidine

framework, which is reminiscent of that of 2-aminopyridine and 2-aminoquinoline-based BACE-1 inhibitors,<sup>81</sup> was considered as a highly effective “recognition unit” for renin, and no efforts were made for further optimization of this particular subunit.<sup>38a</sup> Combining the TS surrogate scaffold at its 5-position with 2,2-disubstituted 1,4-benzoxazin-3-ones bearing a P<sub>3</sub><sup>SP</sup> side chain resulted in analogues (**34–37**) exhibiting high potency in vitro. These inhibitors span the S<sub>4</sub>/S<sub>3</sub> and S<sub>1</sub> sites of the extended  $\beta$ -strand binding active site conformation with closed flap conformation.<sup>38</sup> Various challenges to accomplish a proper balance between potency and desirable physicochemical and ADME properties were encountered for this class of DRIs (vide infra).<sup>15,19,38b</sup>

More than 30 years after the pioneering work by Szelke,<sup>65</sup> the incorporation of a  $\psi$ [CH<sub>2</sub>NH]-reduced amide isostere has regained attraction as a viable concept for the design of new chemotype inhibitors of drug target aspartic proteases. First, this approach demonstrated success in generating open-chain and macrocyclic BACE-1 inhibitors with improved solubility, cell-permeability, and intracellular potency.<sup>40b,82</sup>

More recently, Vitae Pharmaceuticals has reported a new class of DRIs, exemplified by **38–40** (Figure 20), that emerged from an iterative structure-based de novo design (vide supra).<sup>39</sup> These inhibitors comprise a rigid 3-substituted *N*-ureapiperidine skeleton bridging the solubilizing basic amine TS surrogate and a substituted P<sub>3</sub> phenyl extended by a flexible P<sub>3</sub><sup>SP</sup> side chain. Inhibitor **38** was confirmed by X-ray

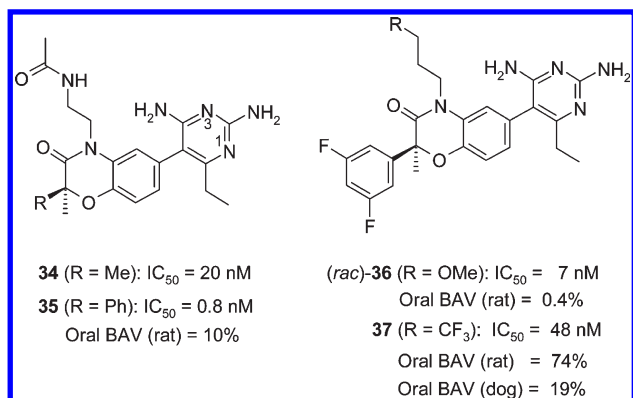


**Figure 19.** 2,4-Diaminopyrimidine-based peptidomimetics (IC<sub>50</sub> in buffer).

to emulate the enzyme-bound  $\beta$ -strand conformation of peptide-derived peptidomimetics, as predicted by modeling. The piperidine scaffold serves to connect the hydrophobic P<sub>1</sub> cyclohexyl and the P<sub>3</sub> meta-Cl-phenyl in a nontopological fashion. The chlorine atom fills an additional hydrophobic subcavity formed by Pro<sub>118</sub>, Phe<sub>119</sub>, Ala<sub>122</sub>, and Phe<sub>124</sub>, resulting in a 15-fold potency increase.<sup>39</sup> Interestingly, the  $\psi$ [CH<sub>2</sub>NH] nitrogen atom is positioned between both catalytic Asp<sub>32</sub> and Asp<sub>215</sub> carboxylates, in contrast to the binding mode observed for other reduced amide isostere inhibitors of aspartic proteases.<sup>28,44,82</sup> The tertiary hydroxyl of **38** was in H-bond distance (2.5 Å) to the  $\gamma$ -oxygen of Ser<sub>219</sub> at the entrance of the S<sub>3</sub><sup>SP</sup> cavity. This again illustrates the key role of Ser<sub>219</sub> for the design of non-peptide DRIs by serving as a potential anchor position for the ligand framework within the enzyme cleft.<sup>13,40b,44,51</sup> Hence, the tertiary phenylcarbinol moiety of **38** constitutes a remarkably compact pharmacophore combining three key structural features important for strong inhibitor binding. Attachment of the P<sub>3</sub><sup>SP</sup> side chain via an ether linkage and removal of the tertiary hydroxyl gave **39** with inferior potency but improved oral bioavailability in rat. Removal of the P<sub>3</sub><sup>SP</sup> ethoxypropoxy chain resulted in a 70-fold IC<sub>50</sub> increase, emphasizing the importance of binding to the S<sub>3</sub><sup>SP</sup> cavity. The methylcarbamate analogue **40** showed a remarkably high potency toward plasma renin. Inhibitors **38** and **40** elicited a sustained BP reduction orally in a double-transgenic rat (dTGR) model.<sup>39</sup>

Further exploration of this chemotype has been a continued effort at Vitae, as judged from the patent literature.<sup>83</sup> Analogue **41** (Figure 20), bearing a regioisomeric modification of the basic amine TS surrogate and a more polar P<sub>1</sub> pyranyl ring, was claimed to be orally efficacious in a dTGR model.<sup>83a</sup> The *N*-carbonylpiperidine and related heterocyclic skeletons have been combined with various classical and novel TSAs.<sup>15</sup> Furthermore, the proximity of the P<sub>3</sub> phenyl and the P<sub>1</sub> cyclohexyl of renin-bound **38** and **40** has suggested growth of the phenyl template into S<sub>1</sub> in a topological fashion,<sup>83b</sup> however, no biological results have been reported to date.

Inhibitors **38–41** are reminiscent of the vicinal-diol TSA inhibitor **42** (CP-265,671) previously reported by Pfizer.<sup>63</sup> The tetrasubstituted cyclohexane provides a rigid vector for the phenethyl chain to reach into S<sub>3</sub> and for the ethyl to fill the S<sub>2</sub> pocket. The tertiary hydroxyl was incorporated to mimic the P<sub>3</sub>/P<sub>2</sub> carbonyl of a peptidic inhibitor for Ser<sub>219</sub>

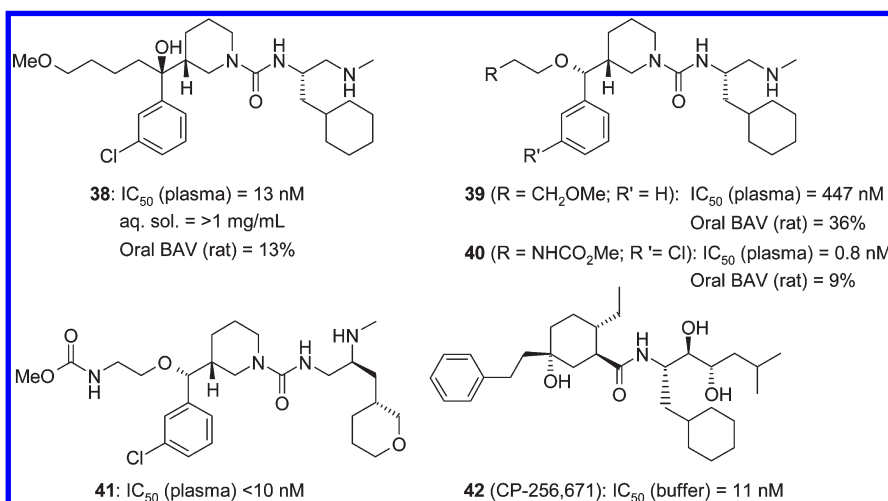


**Figure 20.** Non-peptide peptidomimetic  $\psi$ [CH<sub>2</sub>NH]-reduced amide isosteres.



H-bonding.<sup>44,63</sup> Such compounds were abandoned because of low solubility, weak potency in plasma, and synthetic complexity but laid the foundation for the design of P<sub>3</sub><sup>SP</sup>-tethered inhibitors like **27** (Figure 13).<sup>63</sup>

A diverse array of novel cyclic or acyclic basic “warheads” have been reported to potently inhibit BACE-1<sup>40</sup> and other aspartic proteases.<sup>84</sup> Some of these TS surrogates were utilized for the design of DRIs, such as *N*-acylamidines and *N*-acylguanidines,<sup>15</sup> however, no biological results were disclosed to date. Non-peptide inhibitors displaying a nonclassical binding mode without engaging in direct interactions to the catalytic dyad were identified for BACE-1<sup>64,80</sup> and plasmepsin-II (PM-II).<sup>84</sup> X-ray crystallography revealed a single water-mediated H-bonding between the two aspartates and either an amide NH, as for the BACE-1 ligand,<sup>64</sup> or the basic nitrogen of an *N*-alkylpiperidine as for the PM-II inhibitor.<sup>84</sup> Notably, the water molecules were in a position similar to that of the “catalytic” water of the native enzymes. Spiropiperidine-iminohydantoin BACE-1 inhibitors were found to interact with Asp<sub>32</sub> and Asp<sub>228</sub> via two bridging water molecules, forming a complex H-bonding network involving the *N*-benzylated piperidine and the exocyclic imino nitrogen atom.<sup>80</sup> Remarkably, BACE-1 adopted a different active site conformational topology by forming a new binding site under the flap  $\beta$ -hairpin.<sup>80</sup> While such atypical inhibitors of renin have not been reported, the possibility for a water-mediated mechanism to block the catalytic center may in principle exist also for renin.

### GRAB Peptidomimetic Class of DRIs

The discovery of 3-substituted 4-arylpiperidines as a unique class of potent DRIs, bearing several key structural features unrelated to peptide-derived TSA inhibitors, constitutes a major breakthrough.<sup>36</sup> As already discussed, the finding that the center piperidine acts as a TS surrogate by interacting with the catalytic aspartates has created a new paradigm for the design of non-peptide inhibitors of renin and other aspartic proteases.<sup>36a,43</sup> Most intriguingly, these inhibitors bind to a renin active site topography that is very different from the enzyme conformation targeted by substrate-derived peptidomimetics.

Inhibitors **31** (Figure 16), **43** (RO-66-7219), and **44** (RO-66-1132, Figure 21) represent advanced potent and selective analogues of this new class of inhibitors,<sup>36d</sup> which were derived from the HTS hit *rac*-**8** (Figure 5) via further optimization of the prototype leads **32** and **33** (Figure 18).<sup>36a-c</sup> The bicyclic pharmacophores attached to the piperidine C3 span and partially fill the hydrophobic S<sub>3</sub>-S<sub>1</sub> hot spot and can be further substituted by residues targeting the nonsubstrate S<sub>3</sub><sup>SP</sup> cavity. The lipophilic piperidine C4 phenyl and its extension at the C4' position occupy a large hydrophobic cleft located underneath the S<sub>3</sub>-S<sub>1</sub> pocket at the core of the N-terminal domain, as unveiled by X-ray crystallography of **32** and **33** bound to rh-renin (Figure 24). This cavity results from major conformational movements of the flap adopting a more open conformation, which specifically involve concerted side chain rotations of the Tyr<sub>75</sub>, Leu<sub>73</sub>, and Trp<sub>39</sub> residues. As a consequence, the H-bond between the phenolic OH of Tyr<sub>75</sub> and the indole NH of Trp<sub>39</sub> is disrupted, and the reorientation of the Trp<sub>39</sub> indolylmethyl opens up a buried “deep flap pocket”. Interestingly, this movement of Trp<sub>39</sub> is not observed for the weak affinity inhibitors **8** and **9**, lacking the C4' extension.<sup>36a,b</sup>

The piperidine C4 phenyl of **32** and **33** occupies, in a similar planar orientation, the space of the “gate-keeper” Tyr<sub>75</sub> side

chain<sup>29</sup> and thus reconstitutes the carboxy-terminal boundary of the S<sub>1</sub> pocket by forming an aromatic cluster of edge-to-face interactions with Tyr<sub>75</sub> and Phe<sub>112</sub>.<sup>36a,b</sup> The lipophilic C4' flexible spacer spans the position previously occupied by the Trp<sub>39</sub> indole, while the terminal phenyl moiety is accommodated by an extension of the deep flap cavity generated by additional subtle local rearrangements, particularly by Met<sub>107</sub> (Figure 24). Initial lead optimization included attempts to rigidify the conformational flexibility of the polyether side chain by incorporation of cyclic constraints; however, the ortho-methoxy-benzyloxypropoxy residue (**30**, **31**, **43**, **44**) was found to be optimal for high affinity interactions to the flap binding topography.<sup>36b</sup> The assisting role of the inhibitor C4 phenyl in stabilizing the enzyme complex by replacing the Tyr<sub>75</sub> aromatic ring has inspired to coin this class of DRIs as “group replacement assisted binding” or GRAB peptidomimetics.<sup>29</sup>

The explicitly hydrophobic nature of the early GRAB peptidomimetics is mainly attributed to the large lipophilic (P<sub>3</sub>-P<sub>1</sub>)-scaffold and the C4' extended side chain, both being key contributors to high affinity interactions to renin. Various SAR strategies have been explored to improve the limitations of their physicochemical properties, recognized as the major culprit for significant plasma renin IC<sub>50</sub> shifts, affinity to cytochrome P450 isozymes, and high metabolic clearance. Modifications of the core pharmacophore by replacing either the piperidine C4 phenyl or the side chain terminal phenyl by hydrophilic heteroaryl groups resulted mostly in significant in vitro potency loss.<sup>36b,c</sup> Attachment of solubilizing residues, which could either bind to the renin active site or alternatively point out into bulk solvent was found to be more promising.<sup>36c,d</sup> Inhibitor **31** with a hydrophilic extension into the nonsubstrate S<sub>3</sub><sup>SP</sup> cavity is the most potent GRAB peptidomimetic toward plasma renin reported to date. The piperidine C5 position proved to be amenable for the introduction of polar substituents with up to two hydroxyl and/or alkoxy groups. The methoxymethyl of **32** was shown by X-ray to point toward the reoriented Tyr<sub>75</sub> of the flap, while the C(4)-C(5)-*trans*-configured **43** and **44** potentially extend into the S<sub>2</sub>' pocket. This has generated less hydrophobic analogues, albeit with limited impact on the in vitro potency against plasma renin (cf. **30**, Figure 16).<sup>36c</sup> The preclinical candidate **44** (Figure 21) demonstrated a superior PK profile and displayed a potent sustained BP reduction in dTGR and in monkeys.<sup>36d,e,85b</sup>

This first generation of *trans*-3,4-piperidine GRAB peptidomimetics has inspired other investigators to further exploit this chemotype with the aim to improve the in vitro and in vivo ADME profile. Pfizer has described initially 3-amino-4-arylpiperidines with preferred relative *cis*-configuration, by replacing the ether linkage at the piperidine C3 with a secondary amine spacer.<sup>58a</sup> The most potent analogue, *rac*-**45** (Figure 22), was shown by X-ray crystallography to bind to renin in a similar fashion compared to the 3,4-*trans*-disubstituted alkoxyarylpiperidines but with an additional H-bond formed between Gly<sub>217</sub> and the exocyclic nitrogen atom. Further modifications of the center scaffold were subsequently described by eliminating one chirality center, leading to piperazine and 2-ketopiperazine analogues **46**–**50** with a “reversed” ether linkage.<sup>58b-f</sup> Ketopiperazine **46** showed moderate in vitro activity and short-lasting oral BP lowering effects in hypertensive double-transgenic mice.<sup>58b,c</sup> The 3,4-dihydro-2*H*-quinoline derivatives **47**<sup>58c</sup> and **48**<sup>58d</sup> bearing a P<sub>3</sub><sup>SP</sup> *N*-acetylaminoethyl side chain revealed markedly enhanced in vitro potencies. Further variations of the (P<sub>3</sub>-P<sub>1</sub>)-bicyclic

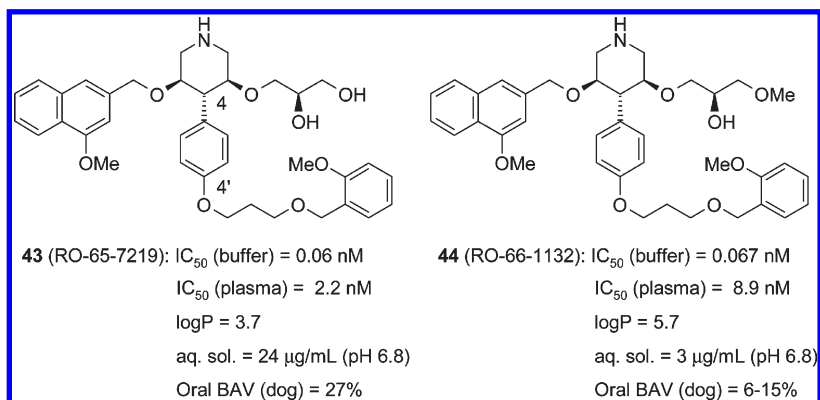


**Figure 21.** Advanced 3,4-piperidine-based GRAB peptidomimetics.

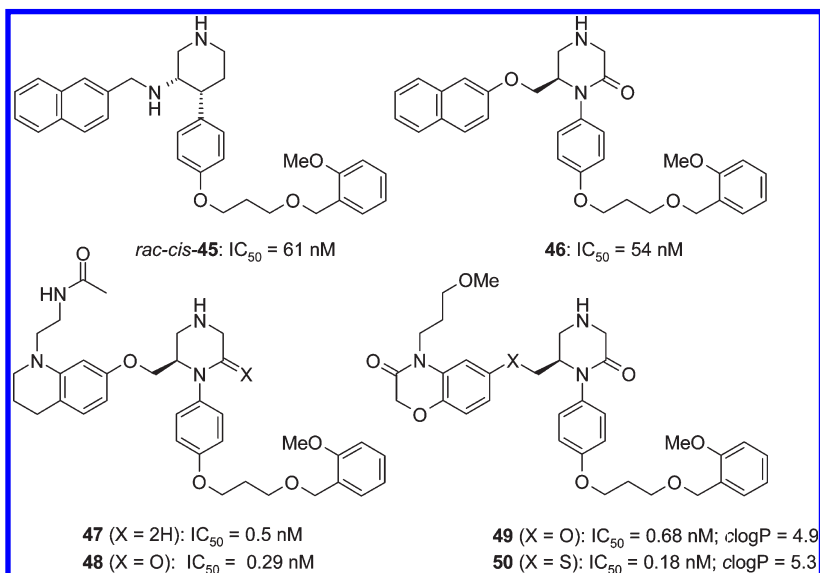


**Figure 22.** Piperidine-derived GRAB peptidomimetic inhibitors ( $IC_{50}$  in buffer).

moiety afforded the potent 1,4-benzoxazin-3-ones **49** and **50**.<sup>58e</sup> The lipophilicity of these inhibitors was reduced but remained noncompliant with Lipinski's rule,<sup>86</sup> suggesting a marked potency drop toward plasma renin to be very likely. Furthermore, most of the potent inhibitors of these series suffered from high affinities to CYP450 isozymes.<sup>19,58</sup> Modifications of the terminal ortho-methoxyphenyl and the propylenedioxy spacer were not envisaged, as this pharmacophore was considered to be optimal for binding into the flap pocket.<sup>58e</sup>

Actelion has reported a novel class of GRAB peptidomimetics based on a 3,9-diazabicyclo[3.3.1]nonene center scaffold (**51** and **52**, Figure 23), as well as modified bicyclic bridged templates.<sup>55</sup> Furthermore, related monocyclic tetrahydropyridine analogues were disclosed, representing the first achiral and in vitro potent DRIs known to date.<sup>55c</sup> Optimized inhibitors **51** and **52** were identified from a structure-based design approach involving multiparallel chemistry. Both analogues were potent toward rh-renin but showed a significant  $\sim 100$ -fold  $IC_{50}$  shift leading to moderate inhibitory affinities against plasma renin in vitro. This was explained by high plasma protein binding ( $> 99\%$  for **52**) in human, dog, and monkey.<sup>55a</sup> The absolute configuration of the dibasic bicyclic core determines which of the two secondary ring nitrogen atoms interacts with the catalytic aspartates by forming H-bonds and expelling the enzyme-bound water, as shown by X-ray for

renin-bound **51** and its equipotent ( $-$ )-(1*S*,5*R*)-enantiomer. The second nitrogen in turn is exposed toward bulk water and has served as anchor point for solubilizing groups, albeit none of the resulting inhibitors had a superior profile. This class of inhibitors comprise a benzylated *N*-cyclopropylcarboxamide as a novel  $P_3$ - $P_1$  motif (cf. Figure 11) providing high potencies toward plasma renin. Emphasis on rigidifying the conformational flexibility of the side chain in para of the 4-phenyl substituent led to the identification of the propyloxy (as in **51**) and 1,2-ethylenedioxy (as in **52**) spacers. A strained 2,6-substitution pattern with at least one ortho-chloro atom at the terminal phenyl, considered as a potential soft spot for metabolism, provided inhibitors with superior potencies. Inhibitors **51** and **52** were well absorbed in Wistar rats and proved to be orally efficacious in a dTGR model,<sup>55a</sup> as well as in salt-restricted, furosemide pretreated rhesus monkeys.<sup>55b</sup> The most preferred analogue, **52**, was progressed to phase IIa clinical trials.

The class of GRAB peptidomimetics is continuing to attract interest, as is implied by the large number of recent patent claims.<sup>15</sup> Design efforts are further exploring modifications of the flap binding motif in combination with new ( $P_3$ - $P_1$ )-scaffolds and central piperidine replacements, including new substitution patterns like 2,4,5-trisubstituted piperidines. Design concepts that address the Trp<sub>39</sub> flap pocket pharmacophore aim to reduce the number of rotatable bonds and to

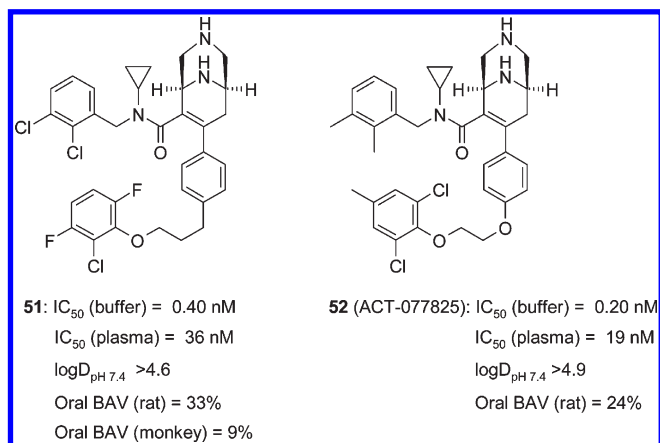


**Figure 23.** Second generation GRAB peptidomimetic DRIs.

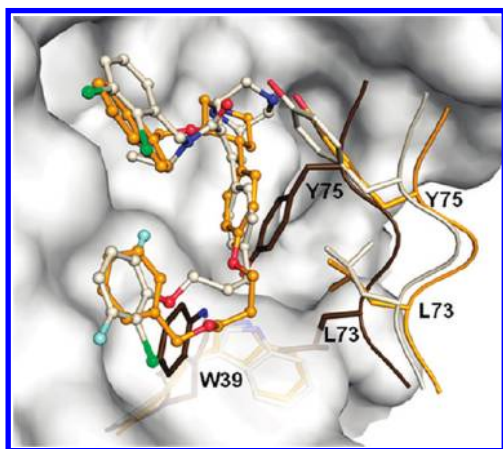


**Figure 24.** Superposition of X-ray structures of rh-renin complexed with GRAB peptidomimetics **33** (orange) and **51** (gray) binding to the open flap conformational topography. Partial peptide backbones and the side chains for Trp<sub>39</sub>, Leu<sub>73</sub>, and Tyr<sub>75</sub> are shown for the two complexes using the same color code. The corresponding portions of the rh-renin-1 complex are overlaid in brown. For the complex with **51** the portion of the active site behind the inhibitor is shown as a transparent surface.

replace the lipophilic C4' portion by small polar side chains lacking the terminal aryl residue. Since more detailed biological data are currently not available, predictions of whether these approaches are likely to succeed in providing clinical candidates would be premature.

Notably, exploration of potent GRAB peptidomimetics, as reported to date, has been restricted to hydrophobic side chains of variable conformational flexibility that are exclusively attached to the para-position of the C4 phenyl binding into the Tyr<sub>75</sub> pocket. Not surprisingly, analysis of X-ray crystal structures showed overall similar van der Waals contacts for such inhibitors to the open flap conformational topography and a conserved alignment of the side chains of Tyr<sub>75</sub>, Leu<sub>73</sub>, and Trp<sub>39</sub> in the renin-inhibitor complexes (Figure 24).<sup>36,55a</sup> The 1,2-ethylenedioxy spacer of **52** adopted a more compact gauche conformation compared to the propyloxy spacer of **51**. Both terminal aryl groups are similarly positioned in the hydrophobic Trp<sub>37</sub> flap pocket, albeit in the case of **52** the phenyl is not entirely filling out the cavity. In both cases, the ortho-chlorine occupied a hydrophobic indent, while the second ortho-halogen pointed straight toward the *N*-cyclopropyl in the S<sub>1</sub> site. The SAR of GRAB peptidomimetic inhibitors of plasmepsin II was shown to correlate with the degree to which the narrow

well-defined flap pocket is filled by flexible ligand alkyl chains, in line with the principle of ideal volume occupancy for host-guest recognition.<sup>77a</sup>

The conformational mobility of the flap  $\beta$ -hairpin characterized by major spatial movements is part of its critical function to open and close the catalytic site, thereby enabling ligand binding and release. The disruption of flap domain H-bonds, such as between Tyr<sub>75</sub> and Trp<sub>39</sub>, is considered to be part of this dynamic process and hence to be at low energy cost involving low barrier conformational changes.<sup>29,36a</sup> It has been suggested that distinct pre-existing conformations of the renin active site are stabilized upon binding of complementary ligand structures rather than by an induced-fit adaptation binding mechanism.<sup>29,87</sup> Energetically favorable conformational ensembles with topographies distinct from that stabilized by known GRAB peptidomimetics may exist, which could be exploited for inhibitor design. Notably, 3,4-piperidine-based inhibitors that comprise a meta-extended C4 phenyl or more space-filling meta-biphenyl, benzothiophene, and *N*-substituted indole moieties at the C4 position of the TS surrogate have been claimed as novel DRIs.<sup>15</sup> Inspection by modeling would suggest that these residues could not be readily accommodated by the small Tyr<sub>75</sub> pocket or may extend into the Trp<sub>37</sub> deep flap pocket in a different manner as in the case of GRAB peptidomimetics bearing a para-phenyl substitution. Hence, distinct conformations of the flap region that could be stabilized by structurally distinct flap-binding pharmacophores are indeed likely to be accessible.

## S<sub>2</sub> Specificity Pocket

Structural modification of the P<sub>2</sub> portion in peptide-derived peptidomimetics has played an important role for optimizing their potency and selectivity, as well as for designing analogues with improved pharmaceutical properties.<sup>21–23</sup> The large and bifurcated hydrophobic S<sub>2</sub> pocket of renin (Ser<sub>76</sub>, Thr<sub>77</sub>, Tyr<sub>220</sub>, Phe<sub>242</sub>, and His<sub>290</sub>-Met<sub>292</sub>), like that of related aspartic proteases, can accommodate a variety of both hydrophobic and polar pharmacophores and thus allows considerable variations in enzyme-ligand interactions. Indeed, a number of peptide-derived DRIs were shown by X-ray crystallography of their complexes to endothiapepsin to adopt a range of distinct P<sub>2</sub> side chain orientations as a consequence of the permissiveness of the S<sub>2</sub> pocket.<sup>28,44,45</sup> The fact that P<sub>2</sub> side chain conformations are not tightly constrained within this binding site has rendered accurate modeling predictions of ligand-enzyme interactions to S<sub>2</sub> rather difficult.<sup>13,38c</sup> The topography of both the S<sub>2</sub> and S<sub>1</sub>' pockets forming a spacious open subsite has been exploited for the design of potent macrocyclic DRIs.<sup>23a</sup>

Most non-peptide classes of DRIs reported to date, including piperidine-based GRAB peptidomimetics (**43**, **44**, and **46–52**), as well as the (S<sub>3</sub>-S<sub>1</sub>)-topological peptidomimetics **1**, **19–22**, are not engaged in binding interactions to the S<sub>2</sub> specificity site. Topographic characteristics and promiscuity have suggested a limited attractiveness for explicitly targeting the S<sub>2</sub> pocket by rational de novo design of DRIs.<sup>13,39</sup> Such considerations, among other key aspects (vide supra), have formed the initial conceptual idea toward the design of (S<sub>3</sub>-S<sub>1</sub>)-topological peptidomimetic inhibitors that eventually led to the discovery of **1**.<sup>12,13,49</sup> Noteworthy, targeting optimized interactions to the S<sub>2</sub> pocket has been seminal in identifying potent inhibitors of BACE-1 with high selectivity against other human aspartic proteases.<sup>40</sup>



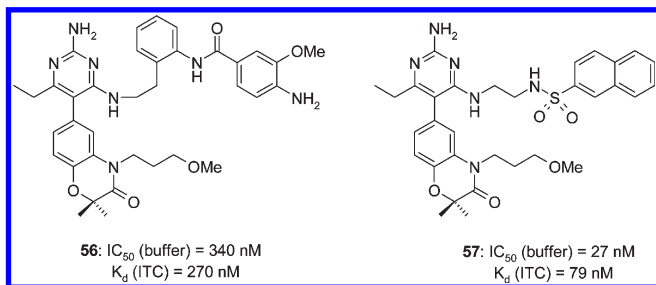


**Figure 25.** Non-peptide peptidomimetic DRIs binding to the  $S_2$  pocket.

Analogues of 5-aryl-2,4-diaminopyrimidines (**34–37**, Figure 19) were shown by X-ray to be positioned with their 4-NH<sub>2</sub> group in close distance to Thr<sub>77</sub> and Ser<sub>76</sub> at the entry of the large  $S_2$  pocket.<sup>38</sup> This suggested extending this position into the  $S_2$  cavity as a strategy for lead optimization. A fragment-based NMR “second-site screening approach” using the 4-aminomethyl analogue of **12** (Figure 6) as the first-site ligand probe in combination with in silico GOLD docking to assess fragments as potential  $S_2$  binders identified the (4-amino-3-methoxyphenyl)benzamide as single hit from a small library. Saturated transfer difference NMR via interligand NOEs in the presence of renin demonstrated this fragment to be an active site coligand.<sup>38c,d</sup> Modeling suggested tethering of the ortho-phenyl position of the fragment to the 4-NH<sub>2</sub> of **12** by an ethylene spacer. Cocrystallization of the resulting inhibitor **56** (Figure 25) with rh-renin confirmed the attached moiety to occupy a significant portion of the  $S_2$  pocket.<sup>38d</sup> However, **56** was found to be 4-fold less potent compared to its direct 4-NH<sub>2</sub> analogue.<sup>38b</sup> ITC data suggested a substantial loss of binding enthalpy for **56**, which is largely compensated by a gain in binding entropy. This was attributed to flexing of the protein to accommodate the extension into  $S_2$  and removal of ordered water from the pocket.<sup>38c</sup>

Guided by both X-ray and thermodynamics considerations, subsequent modifications of the spacer length and incorporation of functional groups predicted to interact more properly with the  $S_2$  polar surface led to inhibitor **57** with improved enzyme inhibition and binding affinity (by ITC). Interestingly, the cocrystal structure of renin-bound **57** revealed two different orientations of the naphthalene extending into the  $S_2$  pocket and alternative H-bonding patterns for the polar sulfonamide functionality at the bottom of this site. Furthermore, a portion of the renin active site determined by the peptide loop of residues Lys<sub>238</sub>–Tyr<sub>244</sub> adopted both a closed and a more open conformation, depending on the orientation of the ligand naphthalene.<sup>38c</sup>

ITC and X-ray data for **56** and **57** and related analogues suggested that binding to the large hydrophobic  $S_2$  pocket is both enthalpy and entropy driven. A proper balance between nonpolar and polar interactions via correctly positioned functional groups that could compensate for displacement of ordered water molecules will likely be required for optimizing the interactions to the  $S_2$  cavity.<sup>38c</sup> Noteworthy, it has been suggested that improving binding affinity is more difficult to achieve for inhibitors with entropically driven interactions, while inhibitors exhibiting favorable binding enthalpy may have a better potential for lead optimization.<sup>88</sup>

### $S_1$ – $S_2'$ Prime Site Specificity Pockets

Optimizing the interactions to the  $S_1'$  and  $S_2'$  recognition sites has played an important role for the initial development

of peptide-based peptidomimetic DRIs. The introduction of polar or basic  $P_2'$  moieties has provided less lipophilic and more soluble analogues with improved PK properties.<sup>23a</sup> Dipeptide isostere TSAs with a truncated C-terminal portion have been designed to seek second generation DRIs with reduced molecular size (Figure 3),<sup>20–23</sup> and as a consequence, targeting the prime site became less attractive. In contrast, optimal interactions to both the  $S_1'$  and  $S_2'$  pockets were found to be critical for tight binding affinity of the ( $S_3$ – $S_1$ )–topological class of TSAs such as **1** and **19–22**.<sup>13</sup> Truncated analogues with an optimized ( $P_3$ – $P_1$ )–pharmacophore, but lacking the prime-site portion, were only moderately potent. The  $\alpha,\alpha$ -diMe  $\beta$ -alanine carboxamide of **1** constitutes a unique  $P_2'$  motif contributing significantly to the picomolar inhibition of plasma renin. Its terminal CONH<sub>2</sub> group forms a network of direct and water-mediated H-bonds to  $S_2'$  residues including Arg<sub>74</sub> of the flap.<sup>12,51</sup>

More recent design approaches toward non-peptide DRIs have centered around the  $S_3$ – $S_1$  hydrophobic hot spot, the nonsubstrate  $S_3^{sp}$  cavity, and the flap  $\beta$ -hairpin binding sites. The prime-site portion of the active site has received much less attention and was even excluded conceptually for de novo inhibitor design.<sup>39</sup> Piperidine-based GRAB peptidomimetics bearing polar residues at the piperidine C5 position, like **43** and **44** (Figure 21) potentially extend into the  $S_2'$  pocket. Such modifications aimed to reduce the high lipophilicity of this class of DRIs.<sup>36c,d</sup>

The primarily hydrophobic  $S_1'$  site and the more polar  $S_2'$  pocket are flanked by Ser<sub>76</sub> and Leu<sub>73</sub>–Arg<sub>74</sub>–Tyr<sub>75</sub>, respectively, of the flexible flap  $\beta$ -hairpin in the inhibitor-bound closed conformation. The known dynamic flexibility of the flap region, and possibly other regions close to  $S_2'$ , would suggest that distinct conformational ensembles of the renin prime site may well exist. Such alternative binding topographies could possibly be exploited for the design of new high-affinity pharmacophores. Interestingly, the renin  $S_2'$  subsite was described recently as a hot spot for binding of fragment-ligand probes using a computational approach based on the FTMAP algorithm for protein mapping.<sup>89</sup> Hence, the potential of the renin  $S_2'$  pocket of the renin active site may not have been fully recognized, albeit emerging evidence suggests that targeting this site has gained more interest recently.<sup>15</sup> The more hydrophilic nature of the  $S_2'$  pocket may offer attractive opportunities for modulating ADME properties or to address off-target selectivity.

### Renin Selectivity Design

The gastric pepsins A and C, the lysosomal cathepsin D, as well as cathepsin E, are key off-targets within the human aspartic protease family for any clinical DRI.<sup>90,91</sup> High selectivity of a DRI against related human aspartic proteases including BACE-1 and -2 is generally considered as an essential criterion in view of a safe, life-long treatment for cardiovascular diseases such as hypertension. The significance of partial inhibition of these enzymes for clinical tolerability and safety, however, has not yet been fully elucidated. Successful design strategies to generate highly selective inhibitors of renin have relied mainly on structural differences of the substrate recognition sites within the enzyme family.<sup>30,91</sup> The emergence of renin active site topographies diverging from the  $\beta$ -strand binding catalytic cleft conformation and the discovery of diverse chemotype DRIs deserve further considerations with respect to enzyme selectivity design.

Piperidine-based TS surrogates have been demonstrated to serve as aspartic protease family specific warheads,<sup>43,78,79</sup>

which may imply a potential risk in achieving adequate selectivity within this protease family for DRIs comprising these and related structural features. Very limited in vitro structure–selectivity relationship data are currently available for newly disclosed potent non-peptide peptidomimetic DRIs.<sup>12</sup> For example, the 3,9-diazabicyclononene **51** (Figure 23) was reported to be a weak inhibitor of cathepsins D and E ( $IC_{50}$  = 2.7 and 8.1  $\mu$ M, respectively).<sup>55b</sup> The 3,4-bis(aminomethyl)pyrrolidine has served as basic center scaffold to generate a submicromolar cathepsin D inhibitor and was predicted by modeling to bind into the  $S_2$ – $S_2'$  specificity pockets.<sup>79</sup> On the other hand, the 2,4-diaminopyrimidine **12** (Figure 6) and related analogues with moderate affinity to renin were devoid of in vitro activity against cathepsins D and E and pepsin up to 100  $\mu$ M.<sup>38a</sup> Also, prototype alkylamines **38** and **40** (Figure 20) of a novel class of  $S_3^{SP}$ -binding DRIs, showed greater than 1000-fold selectivity over pepsin, BACE-1, and cathepsins D and E.<sup>39</sup>

Competitive inhibition of porcine pepsin by a 3-alkoxy-4-arylpiperidine derivative structurally related to **8** (Figure 5) was shown to be pH-dependent with maximal inhibition at pH 5 ( $IC_{50}$  = 1.5  $\mu$ M) and complete loss of in vitro activity at lower pH values.<sup>78</sup> Steady-state enzyme-kinetic studies demonstrated active site-directed inhibition of pepsin and significant conformational changes and perturbation of the ionization state of the catalytic aspartates upon binding of the ligand.<sup>78</sup> Reduced binding affinities under physiologically relevant conditions toward human aspartic proteases that function at low pH range could be a contributing factor leading to renin selectivity for basic TS surrogate classes of non-peptide DRIs.

The nonsubstrate  $S_3^{SP}$  binding cavity (vide supra) is not unique to renin within the human aspartic protease family. Inspection of the known X-ray crystal structures of human pepsin A (PDB code 1qrp), cathepsin D (PDB code 1lyb), and cathepsin E (PDB code 1tzs) revealed the presence of a conserved  $S_3^{SP}$  channel of similar size and topography compared to renin.<sup>64</sup> Interestingly, an aspartic acid (Asp<sub>303</sub> in pepsin A; Asp<sub>323</sub> in cathepsin D; Asp<sub>319</sub> in cathepsin E) is located at the bottom of this channel in all cases, replacing the smaller hydrophobic Ala<sub>303</sub> of renin. This suggests that the design of enzyme-specific ligand binding to the  $S_3^{SP}$  subsite is feasible and that such interactions could significantly contribute to the selectivity toward renin. However, the specific contributions of binding into the renin  $S_3^{SP}$  subsite to the selectivity of reported DRIs against other human aspartic proteases and to human vs nonprimate renin specificity appear less well-defined. Functional groups that could form H-bond or salt bridge interactions to Asp<sub>323</sub>/Asp<sub>319</sub> of the  $S_3^{SP}$  site of cathepsins D and E, respectively, may conceivably reduce renin selectivity. Conversely, the design of selective cathepsin D, E inhibitors by target-specific optimization of interactions to the nonsubstrate  $S_3^{SP}$  site could be explored. To our knowledge, aspects of structure–selectivity relationship related to the conserved  $S_3^{SP}$  channel of human aspartic proteases based on enzyme–inhibitor complex structures have not been studied in more detail.

### Preclinical ADME Properties and Safety Profiling

A key driving force to identify new scaffolds potentially leading to orally efficacious DRIs was the desire to overcome the generally poor PK properties of most substrate-based peptidomimetics. The oral bioavailability of **1** was low to mod-

erate in rat, dog, and marmoset (2.4%, 32%, and 16–30%), with the rat predicting best the human bioavailability.<sup>11–14</sup> Preclinical oral bioavailability data reported for representatives from different new classes of non-peptide DRIs in various species often ranged from low to moderate, albeit significantly higher oral bioavailability has been achieved in some cases.<sup>38b,55c</sup> The 3,9-diazabicyclo[3.3.1]nonene GRAB peptidomimetic **51** (Figure 23) showed bioavailability of 33%, 36%, and 9% in Wistar rat, dog, and rhesus monkey, respectively, with the elimination half-life being shortest in rat (5.5 h) and more sustained in dog and primates (10–11 h).<sup>55b</sup> The close analogue **52** displayed similar PK properties with sustained oral absorption in Wistar rats (24%,  $t_{1/2}$  = 6.6 h,  $t_{max}$  = 10 h).<sup>55a</sup> The oral bioavailability of tetrahydropyridine analogues of **51** and **52**, disclosed by the same investigators, reached as high as 70% in rats.<sup>55c</sup> Oral bioavailability of the alkylamine inhibitor **38** (Figure 20) was modest in cynomolgus monkey (17%) and in rat (13%) because of incomplete GI absorption and high clearance but was significantly higher in dog (38%), with long terminal half-lives of ~16 h in monkey and dog.<sup>39a</sup> All these reports hint at significant efforts invested in improving PK properties and highlight the difficulties in achieving this goal while maintaining other desired properties including potency. It remains to be seen whether any clinical candidate of such novel DRIs will exhibit acceptable ADME properties in humans.

The design of high-affinity DRIs exhibiting optimal ADME characteristics has become more demanding in line with the general paradigm shift in modern drug discovery that requires early evaluation and rigorous optimization of multiple additional parameters that predict, for example, the potential for toxicity.<sup>92</sup> High selectivity against antitargets including proteases, other enzyme classes as well as receptors, low potential for drug–drug interactions, and an acceptable in vitro/in vivo safety profile are considered to be key attributes of successful novel DRIs.

Many of the novel chemotype DRIs reported to date are characterized by relatively high molecular weight (MW > 500) and high lipophilicity ( $\log P \geq 5$ ). A rather large contact surface area within the renin active site appears to be generally required to achieve maximal ligand binding efficacy for each inhibitor class, independent of the targeted enzyme conformation and recognition sites. Unfavorable physicochemical properties such as low aqueous solubility and lipophilicity may affect the in vitro potency against human plasma renin and hence could limit the in vivo efficacy of DRIs at reasonable dose levels.<sup>36,38,49,55</sup> Lipophilicity, molecular size, and H-bonding potential determine the ADME space predicting favorable PK properties, i.e., the potential to be delivered by the oral route.<sup>93</sup> Furthermore, high lipophilicity of compounds has recently been shown to be associated with increased promiscuity, i.e., a higher propensity to bind to multiple targets,<sup>94</sup> and with an increased likelihood of adverse or toxic events in vivo.<sup>95</sup>

A number of inhibitors from different new classes of non-peptide DRIs showed a significant in vitro affinity to cytochrome P450 isozymes, indicating a potential risk for high P450-mediated metabolic clearance and for in vivo drug–drug interactions (DDI). These include aminoarylpiperidines (e.g., **45**; Figure 22),<sup>58a</sup> 2-ketopiperazines (e.g., **47**; Figure 22),<sup>58e</sup> and 5-aryl-2,4-diaminopyrimidines (e.g., **36**; Figure 19).<sup>38b</sup> The in vitro metabolism of the *N*-alkyl-1,2,3,4-tetrahydroquinoline moiety, which has been incorporated as a common  $P_3$ – $P_1$  pharmacophore into several series of potent inhibitors by

human liver microsomes, has shown this moiety to be prone to metabolic aromatization.<sup>58g</sup> Compound **43** and the preclinical candidate **44** (Figure 21), both 3-arylmethoxy-4-arylpiperidine GRAB peptidomimetics, showed only moderate oral bioavailability (27% and 6–15%, respectively) in dogs due to extensive CYP3A4 mediated metabolism and/or P-glycoprotein-mediated efflux.<sup>36c</sup> The more soluble P<sub>3</sub><sup>SP</sup>-substituted analogue **31** (Figure 16) was reported to have significantly inferior PK properties.<sup>36d</sup> The GRAB peptidomimetic **51** showed only weak CYP3A4 affinity (IC<sub>50</sub> > 10 μM). However, analogues in which one nitrogen of the center scaffold was replaced by nonpolar groups proved to be rather potent CYP3A4 inhibitors, and inhibition of CYP3A4 emerged as a selection criteria within this series.<sup>55c</sup> Inhibitor **51** revealed a potential for activation to reactive metabolites and for protein adduct formation in vitro in rat and human liver microsomes. Such effects were apparently less significant for the related clinical phase IIa inhibitor **52**.<sup>55a</sup>

Major hurdles have been encountered by Pfizer during lead optimization of the 2,4-diaminopyrimidine class of DRIs **34–37** (Figure 19) in an attempt to accomplish a favorable inhibitor profile for in vitro potency, CYP450 affinity, and metabolic stability, as well as PK properties.<sup>19,38</sup> Shortcomings of the most potent analogues identified were again attributed to their high lipophilicity. Various approaches for structural modifications were explored to render these inhibitors compliant with Lipinski's rule.<sup>38,86</sup> For example, inhibitor **35** bearing a polar *N*-(2-ethyl)acetamide P<sub>3</sub><sup>SP</sup> side chain exhibited excellent in vitro potency toward rh-renin, good aqueous solubility, high human liver microsomal stability, as well as low affinity for CYP450 isozymes (> 30 μM) rendering it superior to hydrophobic congeners. However, rat oral bioavailability of **35** was low (10%), likely due to low cell permeability and poor intestinal absorption. In contrast, inhibitors bearing an *N*-methoxypropyl P<sub>3</sub><sup>SP</sup> residue and a more lipophilic S<sub>4</sub> residue, such as **36**, demonstrated strong CYP450 interactions, high microsomal clearance due to O-demethylation, and high liver first-pass elimination in rats (oral bioavailability of 0.4%). The 3-hydroxypropyl analogue of **36** showed no CYP450 inhibition (> 30 μM), excellent stability toward liver microsomes, and good rat oral bioavailability (44%) but only moderate renin inhibition (IC<sub>50</sub> = 0.9 μM). Similarly, the CF<sub>3</sub>-analogue **37** revealed high in vitro metabolic stability and improved oral bioavailability in rat (74%; *t*<sub>1/2</sub> = 3 h) and dog (19%; *t*<sub>1/2</sub> = 10 h) but again had only moderate potency and in addition suffered from strong CYP2D6 affinity.<sup>38b</sup> Remarkably, no in vivo pharmacology data have been reported for any analogues exhibiting high in vitro potency in the double-transgenic mouse (dTGM) model.<sup>58c,96</sup> The challenges of accomplishing a proper balance between desired target profile criteria, such as potency and ADME properties, have persisted throughout lead optimization. A preclinical development candidate was not identified from this class of DRIs at the time this research program was terminated.<sup>15,19,38b</sup>

Many of the novel DRIs comprise structural motifs, like the 4-arylpiperidine subunit of GRAB peptidomimetics, which are found in a number of other molecules known to bind to and modulate various types of drug targets or antitargets including G-protein-coupled receptors (GPCRs), transporters, and ion channels.<sup>92</sup> Cardiac ion channels play an increasingly important role. The hERG voltage-gated K<sup>+</sup> channel is widely recognized as a critical antitarget to be avoided from a drug safety perspective, as blocking this channel carries an increased risk of causing arrhythmias and torsades de pointes

(TdP).<sup>97</sup> Several emerging non-peptide DRI chemotypes are characterized by a pharmacophore comprising a basic nitrogen atom, being crucial for the interaction with the catalytic aspartates of renin, in combination with one or more aromatic rings. These structural features may potentially match a well-accepted pharmacophore for hERG channel blockade.<sup>97b,c</sup> *N*-Ureapiperidine-based basic amine DRIs (**38**, Figure 20) were reported to be inactive against hERG (patch clamp IC<sub>50</sub> > 30 μM), while no in vitro affinity profile against GPCRs was disclosed.<sup>39a</sup> The in vitro cardiac safety profile of **1** indicated a very low risk of impacting cardiac repolarization and conduction time. The human hERG channel was very weakly inhibited (patch-clamp IC<sub>25</sub> = 671 μM), and no effects were observed on the action potential in the isolated rabbit heart up to 100 μM, suggesting no interaction of **1** with cardiac ion channels in tissues at clinically relevant concentrations.<sup>98</sup>

Early in vitro profiling for the potential to interfere with other ion channels such as the cardiac voltage-gated sodium (Na<sub>v1.5</sub>) and calcium (Ca<sub>v1.2</sub>) channels has received more attention recently.<sup>99,100</sup> Interfering with the physiological function of the Na<sub>v1.5</sub> channel may exert a malignant proarrhythmic potential in vivo.<sup>99b</sup> Assessment of the potential of novel chemotype DRIs to bind particularly to the Na<sub>v1.5</sub> channel needs to be considered in cases where specific structural alerts have been identified.<sup>99a</sup> Reports describing the binding affinities across antitarget panels of receptors and cardiac ion channels for key representatives of novel class DRIs have remained generally scarce to date.<sup>38b</sup> It will be interesting to learn more about the selectivity and safety profiles of advanced candidates from these series and about the medicinal chemistry path taken to optimize such compounds.

Significant advances have been made in the development of novel non-peptide DRIs with potent in vitro activity and oral efficacy in animal models (vide infra). While the structural diversity has increased remarkably during recent years, lead optimization to identify suitable drug candidates remains a challenge within each compound class. The criteria for candidate selection for cardiovascular indications such as hypertension have become increasingly demanding. Therefore, requirements needed for a long-term safe drug treatment are expected to further raise the hurdles for achieving the desirable preclinical target profile of any new DRI. As a result, the number of novel-class DRIs having reportedly entered clinical trials has remained remarkably low to date and none has progressed toward late stage development.<sup>15</sup>

### Preclinical Pharmacology of Direct Renin Inhibition

Historically, the determination of in vivo potency and efficacy for antihypertensive agents has relied mainly on the use of rodents and dogs and to a lesser extent on other species. Numerous models of hypertension in the rat have been well characterized and are predictive of responses seen in hypertensive patients. However, the high specificity of human renin for human angiotensinogen was widely recognized as a significant limitation to the study of DRIs across species,<sup>101</sup> and the early in vivo assessment of human-specific DRIs has required the use of primates.<sup>102</sup> These animals are typically normotensive, and therefore, to detect effects on BP or changes in plasma renin activity (PRA) or total renin concentration, the use of a low sodium diet or diuretic pretreatment to activate the RAS is required.



The first DRI to demonstrate BP lowering effects following oral administration was *N*2-[(phenylmethoxy)carbonyl]-L-arginyl-L-arginyl-L-prolyl-L-phenylalanyl-L-histidyl-(3*S*,4*S*)-4-amino-3-hydroxy-6-methylheptanoyl-L-isoleucyl-L-histidyl-*N*6-[(1,1-dimethylethoxy)carbonyl]-L-lysinemethyl ester (CGP29287).<sup>103</sup> This modified peptide produced a substantial hypotensive effect in furosemide-treated normotensive marmosets when given at a dose of 100 mg/kg. Several other less peptidic DRIs became available using chemical modifications intended to reduce the overall size and complexity and resulted in second generation inhibitors, including **2**, **4**, and **5** (Figure 3).<sup>21b,23b</sup> Early studies demonstrating BP lowering with **1** also relied on the use of marmosets.<sup>104</sup>

Although species other than non-human primates have been used less frequently, their value is nevertheless apparent from their acceptance as screening models for SAR studies or for basic mechanistic experiments. Early work by Pfizer utilized sodium-depleted guinea pigs or rats infused with hog renin.<sup>35</sup> Pfizer scientists also used the sodium-depleted guinea pig to assess the BP effects of the DRI **3** in combination with an ACEi or ARB, since enzyme affinities in this species are reportedly similar to those in man.<sup>105</sup> These RAS combinations, administered acutely to conscious, unrestrained guinea pigs, resulted in synergistic reductions in BP and were observed over a range of intravenous doses.

The development of transgenic rodent models began in the late 1980s and subsequently offered the potential to assess efficacy of DRIs in small animals. Techniques to measure BP and RAS biomarkers in the rat were already routinely utilized and therefore facilitated a more widespread use of such transgenic models. Early utilization of these transgenic techniques relied on the use of RAS gene constructs that interacted with the host RAS and therefore circumvented concerns of species specificity.<sup>106</sup> Separate lines of normotensive transgenic rats harboring either the human renin or angiotensinogen genes were first established. These strains were subsequently cross bred, yielding the double-transgenic rat (dTGR) characterized by severe hypertension and end organ damage.<sup>107</sup> To our knowledge, **5** was the first DRI shown to reduce arterial BP in this rat model.<sup>107</sup> Subsequent development and phenotyping of the double transgenic mouse (dTGM) essentially revealed pathology similar to that of the dTGR.<sup>108</sup>

These transgenic animals have become valuable tools for the evaluation of various DRI, including **1**. Renin inhibitor programs at several companies have identified novel, potent, and orally active compounds using these models. Piperidine-based GRAB peptidomimetic DRIs<sup>36b-d</sup> have been studied at Hoffmann-LaRoche in the dTGR model. For example, inhibitor **43** (Figure 21) elicited a slight reduction in BP and substantially reduced the progression of albuminuria.<sup>85a</sup> Furthermore, inhibitor **44** was shown to normalize BP and to prevent cardiac hypertrophy and albuminuria over a period of 4 weeks.<sup>85b</sup> The related analogue **30** (Figure 16) was evaluated by Pfizer and was shown to reduce BP, albuminuria, and left ventricular hypertrophy when administered to dTGM over a period of 4 weeks.<sup>96</sup> The group at Pfizer has also reported novel aminoarylpiperidines and 2-ketopiperazines, including **45** and **46** (Figure 22), shown to reduce BP in the same dTGM model.<sup>58a,c</sup> Advanced analogues from the class of diazabicyclononene-based DRIs described by Actelion<sup>55</sup> and the alkylamine inhibitor series discovered by Vitae<sup>39</sup> were shown to elicit long-lasting BP reductions in the dTGR.

A desire to pursue more extensive profiling and ultimately differentiate **1** from other RAS blockers and other antihypertensive agents in general prompted testing in the spontaneously hypertensive rat (SHR), a well established hypertensive rat model. Although a reduction in BP was observed in the SHR, this effect was modest (~25 mmHg), required high doses (100 mg/kg per day), and subcutaneous delivery via osmotic minipump.<sup>104</sup> The moderate *in vitro* potency of **1** for rat renin (IC<sub>50</sub> = 80 nM)<sup>11</sup> was consistent with its weak *in vivo* potency, thus limiting the use of the SHR model for further pharmacological evaluation, for example, for evaluating BP independent effects. Despite these limitations, it was possible to demonstrate a synergistic BP reduction when **1** was given in combination with either an ACEi or an ARB.<sup>104</sup> These findings in the rat corroborated those reported previously by Pfizer using the guinea pig.<sup>105</sup>

The availability of the dTGR overcomes limitations resulting from species cross-reactivity and now makes it feasible to explore potential additional benefits of renin inhibition. In contrast to the mild antihypertensive effect seen in SHR, subsequent studies with **1** in the dTGR demonstrated a potent and substantial BP response.<sup>16</sup> These studies also clearly revealed cardiac and renal benefits, including an improvement in cardiac hypertrophy and function, as well as a reduction in albuminuria and serum creatinine.<sup>16</sup> As already mentioned, similar effects were also observed with two different classes of DRIs, exemplified by **30**<sup>96</sup> and **44**.<sup>85b</sup> Experiments using a very low chronic dose of **1** (0.03 mg/kg per day) in dTGR showed only minimal effects on BP, yet a reduction in cardiac and renal damage.<sup>109</sup> These results implicate the RAS as an important pathophysiologic regulator of organ function and structure and moreover suggest that some of these benefits may be BP independent.

The transgenic (mRen-2)27 rat expressing the murine renin transgene Ren-2 also has become an important rodent model to study the pharmacology of DRIs. Diabetes can be induced readily in these hypertensive rats by the injection of streptozotocin and therefore provides a unique opportunity to assess the therapeutic potential of direct renin inhibition in an animal with the comorbid conditions of hypertension and diabetes. Compound **1** is a potent inhibitor of mouse renin (IC<sub>50</sub> = 4.5 nM) and therefore makes possible the use of the (mRen-2)27 rat.<sup>110</sup> Chronic administration of **1** resulted in substantial antihypertensive and renal protective effects in this model<sup>110</sup> and was also shown to reduce albuminuria, glomerulosclerosis, and interstitial fibrosis<sup>111</sup> and to improve insulin sensitivity and skeletal muscle glucose transport.<sup>112</sup> Inhibitor **1** also decreased oxidative stress, induced beneficial remodeling of pancreatic structure,<sup>113</sup> and resulted in favorable effects on cardiac function and structure in diabetic, hypertensive mRen-2 rats.<sup>114</sup> These data provide evidence supporting organ protective benefits and extend the concept that direct renin inhibition, analogous to RAS inhibition, results in important tissue protective effects.<sup>115</sup>

Evidence to support differentiation is now being gathered as **1** is tested more extensively in animal models. Recent compelling data demonstrating an antiatherosclerotic effect in low density lipoprotein receptor null mice suggest that direct renin inhibition may provide optimal RAS blockade.<sup>116</sup> Inhibitor **1** (25 and 50 mg/kg per day) resulted in substantial reductions in lesion size in both the aortic root and arch. Although this study did not directly compare other RAS blockers, the effects reported with direct renin inhibition appeared to be greater than those described previously for

ACEi and ARBs. Another study using hypertensive apolipoprotein E null mice showed that **1** decreased BP, inhibited lesion progression, stabilized plaques, and reduced lipid core.<sup>117</sup> Improvements in atherosclerotic lesion size have also been demonstrated in Watanabe hypercholesterolemic rabbits.<sup>118</sup> Chronic administration of **1** (40 mg/kg per day; rabbit renin IC<sub>50</sub> = 11 nM)<sup>11</sup> preserved endothelial function, as determined by increased cellular levels of nitric oxide, and reduced plaque area in this model. The overall benefit derived from RAS blockade in atherosclerosis is likely due to preventing the actions of AngII. However, a DRI may provide additional benefit by preventing the generation of AngI, AngII, and Ang breakdown products.<sup>119</sup>

The intracellular RAS is a new and emerging concept with potential therapeutic relevance<sup>120,121</sup> that extends our understanding beyond the classical concept of a systemic and tissue RAS. The importance of this system and its overall regulation are only now being defined. Stimulation of cardiac fibroblasts by high glucose activates the intracellular RAS resulting in elevated levels of intracellular AngII and in turn increased transforming growth factor- $\beta$  and collagen I.<sup>122</sup> These biochemical changes were only partially attenuated by an ARB, whereas **1** completely prevented them. The same investigators also demonstrated that diabetes activates this system in cardiomyocytes and **1** was more effective at preventing increased oxidative stress and fibrosis than either ACE inhibition or AT1 receptor blockade.<sup>123</sup> Consequently, renin inhibition with **1** may offer additional tissue protective benefit in the setting of diabetes.

The prominent role of the RAS, specifically AngII, in the control of renal function has been known for many decades. The conventional view of the RAS had been that of a classical endocrine system. However, as specific pharmacologic tools became available to block the system at various points, evidence began to accrue suggesting the existence of an intrarenal RAS.<sup>57</sup> It soon became clear that the renal effects of AngII, such as renal vasoconstriction, are the result of both a systemic and tissue effect. AngII infused directly into the kidney, at doses that did not alter BP, resulted in renal vasoconstriction.<sup>124</sup> Blocking the effects of AngII therefore offered obvious therapeutic benefit. The early use of ACEi confirmed this idea as a substantial renal vasodilatation was noted.<sup>125</sup> Since it is widely recognized that ACE inhibition can alter the metabolism of several other vasoactive substances, including bradykinin, the ACEi-induced renal vasodilatation may not be due only to the prevention of AngII formation. AngII antagonists available at that time were known to also possess agonist activity, rendering them of limited value in confirming the actions of AngII within the kidney.<sup>126</sup> Comparative studies in the marmoset using the ACEi enalaprilat and a modified peptide renin inhibitor indicated that the renal vasodilatation was primarily due to preventing the formation of AngII.<sup>127</sup> Renal vasodilatation in response to direct renin inhibition was later confirmed using inhibitor **2**.<sup>128</sup>

It was noted that the BP response to **5**, as well as to *N*-[(1*S*,2*R*,3*S*)-1-(cyclohexylmethyl)-3-cyclopropyl-2,3-dihydroxypropyl]- $\alpha$ -[[[(2*S*)-2-[[[1,1-dimethyl-2-(4-morpholinyl)-2-oxoethyl]sulfonyl]methyl]-1-oxo-3-phenylpropyl]amino]-( $\alpha$ *S*)-1*H*-imidazole-4-propanamide (ciprokiren), in squirrel monkeys outlasted their effects on RAS biomarkers.<sup>129</sup> In another study, **5** was shown to induce greater renal vasodilation in squirrel monkeys than inhibitors **2** and **4**.<sup>130</sup> A study with radiolabeled **5** revealed a renal distribution and retention of the compound in the kidney long after its disappearance from the plasma

compartment, suggesting a more pronounced inhibition of kidney renin.<sup>131</sup> Comparative experiments in guinea pigs demonstrated that for an equal effect on BP, **5** increased renal blood flow more than an ARB or an ACEi.<sup>132</sup> Subsequent studies in normal volunteers with **2** showed a greater increase in renal blood flow than with ACE inhibition, a response attributed to a local effect in renal tissue.<sup>133,134</sup> A marked renal vasodilatory response was also demonstrated with inhibitor **6** in normotensive men,<sup>135</sup> and could be explained by the propensity for this compound to penetrate tissues and consequently inhibit the renal RAS. The potential therapeutic benefit of intrarenal RAS inhibition, exclusive of a prominent effect within the plasma compartment, is suggested from comparative results obtained with the DRI **43**, cilazapril, and valsartan in dTGRs.<sup>85a</sup> Despite minimal effects on systemic BP, oral administration of **43** was equally efficacious in reducing albuminuria and in decreasing various biomarkers of renal inflammation. One possible explanation is that the kidney acts as a reservoir to sequester the DRI and thus provides for greater or more prolonged renin inhibition.

Further evidence supporting a unique renal specificity for DRIs has emerged from recent preclinical and clinical profiling studies with **1**. In healthy volunteers, **1** was shown to induce an increase in renal blood flow exceeding that observed with either an ACEi or an ARB.<sup>136</sup> In the rat, **1** distributed extensively to the kidney and was localized in the glomerulus.<sup>110</sup> Three weeks after stopping administration of **1**, drug levels in the kidney remained well above the IC<sub>50</sub> for inhibition of renin, while plasma levels were below the limits of quantitation.<sup>137</sup> Interestingly, **1** was shown to accumulate in renin secretory granules and therefore to bind to renin and prorenin prior to release.<sup>138</sup> Taken together, these data provide a possible explanation for the observed long-lasting BP lowering effect of **1** in hypertensive patients and may support the idea of more complete blockade of the intrarenal RAS with DRIs.

It will be important ultimately to demonstrate that these potentially differentiating characteristics of **1** result in tangible therapeutic benefits. Preclinical data suggest that this is likely to occur. Inhibitor **1** was shown to lower BP, albuminuria, and serum creatinine in the hypertensive dTGR<sup>16</sup> and to reduce cystatin C and neutrophil gelatinase-associated lipocalin, two biomarkers of glomerular filtration and tubular damage, respectively.<sup>139</sup> In this same animal model, **1** reduced albuminuria at a dose that had only minimal effects on BP, suggesting a BP-independent renal protective effect.<sup>109</sup> Inhibitor **1** also reduced BP and albuminuria and suppressed renal transforming growth factor- $\beta$  and collagen I expression in hypertensive, diabetic mRen-2 rats.<sup>110</sup> In a comparative study, **1** and the ACEi perindopril attenuated albuminuria and glomerulosclerosis to a similar extent in diabetic mRen-2 rats, even though BP was reduced to a greater extent by perindopril. Surprisingly, renal interstitial fibrosis was diminished more by **1**.<sup>111</sup> These results support the notion of an intrarenal action of **1** and a BP-independent effect. Increased generation of AngII occurs in renal podocytes in response to high glucose in the diabetic kidney.<sup>140</sup> Elevated AngII levels within the podocyte are causative for inducing podocyte injury, a principal feature of diabetic kidney disease. The DRI **1**, but not the ACEi captopril, decreased AngII production within the podocyte. This finding provides direct mechanistic evidence to functionally distinguish ACE inhibition from renin inhibition in the kidney. The clinical relevance of these findings awaits the outcome of several large ongoing clinical trials with **1**.

However, a small study in type 2 diabetic patients who are already on high dose losartan as background therapy (AVOID Study) has demonstrated an additional renal protective effect (reduction in albuminuria) with the addition of **1** to their daily drug regimen.<sup>141</sup>

### Prorenin, Renin, and the (Pro)Renin Receptor

It is well recognized that the kidney is the primary source of renin and the only tissue capable of processing prorenin to renin. Notably, the kidney also releases prorenin.<sup>142</sup> In other tissues expressing the renin gene, prorenin is both the primary and final product.<sup>143</sup> Interestingly, prorenin represents 80–90% of all renin present in plasma, yet a physiologic or pathophysiologic role has not yet been demonstrated for this protein.<sup>144</sup> Plasma levels of prorenin are elevated in diabetic patients with underlying microvascular complications such as retinopathy and nephropathy,<sup>145</sup> thus implicating prorenin as a biomarker for vascular disease. However, convincing evidence to indicate a pathophysiologic role for plasma prorenin beyond that of a biomarker of disease has yet to be demonstrated.

Prorenin/renin binding proteins within tissues have been known for many years; however, their exact role is unclear.<sup>146,147</sup> Mesangial cells in culture have been shown to specifically bind renin and subsequently induce an increase in plasminogen activator inhibitor-1. These results suggest a potential biologic role for these receptors.<sup>148</sup> Mannose 6-phosphate/insulin-like growth factor II has been identified as another receptor for prorenin and renin<sup>149</sup> but appears to serve primarily as a clearance receptor.

Nguyen et al.<sup>150</sup> identified a novel receptor that binds prorenin and renin, induced intracellular signaling, and is designated as the (pro)renin receptor (P)RR. The (P)RR was localized to the glomerular mesangium and the subendothelium of coronary and renal arteries. Agonist binding resulted in a 4-fold increase in the catalytic activity of the enzyme–receptor complex. In addition to the proteolytic conversion of AngI to AngII, binding also resulted in initiation of an intracellular extracellularly regulated kinase 1/2 cascade that was independent of AngII. The identification of this receptor and the demonstration of an integrated response involving Ang-dependent and -independent mechanisms stimulated intense research into this novel RAS signaling cascade. Further investigation revealed that prorenin binding to this receptor resulted in increased expression of plasminogen activator inhibitor-1 in vascular smooth muscle cells, again an effect independent of AngII.<sup>151</sup> Renin binding was also shown to increase transforming growth factor- $\beta$  and matrix proteins in mesangial cells, an effect that was not blocked by an ACEi, an ARB, or a DRI.<sup>152</sup>

Prorenin harbors a 43-amino-acid N-terminal propeptide that is believed to obstruct substrate access to the active site. Prorenin can be activated either by proteolytic cleavage of the propeptide or by a nonproteolytic mechanism. The latter can be induced by low temperature, low pH, or binding of prorenin to the (pro)renin receptor, all believed to trigger unfolding of the propeptide from the enzymatic cleft. The prosegment contains a “gate and handle” region that is critical for receptor binding during nonproteolytic activation.<sup>153</sup> Although renin and prorenin both have high affinity for the (P)RR, prorenin is considered the endogenous agonist.<sup>154</sup> A condition of mild obesity and impaired glucose tolerance is observed in transgenic rats and mice overexpressing the human renin gene, and these effects are independent of

AngII.<sup>155,156</sup> Overexpression of the human (P)RR, an alternative approach for modulating this system, results in elevations in BP in the rat.<sup>157</sup> Recently, a decoy peptide, presumably binding to the active site of the (P)RR, denoted as the “handle region peptide” was shown to provide organ protective benefits in the kidney, eye, and heart when administered subcutaneously to rodents.<sup>158</sup> However, these results have not been consistently reproduced by other laboratories.<sup>159</sup> In addition, two recent studies have shown that prorenin does not induce any specific organ pathology or vasculopathy. Despite chronically elevated prorenin levels in transgenic mice overexpressing prorenin, no cardiac fibrosis or renal sclerotic changes were evident.<sup>160</sup> These investigators conclude that the mildly increased prorenin levels observed clinically in diabetic patients (3-fold) and those reported in their transgenic mice are insufficient to induce pathological responses. Similarly, glomerulosclerosis did not occur in transgenic rats despite substantial incremental increases in prorenin.<sup>161</sup> These results, taken together with the substantial body of clinical data from thousands of patients receiving chronic therapy with the DRI **1**, do not support a direct pathologic role for elevated prorenin or renin.

The recognition that the (P)RR binds both renin and prorenin and that the catalytic activity of bound renin increases 4-fold raises the intriguing question of whether or not a DRI could modify these effects. Initial studies indicate that **1** does not block the binding of prorenin or renin to the (P)RR.<sup>159</sup> Moreover, it has been shown in rat aortic vascular smooth muscle cells that the half-life of both prorenin and renin is increased by **1** binding to the receptor.<sup>162</sup> While several studies have begun to describe the biological effects that occur following agonist binding to the receptor, its pathophysiological relevance remains to be more fully characterized.

### Clinical Pharmacology of the Direct Renin Inhibitor **1**

A remarkable research effort has been put forth over the past decades directed at the discovery and development of DRIs. Initial clinical characterization of the effects of direct renin inhibition was accomplished with the use of various investigational drugs possessing suboptimal physicochemical and PK properties.<sup>21–23,162</sup> The opportunity to gain considerably more insight into the pharmacodynamic efficacy of DRIs became available with the clinical introduction of **1**.<sup>163</sup> Although the bioavailability of **1** was shown to be only 2.6% in humans, this represents a substantial improvement over that shown historically for DRIs as a class.<sup>164,165</sup> This enhancement represents more than a simple incremental improvement, especially when coupled with the remarkable potency of **1** for human renin, long duration of action, and the potential for distribution to the kidney. Steady-state  $C_{max}$  values are in the range 330–660 nM following a 300 mg dose of **1** and represent concentrations greater than 2 orders of magnitude above the  $IC_{50}$  for renin inhibition.<sup>164,166</sup> Importantly, **1** was also shown to have a long terminal half-life in human plasma.<sup>167</sup> From a functional standpoint and consistent with PK parameters, **1** was shown to induce dose-dependent and long-lasting inhibition of the RAS in humans.<sup>168</sup> Further confirmation of the anticipated benefit of oral renin inhibition came with the demonstration of a dose-dependent (75–300 mg of **1**) BP reduction in patients with mild to moderate hypertension.<sup>169</sup>

Early clinical results demonstrated that **1** has placebo-like tolerability and provides comparable or improved efficacy compared to angiotensin AT1 receptor blockade with



losartan<sup>169</sup> or irbesartan<sup>170</sup> and greater BP reductions than ramipril.<sup>171</sup> The antihypertensive response to **1** is sustained over 24 h (ambulatory BP) with high trough-to-peak ratios and thus represents a true once daily RAS blocker.<sup>172</sup> In a head-to-head comparative study, **1** (150 mg) was shown to reduce BP to a similar extent as 150 mg of irbesartan. Higher doses of **1** provided additional RAS blockade and greater BP reductions.<sup>173</sup> This study also demonstrated a potentially important biomarker divergence, showing that irbesartan and **1** both raised PRC; however, only **1** effectively inhibited PRA. In heart failure patients, an association between high PRA and increased cardiovascular risk has been shown.<sup>174</sup>

Combination therapy has become a cornerstone of the physician's approach to effective management of hypertension. Despite the vast armamentarium of antihypertensive drugs available today, high BP remains difficult to treat, especially in elderly individuals and in patients with existing comorbidities such as diabetes.<sup>175</sup> Inhibitor **1** has been shown to provide additive BP lowering efficacy when administered in combination with the diuretic hydrochlorothiazide, the ACEi ramipril, the ARBs irbesartan and valsartan,<sup>176–178</sup> and amlodipine.<sup>179</sup> These results indicate that **1** effectively reduced BP when administered alone or in combination with other antihypertensive agents. In summary, **1** offers an effective option for treating hypertensive patients.

With a wide variety of effective therapeutic options available, the decision of which agent to use can be a challenge for the physician. Efficacy and safety are clearly important factors. However, additional benefit that could be directly attributed to the use of a specific agent would be important in decision making. Unfortunately, with the introduction of any new agent, additional or unique benefit is usually theoretical rather than proven. It should be emphasized that the ultimate goal for controlling BP is to reduce the overall incidence of end organ failure. To this end, evidence is sought to demonstrate reduced cardiovascular morbidity and mortality.

Results from several small clinical studies have demonstrated a benefit beyond BP lowering. The intent is to use these findings to support larger, pivotal outcome studies that will ultimately demonstrate the long-term value of **1**. Collectively, the clinical program to evaluate the potential long-term benefit of **1** has been initiated and is known as the "Aspire Higher" clinical trial program.<sup>5</sup> It consists of a set of small scale studies focused on demonstrating cardiorenal protection in a short-term setting. These will then be followed by larger, long-term outcome studies aimed at directly demonstrating an organ protective benefit. One such acute study in healthy volunteers has recently demonstrated that **1** elicits a prominent renal vasodilation and that this response surpasses that seen with ACEi and ARBs.<sup>136</sup> This effect was long-lasting and associated with a natriuretic response. The now completed AVOID study demonstrated that **1**, when added to background therapy (losartan), further reduced the albumin/creatinine ratio in patients with type 2 diabetes and nephropathy.<sup>141</sup> This effect was independent of an effect on BP. These results further extend the preclinical observations and suggest a potentially important role for direct renin inhibition in renal (patho)physiology.

Two additional studies, ALLAY and ALOFT, provided early evidence to support a role for **1** in cardiac protection. The DRI **1** was shown to be as effective as losartan in attenuating left ventricular hypertrophy in hypertensive patients.<sup>180</sup> In patients with symptomatic heart failure (New York Heart Association class II to class IV), the addition of **1** to con-

ventional therapy (ACEi or ARB, and a  $\beta$ -adrenoceptor antagonist) resulted in a further decrease in N-terminal pro-Brain natriuretic peptide, a proven biomarker that correlates with severity of cardiac severity.<sup>181</sup>

### Future Directions

The disclosure of new classes of nonpeptide DRIs has continued over the past decade, suggesting that the opportunities offered by the newly uncovered topographical space and the increasing druglike ligand chemical space have not been fully exploited yet. The structural diversity of small-molecule DRIs is likely to further expand, and novel inhibitors are anticipated to be discovered in the future that may hold promise as candidates for clinical investigations. Future DRIs will need to demonstrate a favorable and differential clinical profile over existing therapies at attractive cost-benefit while facing increasingly demanding safety and tolerability standards by the regulatory authorities for cardiovascular drugs.

Several DRIs have reportedly progressed recently to the stage of early clinical investigations, indicating a revival of interest by several pharmaceutical companies in the development of DRIs.<sup>15</sup> The prospect of such more advanced DRIs reaching the patient for the treatment of cardiovascular diseases is difficult to predict, since only limited preclinical information is currently available. Preliminary data have been reported by Speedel on SPP635, SPP676, and SPP1148 (structures not disclosed) from phase I and on SPP635 from phase II clinical trials.<sup>182</sup> After a single dose in normal volunteers, SPP635 (100 mg) and SPP676 (30 mg) inhibited PRA to a similar extent as a 150 mg dose of **1**. SPP676 and SPP1148 were shown to be safe and well tolerated up to doses of 1800 and 600 mg, respectively. While SPP676 had a relatively short terminal half-life (~8 h), SPP1148 was reported to have a longer half-life of ~30 h and to maximally inhibit PRA at the 50 mg single oral dose. SPP635, derived from the 3,4-piperidine GRAB peptidomimetics, showed an oral bioavailability of ~30% and an elimination half-life of ~24 h in phase I studies, in good agreement with the PK parameters determined by a microdosing approach. These data may suggest the potential for a favorable PK profile of SPP635 at clinically effective doses.<sup>182</sup> In a phase IIa study in patients with mild to moderate hypertension, SPP635 significantly reduced PRA and resulted in double-digit reductions in daytime ambulatory BP.<sup>182</sup> Novartis acquired Speedel and its portfolio of follow-up DRIs in 2008.

VTP-27999 (Vitae Pharmaceuticals, structure not disclosed) represents another novel DRI that has just entered phase I clinical trials.<sup>183</sup> VTP-27999 will be evaluated in a randomized double blind placebo controlled study in healthy volunteers to assess efficacy based on relevant biomarkers, as well as safety, tolerability, and PK.

The second generation GRAB peptidomimetic **52**<sup>55a</sup> has been reported by Actelion and Merck to be under codevelopment for the treatment of cardiovascular indications including renal and heart failure and hypertension.<sup>184a</sup> A randomized double-blind placebo and active comparator-controlled (enalapril 20 mg/day) study to determine the effectiveness and tolerability of **52** was completed. The drug candidate was given at 250 and 500 mg once daily over a 4-week treatment period to hypertensive patients. Results of this phase IIa trial have not been disclosed yet; however, further development of **52** has been recently discontinued.<sup>184b</sup>

As with any first-in-class drug, it is imperative that further characterization of **1** be undertaken. The intent is to more comprehensively define its clinical actions and to enhance our understanding of direct renin inhibition as a novel point of clinical intervention along the RAS cascade. With its market introduction, it now becomes possible for the first time to define in humans what had been for decades only a theoretical promise for direct renin inhibition. From a scientific perspective, **1** represents a novel and important pharmacologic probe that can be used to further expand our knowledge on the RAS in normal and diseased states. From a therapeutic point of view, it is important now to fully profile the effects of **1** in different patient populations and to clearly define the benefit derived from such an approach. The ultimate goal is to optimize therapy and to provide maximum benefit to the patient.

The accumulated evidence to date with **1** in cardiorenal disease indicates a potential for long-term benefit and provides a strong foundation on which to build our understanding of direct renin inhibition in cardiovascular disease. Outcome data from the planned and ongoing end point trials will provide definitive proof. One such study, ALTITUDE, aims to determine the effect of **1** added to conventional standard of care therapy (ACEi or ARB) in patients with type 2 diabetes and varying degrees of renal dysfunction.<sup>185</sup> The upcoming years will be an exciting time, as new data are forthcoming. This will hopefully provide evidence to support the hypothesis put forth more than 50 years ago that inhibition of AngI generation from angiotensinogen is the therapeutic approach “most likely to succeed” because renin is the initial and rate-limiting step of the RAS cascade.<sup>3</sup>

## Methods

PDB codes, space groups, and resolution of the X-ray structures discussed in this article are as follows: glycosylated rh-renin (2ren, space group *I4*, 2.5 Å resolution);<sup>31</sup> **1** (2v0z, *P2*<sub>1</sub>3, 2.2 Å);<sup>51</sup> **4** (1rne, *P4*<sub>2</sub>2<sub>1</sub>, 2.4 Å);<sup>32</sup> **29** (2v11, *P2*<sub>1</sub>3, 3.1 Å);<sup>51</sup> analogue of **22** (2v12, *P2*<sub>1</sub>3, 3.2 Å);<sup>51</sup> **28** (2v16, *P2*<sub>1</sub>3, 2.8 Å);<sup>51</sup> **34** (2g1r, *P2*<sub>1</sub>3, 2.4 Å);<sup>38b</sup> **38** (3gw5, *P2*<sub>1</sub>2<sub>1</sub>2<sub>1</sub>, 2.0 Å);<sup>39</sup> *N*-hydroxypropyl analogue of **48** (2fs4, *P2*<sub>1</sub>3, 2.2 Å);<sup>58c</sup> **51** (3g70, *P2*<sub>1</sub>2<sub>1</sub>2<sub>1</sub>, 2.0 Å);<sup>55a</sup> **52** (3g6z, *P2*<sub>1</sub>2<sub>1</sub>2<sub>1</sub>, 2.0 Å).<sup>55a</sup> The X-ray structures (PDB codes, space groups, resolution) for **9** (1pr7, *P2*<sub>1</sub>3, 3.65 Å),<sup>36a</sup> **32** (1pr8, *P4*<sub>2</sub>2<sub>1</sub>2, 2.9 Å),<sup>36a</sup> and **33** (1uhq)<sup>36b</sup> had been made publicly available by the Protein Data Bank during a restricted time period. These data have been retracted in the meantime for unknown reasons. Shown X-ray structures were aligned onto the aliskiren complex using Coot (Emsley, P.; Cowtan, K. Coot: model-building tools for molecular graphics. *Acta Crystallogr.* **2004**, *D60*, 2126–2132). Figures were generated using PyMOL (DeLano, W. L. *The PyMOL Molecular Graphics System*; DeLano Scientific: San Carlos, CA, 2002; <http://www.pymol.org>).

## Biographies

**Randy L. Webb** is Executive Director in the Cardiovascular and Metabolic Disease area. He graduated from the University of Iowa and received his Ph.D. in Pharmacology. He was a postdoctoral fellow in 1984 in the Department of Physiology at the Medical College of Wisconsin. He joined Ciba-Geigy (now Novartis) in 1984 where he worked on various cardiovascular drug discovery and late-stage development projects. He has performed studies supporting the regulatory submissions for benazepril, valsartan, and aliskiren.

**Nikolaus Schiering** received his Ph.D. from the University of Heidelberg (Germany) in 1991 for work conducted at the Max-Planck-Institute for Medical Research, Department of Biophysics, in the group of Emil F. Pai. From 1992 to 1995

he pursued postdoctoral studies at the Rosenstiel Center of Brandeis University, Waltham, MA, under the guidance of Gregory A. Petsko and Dagmar Ringe. He joined Pharmacia (Nerviano, Italy) in 1995 as a Research Scientist in the Department of Structural Chemistry. Since 2003, he has been working in the Structural Sciences Unit of the Expertise Platform Proteases at Novartis in Basel, Switzerland, as a Research Investigator.

**Richard Sedrani** is Executive Director in the Expertise Platform Proteases at Novartis in Basel, Switzerland. He studied at the Université Pierre et Marie Curie in Paris, France, where he obtained his Ph.D. in Organic Chemistry in 1990 working under the guidance of Professor Alexandre Alexakis. From 1990 to 1991 he was a postdoctoral fellow at the University of South Carolina working in the group of Professor James A. Marshall. He joined Sandoz Pharma, now Novartis, in 1991, where he has been working in drug discovery projects in various therapeutic areas. He is co-inventor of everolimus, the active principle in Certican, used for the prevention of transplant rejection, and in Afinitor, a treatment for patients with advanced kidney cancer.

**Jürgen Maibaum** is Director and Leading Scientist within the Expertise Platform Proteases at NIBR in Basel, Switzerland. He graduated from the University of Münster, Germany, where he received his Ph.D. in Medicinal Chemistry in 1983 under the guidance of Professor Gottfried Blaschke. He was postdoctoral fellow between 1985 and 1987 at the University of Wisconsin, Madison, under the guidance of Professor Daniel H. Rich. He joined Ciba-Geigy (now Novartis) in 1989, where he has been engaged in drug discovery projects in the areas of cardiovascular disease, osteoporosis, metabolic disorders and obesity, and ophthalmology. In 2009, Jürgen was honored with the “Hero of Chemistry Award” by the American Chemical Society for his contributions to the discovery of aliskiren.

## References

- (1) Tigerstedt, R.; Bergman, P. G. Niere und Kreislauf. *Skand. Arch. Physiol.* **1898**, *8*, 223–271.
- (2) Aurell, M. The renin–angiotensin system: the centenary jubilee. *Blood Pressure* **1998**, *7*, 71–75.
- (3) Skeggs, L. T., Jr.; Kahn, J. R.; Lentz, K.; Shumway, N. P. The preparation, purification, and amino acid sequence of a polypeptide renin substrate. *J. Exp. Med.* **1957**, *106*, 439–453.
- (4) Azizi, M.; Webb, R.; Nussberger, J.; Hollenberg, N. K. Renin inhibition with aliskiren: Where are we now, and where are we going? *J. Hypertens.* **2006**, *24*, 243–256.
- (5) Sever, P. S.; Gradman, A. H.; Azizi, M. Managing cardiovascular and renal risk: the potential of direct renin inhibition. *J. Renin–Angiotensin–Aldosterone Syst.* **2009**, *10*, 65–76.
- (6) Brown, M. J. Direct renin inhibition—a new way of targeting the renin system. *J. Renin–Angiotensin–Aldosterone Syst.* **2006**, *7*, S7–S11. The terminology “direct renin inhibition” indicates an action that directly involves renin inhibition rather than an “indirect inhibition” that can occur somewhere along the pathway and will result in suppression of the cascade and eventually of renin release. The term DRI does not refer to the mechanism of ligand–enzyme interaction, e.g., active site vs allosteric site binders. To the best of our knowledge, allosteric renin inhibitors have not been reported to date.
- (7) Ong, K. L.; Cheung, B. M. Y.; Man, Y. B.; Lau, C. P.; Lam, K. S. L. Prevalence, awareness, treatment, and control of hypertension among United States adults 1999–2004. *Hypertension* **2007**, *49*, 69–75.
- (8) Kearney, P. M.; Whelton, M.; Reynolds, K.; Muntner, P.; Whelton, P. K.; He, H. Global burden of hypertension: analysis of worldwide data. *Lancet* **2005**, *365*, 217–223.
- (9) Ondetti, M. A.; Cushman, D. W. Inhibition of the renin angiotensin system: a new approach to the therapy of hypertension. *J. Med. Chem.* **1981**, *24*, 355–361.
- (10) Timmermans, P. B.; Carini, D. J.; Chiu, A. T.; Duncia, J. V.; Price, W. A., Jr.; Wells, G. J.; Wong, P. C.; Wexler, R. R.; Johnson, A. L. Angiotensin II receptor antagonists: from discovery to antihypertensive drugs. *Hypertension* **1991**, *18* (Suppl. III), 136–142.
- (11) Wood, J. M.; Maibaum, J.; Rahuel, J.; Grütter, M. G.; Cohen, N. C.; Rasetti, V.; Rüeger, H.; Göschke, R.; Stutz, S.; Fuhrer, W.; Schilling, W.; Rigollier, P.; Yamaguchi, Y.; Cumin, F.; Baum, H. P.; Schnell, C. R.; Herold, P.; Mah, R.; Jensen, C.; O'Brien, E.; Stanton, A.; Bedigian, M. P. Structure-based design of aliskiren, a



- novel orally effective renin inhibitor. *Biochem. Biophys. Res. Commun.* **2003**, *308*, 698–705.
- (12) Maibaum, J.; Stutz, S.; Göschke, R.; Rigollier, P.; Yamaguchi, Y.; Cumin, F.; Rahuel, J.; Baum, H. P.; Cohen, N. C.; Schnell, C. R.; Fuhrer, W.; Grütter, M. G.; Schilling, W.; Wood, J. M. Structural modification of the P2' position of 2,7-dialkyl-substituted 5(S)-amino-4(S)-hydroxy-8-phenyl-octanecarboxamides: the discovery of aliskiren, a potent nonpeptide human renin inhibitor active after once daily dosing in marmosets. *J. Med. Chem.* **2007**, *50*, 4832–4844.
  - (13) Maibaum, J.; Feldman, D. L. Case history on Tekturna/Rasilez (aliskiren), a highly efficacious direct oral renin inhibitor as a new therapy for hypertension. *Annu. Rev. Med. Chem.* **2009**, *44*, 105–127.
  - (14) Jensen, C.; Herold, P.; Brunner, H. R. Aliskiren: the first renin inhibitor for clinical treatment. *Nat. Rev. Drug Discovery* **2008**, *7*, 399–410.
  - (15) Yokokawa, F.; Maibaum, J. Recent advances in the discovery of non-peptidic direct renin inhibitors as antihypertensives: new patent applications in years 2000–2008. *Expert Opin. Ther. Pat.* **2008**, *18*, 581–602. A total of 62 new patents claiming novel renin inhibitors have been disclosed in the years 2008–2009, as based on a search in SciFinder. For more recent reports on DRI clinical development compounds, see refs 182–184.
  - (16) Pilz, B.; Shagdasuren, E.; Wellner, M.; Fiebler, A.; Dechend, R.; Gratzke, P.; Meiners, S.; Feldman, D. L.; Webb, R. L.; Garrelts, I. M.; Danser, A. H. J.; Luft, F. C.; Müller, D. N. Aliskiren, a human renin inhibitor, ameliorates cardiac and renal damage in double-transgenic rats. *Hypertension* **2005**, *46*, 569–576.
  - (17) A revised definition of “peptide-derived peptidomimetic” and “non-peptide peptidomimetic” protease inhibitors has been proposed by Rich et al.<sup>29</sup> Non-peptide peptidomimetics can be further distinguished in two major classes: those accessing exclusively the substrate-derived extended  $\beta$ -strand binding active site topography and those binding to a distinct active site conformational topography not recognized by substrate-derived inhibitors. We use this terminology throughout the discussion in this article.
  - (18) Tice, C. M. Renin inhibitors. *Annu. Rep. Med. Chem.* **2006**, *41*, 155–167.
  - (19) Kasai, A.; Subedi, R.; Stier, M.; Holsworth, D. D. Cardiovascular agents: renin inhibitors and factor Xa inhibitors. *Heterocycles* **2007**, *73*, 47–85.
  - (20) Rich, D. H. Inhibitors of Aspartic Proteinases. In *Research Monographs in Cell and Tissue Physiology, Vol. 12, Proteinase Inhibitors*; Barrett, A. J., Salvesen, G., Eds.; Elsevier: Amsterdam, 1986; pp 179–217 and references therein.
  - (21) (a) Greenlee, W. J. Renin inhibitors. *Med. Res. Rev.* **1990**, *2*, 173–236. (b) Greenlee, W. J. Hypertension: Treatment by Blockade of the Renin–Angiotensin System. In *Proceedings of the 14th International Symposium on Medicinal Chemistry*; Awouters, F., Ed.; Elsevier Science: Amsterdam, 1997; pp 97–107.
  - (22) (a) Raddatz, P. Recent developments in renin inhibitors: Part I. *Expert Opin. Ther. Pat.* **1994**, *4*, 489–504. (b) Raddatz, P. Recent developments in renin inhibitors: Part II. *Expert Opin. Ther. Pat.* **1994**, *4*, 1347–1359.
  - (23) (a) Rosenberg, S. H. Renin inhibitors. *Progr. Med. Chem.* **1995**, *32*, 37–114. (b) Rosenberg, S. H.; Boyd, S. A. Renin Inhibitors. In *Antihypertensive Drugs*; Van Zwieten, P. A., Greenlee, W. J., Eds.; Harwood: Amsterdam, 1997; pp 77–111. (c) Rosenberg, S. H.; Kleinert, H. D. Renin inhibitors. *Pharm. Biotechnol.* **1998**, *11*, 7–28.
  - (24) (a) Appelt, K.; Bacquet, R. J.; Bartlett, C. A.; Booth, C. L.; Freer, S. T.; Fuhry, M. A.; Gehring, M. R.; Herrmann, S. M.; Howland, E. F.; Janson, C. A.; Jones, T. R.; Kan, C.-C.; Kathardekar, V.; Lewis, K. K.; Marzoni, G. P.; Matthews, D. A.; Mohr, C.; Moomaw, E. W.; Morse, C. A.; Oatley, S. J.; Ogden, R. C.; Reddy, M. R.; Reich, S. H.; Schoettlin, W. S.; Smith, W. W.; Varney, M. D.; Villafranca, J. E.; Ward, R. W.; Webber, S.; Webber, S. E.; Welch, K. M.; White, J. Design of enzyme inhibitors using iterative protein crystallographic analysis. *J. Med. Chem.* **1991**, *34*, 1925–1934. (b) Murray, C. W.; Rees, D. C. The rise of fragment-based drug discovery. *Nat. Chem.* **2009**, *1*, 187–192. (c) de Kloe, G. E.; Bailey, D.; Leurs, R.; de Esch, I. J. P. Transforming fragments into candidates: small becomes big in medicinal chemistry. *Drug Discovery Today* **2009**, *14*, 630–646.
  - (25) Rich, D. H. Pepstatin-derived inhibitors of aspartic proteinases. A close look at an apparent transition-state analog inhibitor. *J. Med. Chem.* **1985**, *28*, 263–273.
  - (26) Guruprasad, K.; Dhanaraj, V.; Groves, M.; Blundell, T. L. Aspartic proteinases: the structures and functions of a versatile superfamily of enzymes. *Perspect. Drug Discovery Des.* **1995**, *2*, 329–341.
  - (27) Dunn, B. Structure and mechanism of the pepsin-like family of aspartic peptidases. *Chem. Rev.* **2002**, *102*, 4431–4458. See also the following: Babine, R. E.; Bender, S. L. Molecular recognition of protein–ligand complexes: applications to drug design. *Chem. Rev.* **1997**, *97*, 1359–1472.
  - (28) Cooper, J. B. Aspartic proteinases in disease: a structural perspective. *Curr. Drug Targets* **2002**, *3*, 155–173.
  - (29) (a) Bursavich, M. G.; Rich, D. H. Designing non-peptide peptidomimetics in the 21st century: inhibitors targeting conformational ensembles. *J. Med. Chem.* **2002**, *45*, 541–558. (b) Bursavich, M. G.; West, C. W.; Rich, D. H. From peptides to non-peptide peptidomimetics: design and synthesis of new piperidine inhibitors of aspartic peptidases. *Org. Lett.* **2001**, *3*, 2317–2320.
  - (30) Dhanaraj, V.; Dealwis, C. G.; Frazao, C.; Badasso, M.; Sibanda, B. L.; Tickle, I. J.; Cooper, J. B.; Driessen, H. P. C.; Newman, M.; Aguilár, C.; Wood, S. P.; Blundell, T. L.; Hobart, P. M.; Geoghegan, K. F.; Ammirati, M. J.; Danley, D. E.; O'Connor, B. A.; Hoover, D. J. X-ray analyses of peptide–inhibitor complexes define the structural basis of specificity for human and mouse renins. *Nature* **1992**, *357*, 466–472.
  - (31) Sielecki, A. R.; Hayakawa, K.; Fujinaga, M.; Murphy, M. E. P.; Fraser, M.; Muir, A. K.; Carilli, C. T.; Lewicki, J. A.; Baxter, J. D.; James, M. N. G. Structure of recombinant human renin, a target for cardiovascular-active drugs, at 2.5 Å resolution. *Science* **1989**, *243*, 1346–1351.
  - (32) Rahuel, J.; Priestle, J. P.; Grütter, M. G. The crystal structures of recombinant glycosylated human renin alone and in complex with a transition state analog inhibitor. *J. Struct. Biol.* **1991**, *107*, 227–236.
  - (33) Wolfenden, R. Transition state analog inhibitors and enzyme catalysis. *Annu. Rev. Biophys. Bioengin.* **1976**, *5*, 271–306.
  - (34) Wiley, R. A.; Rich, D. H. Peptidomimetics derived from natural products. *Med. Chem. Rev.* **1993**, *13*, 327–384.
  - (35) Hoover, D. J.; Lefker, B. A.; Rosati, R. L.; Wester, R. T.; Kleinman, E. F.; Bindra, J. S.; Holt, W. F.; Murphy, W. R.; Mangiapane, M. L.; Hockel, G. M.; Williams, I. H.; Smith, W. H.; Gumkowski, M. J.; Shepard, R. M.; Gardner, M. J.; Nocerini, M. R. Discovery of inhibitors of human renin with high oral bioavailability. *Adv. Exp. Med. Biol.* **1995**, *362*, 167–180.
  - (36) (a) Oefner, C.; Binggeli, A.; Breu, V.; Bur, D.; Clozel, J.-P.; D'Arcy, A.; Dorn, A.; Fischli, W.; Grüninger, F.; Güller, R.; Hirth, G.; Märki, H. P.; Mathews, S.; Müller, M.; Ridley, R. G.; Stadler, H.; Vieira, E.; Wilhelm, M.; Winkler, F. K.; Westl, W. Renin inhibition by substituted piperidines: a novel paradigm for the inhibition of monomeric aspartic proteinases? *Chem. Biol.* **1999**, *6*, 127–131. (b) Vieira, E.; Binggeli, A.; Breu, V.; Bur, D.; Fischli, W.; Güller, R.; Hirth, G.; Märki, H. P.; Müller, M.; Oefner, C.; Scalone, M.; Stadler, H.; Wilhelm, M.; Westl, W. Substituted piperidines: highly potent renin inhibitors due to induced fit adaptation of the active site. *Bioorg. Med. Chem. Lett.* **1999**, *9*, 1397–1402. (c) Güller, R.; Binggeli, A.; Breu, V.; Bur, D.; Fischli, W.; Hirth, G.; Jenny, C.; Kansy, M.; Montavon, F.; Müller, M.; Oefner, C.; Stadler, H.; Vieira, E.; Wilhelm, M.; Westl, W.; Märki, H. P. Piperidine–renin inhibitors compounds with improved physicochemical properties. *Bioorg. Med. Chem. Lett.* **1999**, *9*, 1403–1408. (d) Märki, H. P.; Binggeli, A.; Bittner, B.; Bohner-Lang, V.; Breu, V.; Bur, D.; Coassolo, P.; Clozel, J. P.; D'Arcy, A.; Doebeli, H.; Fischli, W.; Funk, C.; Foricher, J.; Giller, T.; Grüninger, F.; Guenzi, A.; Güller, R.; Hartung, T.; Hirth, G.; Jenny, C.; Kansy, M.; Klinkhammer, U.; Lave, T.; Lohri, B.; Luft, F. C.; Mervaala, E. M.; Müller, D. N.; Müller, M.; Montavon, F.; Oefner, C.; Qiu, C.; Reichel, A.; Sanwald-Ducray, P.; Scalone, M.; Schleimer, M.; Schmid, R.; Stadler, H.; Treiber, A.; Valdenaire, O.; Vieira, E.; Waldmeier, P.; Wiegand-Chou, R.; Wilhelm, M.; Westl, W.; Zell, M.; Zell, R. Piperidine renin inhibitors: from leads to drug candidates. *Il Farmaco* **2001**, *56*, 21–27. (e) Bittner, B.; Chou, R.; Schleimer, M.; Morgenroth, B.; Zell, M.; Lavé, T. Preformulation approaches to improve the oral bioavailability of two novel piperidine renin inhibitors in dog. *Arzneim.-Forsch./Drug Res.* **2002**, *52*, 593–599.
  - (37) Keserü, G. M.; Makara, G. M. The influence of lead discovery strategies on the properties of drug candidates. *Nat. Rev. Drug Discovery* **2009**, *8*, 203–212.
  - (38) (a) Holsworth, D. D.; Jalaie, M.; Belliotti, T.; Cai, C.; Collard, W.; Ferreira, S.; Powell, N. A.; Stier, M.; Zhang, E.; McConnell, P.; Mochalkin, I.; Ryan, M. J.; Bryant, J.; Li, T.; Kasani, A.; Subedi, R.; Maiti, S. N.; Edmunds, J. J. Discovery of 6-ethyl-2,4-diaminopyrimidine-based small molecule renin inhibitors. *Bioorg. Med. Chem. Lett.* **2007**, *17*, 3575–3580. (b) Powell, N. A.; Ciske, F. L.; Cai, C.; Holsworth, D. D.; Mennen, K.; Van Huis, C. A.; Jalaie, M.; Day, J.; Mastronardi, M.; McConnell, P.; Mochalkin, I.; Zhang, E.; Ryan, M. J.; Bryant, J.; Collard, W.; Ferreira, S.; Gu, C.; Collins, R.; Edmunds, J. J. Rational design of 6-(2,4-diaminopyrimidinyl)-1,4-benzoxazin-3-ones as small molecule renin inhibitors. *Bioorg. Med.*



- Chem.* **2007**, *15*, 5912–5949. (c) Sarver, R. W.; Peevers, J.; Cody, W. L.; Ciske, F. L.; Dyer, J.; Emerson, S. D.; Hagadorn, J. C.; Holsworth, D. D.; Jalaie, M.; Kaufman, M.; Mastronardi, M.; McConnell, P.; Powell, N. A.; Quinn, J.; Van Huis, C. A.; Zhang, E.; Mochalkin, I. Binding thermodynamics of substituted diaminopyrimidine renin inhibitors. *Anal. Biochem.* **2007**, *360*, 30–40. (d) Holsworth, D. D.; Bury, M.; Cody, W. L.; Emerson, D.; Van Huis, C.; Jalaie, M.; Kaufman, M.; McConnell, P.; Powell, N. A.; Sahasrabudhe, P.; Sarver, R. W.; Thanabal, V.; Zhang, E. NMR Auxillary Binding Screen for Lead Optimization: Design of Novel Renin Inhibitors That Access Both the S2 and S3 Pockets of Renin. *Abstracts of Papers*, 231st National Meeting of the American Chemical Society: Atlanta, GA, March 26–30, 2006; American Chemical Society: Washington, DC, 2006; MEDI-086.
- (39) (a) Tice, C. M.; Xu, Z.; Yuan, J.; Simpson, R. D.; Cacatian, S. T.; Flaherty, P. T.; Zhao, W.; Guo, J.; Ishchenko, A.; Singh, S. B.; Wu, Z.; Scott, B. B.; Bukhtiyarov, Y.; Berbaum, J.; Mason, J.; Panemangalore, R.; Cappiello, M. G.; Mueller, D.; Harrison, R. K.; McGeehan, G. M.; Dillard, L. W.; Baldwin, J. J.; Claremon, D. A. Design and optimization of renin inhibitors: orally bioavailable alkyl amines. *Bioorg. Med. Chem. Lett.* **2009**, *19*, 3541–3545. (b) Xu, Z.; Cacatian, S.; Yuan, J.; Simpson, R. D.; Jia, L.; Zhao, W.; Tice, C. M.; Flaherty, P. T.; Guo, J.; Ishchenko, A.; Singh, S. B.; Wu, Z.; McKeever, B. M.; Scott, B. B.; Bukhtiyarov, Y.; Berbaum, J.; Mason, J.; Panemangalore, R.; Cappiello, M. G.; Bentley, R.; Doe, C. P.; Harrison, R. K.; McGeehan, G. M.; Dillard, L. W.; Baldwin, J. J.; Claremon, D. A. Optimization of orally bioavailable alkyl amine renin inhibitors. *Bioorg. Med. Chem. Lett.* **2010**, *20*, 694–699.
- (40) (a) Hills, I. D.; Vacca, J. P. Progress toward a practical BACE-1 inhibitor. *Curr. Opin. Drug Discovery Dev.* **2007**, *10*, 383–391. (b) Silvestri, R. Boom in the development of non-peptidic  $\beta$ -secretase (BACE1) inhibitors for the treatment of Alzheimer's disease. *Med. Res. Rev.* **2009**, *29*, 295–338.
- (41) Hong, L.; Koelsch, G.; Lin, X.; Wu, S.; Terzyan, S.; Ghosh, A. K.; Zhang, X. C.; Tang, J. Structure of the protease domain of memapsin 2 ( $\beta$ -secretase) complexed with inhibitor. *Science* **2000**, *290*, 150–153.
- (42) Nantermet, P. G.; Rajapakse, H. A.; Stanton, M. G.; Stauffer, S. R.; Barrow, J. C.; Grego, A. R.; Moore, K. P.; Steinbeiser, M. A.; Swestock, J.; Selnick, H. G.; Graham, S. L.; McGaughey, G. B.; Colussi, D.; Lai, M.-T.; Sankaranarayanan, S.; Simon, A. J.; Munshi, S.; Cook, J. J.; Holahan, M. A.; Michener, M. S.; Vacca, J. P. Evolution of tertiary carbinamine BACE-1 inhibitors:  $A\beta$  reduction in rhesus CSF upon oral dosing. *ChemMedChem* **2009**, *4*, 37–40.
- (43) Müller, G. Target Family-Directed Masterkeys in Chemogenomics. In *Chemogenomics in Drug Discovery: A Medicinal Chemistry Perspective*; Kubinyi, H., Mueller, G., Eds.; Wiley-VCH: Weinheim, Germany, 2004; pp 7–41.
- (44) Foundling, S. I.; Cooper, J.; Watson, F. E.; Cleasby, A.; Pearl, L. H.; Sibanda, B. L.; Hemmings, A.; Wood, S. P.; Blundell, T. L.; Valler, M. J.; Norey, C. G.; Kay, J.; Boger, J.; Dunn, B. M.; Leckie, B. J.; Jones, D. M.; Atrash, B.; Hallett, A.; Szelke, M. High resolution X-ray analyses of renin inhibitor–aspartic protease complexes. *Nature* **1987**, *327*, 349–352.
- (45) Blundell, T. L.; Cooper, J.; Foundling, S. I.; Jones, D. M.; Atrash, B.; Szelke, M. On the rational design of renin inhibitors: X-ray studies of aspartic proteinases complexed with transition-state analogs. *Biochemistry* **1987**, *26*, 5585–5590.
- (46) Brotherton-Pleiss, C. E.; Newman, S. R.; Waterbury, L. D.; Schwartzberg, M. S. Design and Synthesis of Conformationally Restricted Renin Inhibitors. *Peptides: Chemistry and Biology*, Proceedings of the 12th American Peptide Symposium, Cambridge, MA, 1991; Smith, J. A., Rivier, J. E., Eds.; Escam Science, Leiden, The Netherlands, 1992; pp 816–817.
- (47) (a) Plummer, M. S.; Shahripour, A.; Kaltenbronn, J. S.; Lunney, E. A.; Steinbaugh, B. A.; Hamby, J. M.; Hamilton, H. W.; Sawyer, T. K.; Humblet, C.; Doherty, A. M.; Taylor, M. D.; Hingorani, G.; Batley, B. L.; Rapundalo, S. T. Design and synthesis of renin inhibitors: Incorporation of transition-state isostere side chains that span from the S1 to the S3 binding pockets and examination of P3-modified renin inhibitors. *J. Med. Chem.* **1995**, *38*, 2893–2905. (b) Plummer, M.; Hamby, J. M.; Hingorani, G.; Batley, B. L.; Rapundalo, S. T. Peptidomimetic inhibitors of renin incorporating topographically modified isosteres spanning the P1(→P3)-P1 sites. *Bioorg. Med. Chem. Lett.* **1993**, *3*, 2119–2124.
- (48) Lefker, B. A.; Hada, W. A.; Wright, A. S.; Martin, W. H.; Stock, I. A.; Schulte, G. K.; Pandit, J.; Danley, D. E.; Ammirati, M. J.; Sneddon, S. F. Rational design, synthesis and X-ray structure of renin inhibitors with extended P1 side-chains. *Bioorg. Med. Chem. Lett.* **1995**, *5*, 2623–2626.
- (49) Göschke, R.; Stutz, S.; Rasetti, V.; Cohen, N. C.; Rahuel, J.; Rigollier, P.; Baum, H. P.; Forgiarini, P.; Schnell, C. R.; Wagner, T.; Grütter, M. G.; Fuhrer, W.; Schilling, W.; Cumin, F.; Wood, J. M.; Maibaum, J. Novel 2,7-dialkyl-substituted 5(S)-amino-4(S)-hydroxy-8-phenyl-octanecarboxamide transition state peptidomimetics are potent and orally active inhibitors of human renin. *J. Med. Chem.* **2007**, *50*, 4818–4831.
- (50) Hajduk, P. J.; Huth, J. R.; Fesik, S. W. D. Druggability indices for protein targets derived from NMR-based screening data. *J. Med. Chem.* **2005**, *48*, 2518–2525.
- (51) Rahuel, J.; Rasetti, V.; Maibaum, J.; Rüeger, H.; Göschke, R.; Cohen, N. C.; Stutz, S.; Cumin, F.; Fuhrer, W.; Wood, J. M.; Grütter, M. G. Structure-based drug design: the discovery of novel nonpeptide orally active inhibitors of human renin. *Chem. Biol.* **2000**, *7*, 493–504.
- (52) Cooper, J. B.; Foundling, S. I.; Blundell, T. L.; Arrowsmith, R. J.; Harris, C. J.; Champness, J. N. A rational approach to the design of antihypertensives: X-ray studies of complexes between aspartic proteinases and aminoalcohol renin inhibitors. *Top. Med. Chem.* **1988**, *65*, 308–313.
- (53) Arrowsmith, R. J.; Harris, C. J.; Davies, D. E.; Morton, J. A.; Dann, J. G.; Champness, J. N. The discovery and design of substrate-based proteinase inhibitors—problems and lessons from the development of renin inhibitors as potential antihypertensive drugs. *Spec. Publ.—R. Soc. Chem.* **1989**, *78* (Mol. Recognit.: Chem. Biochem. Probl.), 112–122.
- (54) Evans, B. E.; Rittle, K. E.; Bock, M. G.; Bennett, C. D.; DiPardo, R. M.; Boger, J.; Poe, M.; Ulm, E. H.; LaMont, B. I.; Blaine, E. H.; Fanelli, G. M.; Stabilito, I. I.; Veber, D. V. A uniquely potent renin inhibitor and its unanticipated plasma binding component. *J. Med. Chem.* **1985**, *28*, 1755–1756.
- (55) (a) Bezencon, O.; Bur, D.; Weller, T.; Richard-Bildstein, S.; Remen, L.; Sifferlen, T.; Corminboeuf, O.; Grisostomi, C.; Boss, C.; Prade, L.; Delahaye, S.; Treiber, A.; Strickner, P.; Binkert, C.; Hess, P.; Steiner, B.; Fischli, W. Design and preparation of potent, nonpeptidic, bioavailable renin inhibitors. *J. Med. Chem.* **2009**, *52*, 3689–3702. (b) Bezencon, O.; Bur, D.; Weller, T.; Richard-Bildstein, S.; Remen, L.; Sifferlen, T.; Corminboeuf, O.; Grisostomi, C.; Prade, L.; Delahaye, S.; Treiber, A.; Strickner, P.; Hess, P.; Steiner, B.; Fischli, W. Potent, Non-Peptidic, Bioavailable Renin Inhibitors. Presented at the 20th International Symposium on Medicinal Chemistry, EFMC-ISMC 2008, Vienna, Austria, Aug 31–Sep 4, **2008**; Poster P012. (c) Remen, L.; Bezencon, O.; Richard-Bildstein, S.; Bur, D.; Prade, L.; Corminboeuf, O.; Boss, C.; Grisostomi, C.; Sifferlen, T.; Strickner, P.; Hess, P.; Delahaye, S.; Treiber, A.; Weller, T.; Binkert, C.; Steiner, B.; Fischli, W. New classes of potent and bioavailable human renin inhibitors. *Bioorg. Med. Chem. Lett.* **2009**, *19*, 6762–6765.
- (56) Yamaguchi, Y.; Menear, K.; Cohen, N.-C.; Mah, R.; Cumin, F.; Schnell, C.; Wood, J. M.; Maibaum, J. The P1 *N*-isopropyl motif bearing hydroxyethylene dipeptide isostere analogs of aliskiren are in vitro potent inhibitors of the human aspartyl protease renin. *Bioorg. Med. Chem. Lett.* **2009**, *19*, 4863–4867.
- (57) Levens, N. R.; Peach, M. J.; Carey, R. M. Role of the intrarenal renin–angiotensin system in the control of renal function. *Circ. Res.* **1981**, *48*, 157–167.
- (58) (a) Cody, W. L.; Holsworth, D. D.; Powell, N. A.; Jalaie, M.; Zhang, E.; Wang, W.; Samas, B.; Bryant, J.; Ostroski, R.; Ryan, M. J.; Edmunds, J. J. The discovery and preparation of disubstituted novel amino-aryl-piperidine-based renin inhibitors. *Bioorg. Med. Chem.* **2005**, *13*, 59–68. (b) Powell, N. A.; Clay, E. H.; Holsworth, D. D.; Bryant, J. W.; Ryan, M. J.; Jalaie, M.; Zhang, E.; Edmunds, J. J. Equipotent activity in both enantiomers of a series of ketopiperazine-based renin inhibitors. *Bioorg. Med. Chem. Lett.* **2005**, *15*, 2371–2374. (c) Holsworth, D. D.; Powell, N. A.; Downing, D. M.; Cai, C.; Cody, W. L.; Ryan, J. M.; Ostroski, R.; Jalaie, M.; Bryant, J. W.; Edmunds, J. J. Discovery of novel non-peptidic ketopiperazine-based renin inhibitors. *Bioorg. Med. Chem.* **2005**, *13*, 2657–2664. (d) Powell, N. A.; Clay, E. H.; Holsworth, D. D.; Bryant, J. W.; Ryan, M. J.; Jalaie, M.; Edmunds, J. J. Benzyl ether structure–activity relationships in a series of ketopiperazine-based renin inhibitors. *Bioorg. Med. Chem. Lett.* **2005**, *15*, 4713–4716. (e) Holsworth, D. D.; Cai, C.; Cheng, X.-M.; Cody, W. L.; Downing, D. M.; Erasga, N.; Lee, C.; Powell, N. A.; Edmunds, J. J.; Stier, M.; Jalaie, M.; Zhang, E.; McConnell, P.; Ryan, M. J.; Bryant, J.; Li, T.; Kasani, A.; Hall, E.; Subedi, R.; Rahim, M.; Maiti, S. Ketopiperazine-based renin inhibitors: optimization of the “C” ring. *Bioorg. Med. Chem. Lett.* **2006**, *16*, 2500–2504. (f) Cai, C.; Bryant, J.; Cheng, X. M.; Cody, W. L.; Collard, W.; Downing, D. M.; Erasga, N.; Ferreira, S.; Hall, E.; Holsworth, D. D.; Jalaie, M.; Kasani, A.; Lee, C.; Li, T.; Maiti, S.; McConnell, P.; Powell, N. A.; Rahim, M.; Ryan, M.; Stier, M. A.; Subedi, R.; Zhang, E.; Edmunds, J. J. Ketopiperazine-Based Renin Inhibitors: Incorporation of Indole Rings. Presented at the 231st

- National Meeting of the American Chemical Society, Atlanta, GA, March 26–30, 2006; MEDI-091. PDB code 2g27. (g) Gu, C.; Collins, R.; Holsworth, D. D.; Walker, G. S.; Voorman, R. L. Metabolic aromatization of N-alkyl-1,2,3,4-tetrahydroquinoline substructures to quinolinium by human liver microsomes and horseradish peroxidase. *Drug Metab. Dispos.* **2006**, *34*, 2044–2055.
- (59) Ehara, T.; Grosche, P.; Irie, O.; Iwaki, Y.; Kanazawa, T.; Kawakami, S.; Konishi, K.; Mogi, M.; Suzuki, M.; Yokokawa, F. Preparation of 3,5-Substituted Piperidine Compounds as Renin Inhibitors. *PCT Int. Appl. WO 2007/077005A1*, 2007.
- (60) Herold, P.; Mah, R.; Tschinke, V.; Stutz, S.; Stojanovic, A.; Marti, C.; Behnke, D.; Jelakovic, S. Preparation of 5-Amino-4-hydroxy-7-[imidazo[1,2-a]pyridin-6-ylmethyl]-8-methylnonanamide and Related Compounds as Renin Inhibitors for Treatment of Hypertension. *PCT Int. Appl. WO2007/031558A1*, 2007.
- (61) Hanson, G. J.; Clare, M.; Summers, N. L.; Lim, L. W.; Neidhart, D. J.; Shieh, H. S.; Stevens, A. N. Renin inhibitor SC-51106 complexed with human renin: discovery of a new binding site adjacent to P3. *Bioorg. Med. Chem.* **1994**, *2*, 909–918.
- (62) Tong, L.; Pav, S.; Lamarre, D.; Pilote, L.; LaPlante, S.; Anderson, P. C.; Jung, G. High resolution crystal structures of recombinant human renin in complex with polyhydroxymonoamide inhibitors. *J. Mol. Biol.* **1995**, *250*, 211–222.
- (63) Lefker, B. Structure Based Drug Design. Rational Design of Non-Peptide Enzyme Inhibitors. Presented at the 1st Winter Conference on Medicinal and Bioorganic Chemistry, Steamboat Springs, CO, January 29–February 2, 1995. The author (J.M.) is grateful to Dr. Hans-Peter Märki (Hoffman-La Roche, Basel, Switzerland) for bringing this paper to his attention and to Dr. Bruce Lefker (Pfizer, Groton, CT) for providing a copy of the 1995 presentation. The X-ray structure of **27** in complex with renin has not been published to date.
- (64) For the first report on the presence of the S<sub>3</sub> subpocket (S<sub>3</sub><sup>SP</sup>) in BACE-1: Coburn, C. A.; Stachel, S. J.; Li, Y.-M.; Rush, D. M.; Steele, T. G.; Chen-Dodson, E.; Holloway, M. K.; Xu, M.; Huang, Q.; Lai, M.-T.; DiMuzio, J.; Crouthamel, M.-C.; Shi, X.-P.; Sardana, V.; Chen, Z.; Munshi, S.; Kuo, L.; Makara, G. M.; Annis, D. A.; Tadikonda, P. K.; Nash, H. M.; Vacca, J. P. Identification of a small molecule nonpeptide active site  $\beta$ -secretase inhibitor that displays a nontraditional binding mode for aspartyl proteases. *J. Med. Chem.* **2004**, *47*, 6117–6119. See also the following: Stauffer, S. R.; Stanton, M. G.; Grego, A. R.; Steinbeiser, M. A.; Shaffer, J. R.; Nantermet, P. G.; Barrow, J. C.; Rittle, K. E.; Collusi, D.; Espeseth, A. S.; Lai, M.-T.; Pietrak, B. L.; Holloway, M. K.; McGaughey, G. B.; Munshi, S. K.; Hochman, J. H.; Simon, A. J.; Selnick, H. G.; Graham, S. L.; Vacca, J. P. Discovery and SAR of isonicotinamide BACE-1 inhibitors that bind  $\beta$ -secretase in a N-terminal 10s-loop down conformation. *Bioorg. Med. Chem. Lett.* **2007**, *17*, 1788–1792.
- (65) Parry, M. J.; Russel, A. B.; Szelke, M. Bio-Isosteres of a Peptide Renin Inhibitor. In *Chemistry and Biology of Peptides*; Meinehofer, J., Ed.; Ann Arbor Science Publishers: Ann Arbor, MI, 1972; pp 541–544.
- (66) Szelke, M.; Leckie, B.; Hallett, A.; Jones, D. M.; Sueiras, J.; Attrash, B.; Lever, A. F. Potent new inhibitors of human renin. *Nature* **1982**, *299*, 555–557.
- (67) Webb, D. J.; Manhem, P. J. O.; Ball, S. G.; Inglis, G.; Leckie, B. J.; Lever, A. F.; Morton, J. J.; Robertson, J. I. S.; Murray, G. D.; Ménard, J.; Hallett, A.; Jones, D. M.; Szelke, M. A study of the renin inhibitor H142 in man. *J. Hypertens.* **1985**, *3*, 653–658.
- (68) James, M. N. G.; Sielecki, A. R. Stereochemical analysis of peptide bond hydrolysis catalyzed by the aspartic proteinase penicillopepsin. *Biochemistry* **1985**, *24*, 3701–3713. The high-resolution X-ray structure of porcine pepsinogen (PDB code 2psg) has shown the N-terminal sequence of the zymogen to fold back into the intact active site conformation, forming electrostatic interactions of the Lys<sub>36</sub> side chain amine with both Asp<sub>32</sub> and Asp<sub>215</sub> as a self-inhibitory mechanism preventing substrate binding: Sielecki, A. R.; Fujinaga, M.; Read, R. J.; James, M. N. G. Refined structure of porcine pepsinogen at 1.8 Å resolution. *J. Mol. Biol.* **1991**, *219*, 671–692.
- (69) Boger, J.; Lohr, N. S.; Ulm, E. H.; Poe, M.; Blaine, E. H.; Fanelli, G. M.; Lin, T.-Y.; Payne, L. S.; Schorn, T. W.; LaMont, B. I.; Vassil, T. C.; Sabilito, I. I.; Veber, D. F.; Rich, D. H.; Boparai, A. S. Novel renin inhibitors containing the amino acid statine. *Nature* **1983**, *303*, 81–84.
- (70) (a) Sueiras-Diaz, J.; Jones, D. M.; Szelke, M.; Leckie, B. J.; Beattie, S. R.; Beattie, C.; Morton, J. J. Potent in vivo inhibitors of rat renin: analogs of human and rat angiotensinogen sequences containing different classes of pseudodipeptides at the scissile site. *J. Pept. Res.* **1997**, *50*, 239–247. (b) Jones, D. M.; Leckie, B. J.; Svensson, L.; Szelke, M. A Novel Non-Hydrolyzable Isostere of the Peptide Transition State and a New Synthesis of the Hydroxy-ethylene Isostere. *Peptides: Chemistry, Structure and Biology*, Proceedings of the 11th Peptide Symposium; Escam: Leiden, The Netherlands, 1990; pp 971–972.
- (71) Yang, W.; Lu, W.; Lu, Y.; Zhong, M.; Sun, J.; Thomas, A. E.; Wilkinson, J. M.; Fucini, R. V.; Lam, M.; Randal, M.; Shi, X.-P.; Jacobs, J. W.; McDowell, R. S.; Gordon, E. M.; Ballinger, M. D. Aminoethylenes, a tetrahedral intermediate isostere yielding potent inhibitors of the aspartyl protease BACE-1. *J. Med. Chem.* **2006**, *49*, 839–842.
- (72) (a) Jones, M.; Sueiras-Diaz, J.; Szelke, M.; Leckie, B.; Beattie, S. Renin Inhibitors Containing the Novel Amino Acid 3-Amino-deoxystatine. *Peptides: Structure and Function*, Proceedings of the 9th American Peptide Symposium; Pierce Chemical Company: Rockford, IL, 1985; pp 759–762. (b) Arrowsmith, R. J.; Carter, K.; Dann, J. G.; Davies, D. E.; Harris, C. J.; Morton, J. A.; Lister, P.; Robinson, J. A.; Williams, D. J. Novel renin inhibitors: synthesis of aminostatine and comparison with statine-containing analogs. *J. Chem. Soc., Chem. Commun.* **1986**, *10*, 755–757. (c) Thaisrivongs, S.; Schostarez, H. J.; Pals, D. T.; Turner, S. R.  $\alpha,\alpha$ -Difluoro- $\beta$ -aminodeoxystatine-containing renin-inhibitory peptides. *J. Med. Chem.* **1987**, *30*, 1837–1842.
- (73) Bradbury, R. H.; Rivett, J. E. 1,2,4-Triazololo[4,3-a]pyrazine derivatives with human renin inhibitory activity. 3. Synthesis and biological properties of aminodeoxystatine and difluorostatone derivatives. *J. Med. Chem.* **1991**, *34*, 151–157.
- (74) Dann, J. G.; Stammers, D. K.; Harris, C. J.; Arrowsmith, R. J.; Davies, D. E.; Hardy, G. W.; Morton, J. A. Human renin: a new class of inhibitors. *Biochem. Biophys. Res. Commun.* **1986**, *134*, 71–77.
- (75) (a) Arrowsmith, R. J.; Dann, J. G.; Davies, D. E.; Fogden, Y. C.; Harris, C. J.; Morton, J. A.; Ogden, H. Inhibitors of Human Renin: Synthesis and Comparative SAR of P3-P1 Tripeptide-Based Aminoalcohols. *Peptides 1988*, Proceedings of the 20th European Peptide Symposium, Sep 4–9, 1988; W. de Gruyter: Berlin, Germany, 1989; pp 393–395. (b) Breipohl, G.; Geiger, R.; Henke, S.; Kleeman, H. W.; Knolle, J.; Ruppert, D.; Schoelkens, B. A.; Urbach, H.; Wagner, A.; Wegmann, H. Studies on renin inhibitors. *Spec. Publ.-R. Soc. Chem.* **1988**, *65* (Top. Med. Chem.), 101–127. (c) Luly, J. R.; Yi, N.; Soderquist, J.; Stein, H.; Cohen, J.; Perun, T. J.; Plattner, J. J. New inhibitors of human renin that contain novel Leu-Val replacements. *J. Med. Chem.* **1987**, *30*, 1609–1616.
- (76) (a) Wlodawer, A.; Vondrasek, J. Inhibitors of HIV-1 protease: a major success of structure-assisted drug design. *Annu. Rev. Biophys. Biomol. Struct.* **1998**, *27*, 249–284. (b) Wlodawer, A. Rational approach to AIDS drug design through structural biology. *Annu. Rev. Med.* **2002**, *53*, 595–614.
- (77) (a) Zürcher, M.; Gottschalk, T.; Meyer, S.; Bur, D.; Diederich, F. Exploring the flap pocket of the antimalarial target plasmeprin II: the “55 % rule” applied to enzymes. *ChemMedChem* **2008**, *3*, 237–240. (b) Bjelic, S.; Nervall, M.; Gutierrez-de-Teran, H.; Ersmark, K.; Hallberg, A.; Aqvist, J. Computational inhibitor design against malaria plasmeprins. *Cell. Mol. Life Sci.* **2007**, *64*, 2285–2305. (c) Luksch, T.; Chan, N.-S.; Brass, S.; Sotriffer, C. A.; Klebe, G.; Diederich, W. E. Computer-aided design and synthesis of nonpeptidic plasmeprin II and IV inhibitors. *ChemMedChem* **2008**, *3*, 1323–1336.
- (78) Marcinkeviciene, J.; Kopcho, L. M.; Yang, T.; Copeland, R. A.; Glass, B. M.; Combs, A. P.; Falahatpisheh, N.; Thompson, L. Novel inhibition of porcine pepsin by a substituted piperidine. Preference for one of the enzyme conformers. *J. Biol. Chem.* **2002**, *277*, 28677–28682.
- (79) Specker, E.; Böttcher, J.; Brass, S.; Heine, A.; Lilie, H.; Schoop, A.; Müller, G.; Griebenow, N.; Klebe, G. Unexpected novel binding mode of pyrrolidine-based aspartyl protease inhibitors: design, synthesis and crystal structure in complex with HIV protease. *ChemMedChem* **2006**, *1*, 106–117.
- (80) Barrow, J. C.; Stauffer, S. R.; Rittle, K. E.; Ngo, P. L.; Yang, Z.; Selnick, H. G.; Graham, S. L.; Munshi, S.; McGaughey, G. B.; Holloway, M. K.; Simon, A. J.; Price, E. A.; Sankaranarayanan, S.; Collusi, D.; Tugusheva, K.; Lai, M.-T.; Espeseth, A. S.; Xu, M.; Huang, Q.; Wolfe, A.; Pietrak, B.; Zuck, P.; Levorse, D. A.; Hazuda, D.; Vacca, J. P. Discovery and X-ray crystallographic analysis of a spiro-piperidine iminohydantoin inhibitor of  $\beta$ -secretase. *J. Med. Chem.* **2008**, *51*, 6259–6262. See also: Kuglstatler, A.; Stahl, M.; Peters, J.-U.; Huber, W.; Stihle, M.; Schlatter, D.; Benz, J.; Ruf, A.; Roth, D.; Enderle, T.; Hennig, M. Tyramine fragment binding to BACE-1. *Bioorg. Med. Chem. Lett.* **2008**, *18*, 1304–1307.
- (81) (a) Congreve, M.; Aharony, D.; Albert, J.; Callaghan, O.; Campbell, J.; Carr, R. A. E.; Chessari, G.; Cowan, S.; Edwards, P. D.; Frederickson, M.; McMenamin, R.; Murray, C. W.; Patel, S.; Wallis, N. Application of fragment screening by X-ray crystallography to the discovery of aminopyridines as inhibitors of  $\beta$ -secretase. *J. Med. Chem.* **2007**, *50*, 1124–1132. (b) Murray, C. W.;



- Callaghan, O.; Chessari, G.; Cleasby, A.; Congreve, M.; Frederickson, M.; Hartshorn, M. J.; McMenamin, R.; Patel, S.; Wallis, N. Application of fragment screening by X-ray crystallography to  $\beta$ -Secretase. *J. Med. Chem.* **2007**, *50*, 1116–1123.
- (82) Coburn, C. A.; Stachel, S. J.; Jones, K. G.; Steele, T. G.; Rush, D. M.; DiMuzio, J.; Pietrak, B. L.; Lai, M.-T.; Huang, Q.; Lineberger, J.; Jin, L.; Munshi, S.; Holloway, M. K.; Espeseth, A.; Simon, A.; Hazuda, D.; Graham, S. L.; Vacca, J. P. BACE-1 inhibition by a series of  $\psi$ [CH<sub>2</sub>NH] reduced amide isosteres. *Bioorg. Med. Chem. Lett.* **2006**, *16*, 3635–3638.
- (83) (a) Baldwin, J. J.; Claremon, D. A.; Tice, C.; Cacatian, S.; Dillard, L. W.; Ishchenko, A. V.; Yuan, J.; Xu, Z.; McGeehan, G.; Simpson, R. D.; Singh, S. B.; Zhao, W.; Flaherty, P. T. Piperidine Derivatives as Aspartic Protease Inhibitors and Their Preparation, Pharmaceutical Compositions and Use in the Treatment of Aspartic Protease Mediated Diseases. PCT Int. Appl. WO2007/070201A1, 2007. (b) See, for example, the following: Baldwin, J. J.; Cacatian, S.; Claremon, D.; Dillard, L. W.; Flaherty, P. T.; Ghavimi-Alagha, B.; Ghirlanda, D.; Ishchenko, A. V.; Kallander, L. S.; Lawhorn, B.; Lu, Q.; McGeehan, G.; Terrell, L. R.; Zhang, J.; Leach, C. A.; Stoy, P.; Patterson, J. R.; Simpson, R. D.; Singh, S. B.; Tice, C.; Xu, Z.; Yuan, C. C. K.; Zhao, W. Preparation of Substituted Benzoyl-piperidine Derivatives and Analogs as Renin Inhibitors. PCT Int. Appl. WO2008/124575A1, 2008.
- (84) Prade, L.; Jones, A. F.; Boss, C.; Richard-Blichstein, S.; Meyer, S.; Binkert, S.; Bur, D. X-ray structure of plasmepsin II complexed with a potent achiral inhibitor. *J. Biol. Chem.* **2005**, *280*, 23837–23843.
- (85) (a) Mervaala, E. M. A.; Müller, D. N.; Park, J. K.; Schmidt, F.; Lohn, M.; Breu, V.; Dragun, D.; Ganten, D.; Haller, H.; Luft, F. C. Monocyte infiltration and adhesion molecules in a rat model of high human renin hypertension. *Hypertension* **1999**, *33*, 389–395. (b) Mervaala, E.; Müller, D. N.; Schmidt, F.; Park, J. K.; Gross, V.; Bader, M.; Breu, V.; Ganten, D.; Haller, H.; Luft, F. C. Blood pressure-independent effects in rats with human renin and angiotensinogen genes. *Hypertension* **2000**, *35*, 587–594.
- (86) Lipinski, C. A.; Lombardo, F.; Dominy, B. W.; Feeney, P. J. Experimental and computational approaches to estimate solubility and permeability in drug discovery and development settings. *Adv. Drug Delivery Rev.* **2001**, *46*, 3–26.
- (87) Boehr, D. D.; Nussinov, R.; Wright, P. E. The role of dynamic conformational ensembles in biomolecular recognition. *Nat. Chem. Biol.* **2009**, *5*, 789–796.
- (88) Freire, E. Isothermal titration calorimetry: controlling binding forces in lead optimization. *Drug Discovery Today: Technol.* **2004**, *1*, 295–299.
- (89) Brenke, R.; Kozakov, D.; Chuang, G.-Y.; Beglov, D.; Hall, D.; Landon, M. R.; Mattos, C.; Vajda, S. Fragment-based identification of druggable “hot-spots” of proteins using Fourier domain correlation techniques. *Bioinformatics* **2009**, *25*, 621–627.
- (90) (a) Dash, C.; Kulkarni, A.; Dunn, B.; Rao, M. Aspartic peptidase inhibitors: implications in drug development. *Crit. Rev. Biochem. Mol. Biol.* **2003**, *38*, 89–119. (b) Zaidi, N.; Hermann, C.; Herrmann, T.; Kalbacher, H. Emerging functional roles of cathepsin E. *Biochem. Biophys. Res. Commun.* **2008**, *377*, 327–330.
- (91) Rao, C. M.; Scarborough, P. E.; Kay, J.; Batley, B.; Rapundalo, S.; Klutchko, S.; Taylor, M. D.; Lunney, E. A.; Humblet, C. C.; Dunn, B. M. Specificity in the binding of inhibitors to the active site of human/primate aspartic proteinases: analysis of P2-P1-P1'-P2' variation. *J. Med. Chem.* **1993**, *36*, 2614–2620.
- (92) (a) Faller, B.; Urban, L., Eds. *Hit and Lead Profiling, Identification and Optimization of Drug-like Molecules*. Methods and Principles in Medicinal Chemistry, Vol. 43; Wiley-VCH: Weinheim, Germany, 2009. (b) Hamon, J.; Whitebread, S.; Techer-Etienne, V.; Le Coq, H.; Azzaoui, K.; Urban, L. In vitro safety pharmacology profiling: What else beyond hERG? *Future Med. Chem.* **2009**, *1*, 645–665.
- (93) Beaumont, K.; Smith, D. A. Does human pharmacokinetic prediction add significant value to compound selection in drug discovery research? *Curr. Opin. Drug Discovery Dev.* **2009**, *12*, 61–71.
- (94) Leeson, P. D.; Springthorpe, B. The influence of drug-like concepts on decision-making in medicinal chemistry. *Nat. Rev. Drug Discovery* **2007**, *6*, 881–890.
- (95) Hughes, J. D.; Blagg, J.; Price, D. A.; Bailey, S.; DeCrescenzo, G. A.; Devraj, R. V.; Ellsworth, E.; Fobian, Y. M.; Gibbs, M. E.; Gilles, R. W.; Greene, N.; Huang, E.; Krieger-Burke, T.; Loesel, J.; Wager, T.; Whiteley, L.; Zhang, Y. Physicochemical drug properties associated with in vivo toxicological outcomes. *Bioorg. Med. Chem. Lett.* **2008**, *18*, 4872–4875.
- (96) Major, T. C.; Olszewski, B.; Rosebury, W.; Okerberg, C.; Carlson, T.; Ostroski, R.; Schroeder, R.; Kowala, M. C.; Leadley, R. A. nonpeptide, piperidine renin inhibitor provides renal and cardiac protection in double-transgenic mice expressing human renin and angiotensinogen genes. *Cardiovasc. Drugs* **2008**, *22*, 469–478.
- (97) (a) Rossenbacker, T.; Priori, S. New insights into the long-QT syndrome. *Rev. Esp. Cardiol.* **2007**, *60*, 675–682. (b) Cavalli, A.; Poluzzi, E.; De Ponti, F.; Recanatini, M. Toward a pharmacophore for drugs inducing the long QT syndrome: insights from a COMFA study of hERG K<sup>+</sup> channel blockers. *J. Med. Chem.* **2002**, *45*, 3844–3853. (c) Pearlstein, R.; Vaz, R.; Rampe, D. Understanding the structure–activity relationship of the human ether-a-go-go-related gene cardiac K<sup>+</sup> channel. A model for bad behavior. *J. Med. Chem.* **2003**, *46*, 2017–2022.
- (98) Ayalalomasajula, S.; Yeh, C.-M.; Vaidyanathan, S.; Flannery, B.; Dieterich, H. A.; Howard, D.; Bedigian, M. P.; Dole, W. P. Effects of aliskiren, a direct renin inhibitor, on cardiac repolarization and conduction in healthy subjects. *J. Clin. Pharmacol.* **2008**, *48*, 799–811.
- (99) (a) Huang, C.-J.; Harootunian, A.; Maher, M. P.; Quan, C.; Raj, C. D.; McCormack, K.; Numann, R.; Negulescu, P. A.; González, J. E. Characterization of voltage-gated sodium-channel lockers by electrical stimulation and fluorescence detection of membrane potential. *Nat. Biotechnol.* **2006**, *24*, 439–446. (b) Balsler, J. R. The cardiac sodium channel: gating function and molecular pharmacology. *J. Mol. Cell. Cardiol.* **2001**, *33*, 599–613.
- (100) Splawski, I.; Timothy, K. W.; Decher, N.; Kumar, P.; Sachse, F. B.; Beggs, A. H.; Sanguinetti, M. C.; Keating, M. T. Severe arrhythmia disorder caused by cardiac L-type calcium channel mutations. *Proc. Natl. Acad. Sci. U.S.A.* **2005**, *102*, 8089–8096.
- (101) Oliver, W. J.; Gross, F. Unique specificity of mouse angiotensinogen to homologous renin. *Proc. Soc. Exp. Biol. Med.* **1966**, *122*, 923–926.
- (102) Lin, C.; Frishman, W. H. Renin inhibition: a novel therapy for cardiovascular disease. *Am. Heart J.* **1996**, *131*, 1024–1034.
- (103) Wood, J. M.; Gulati, N.; Forgiarini, P.; Fuhrer, W.; Hofbauer, K. G. Effects of a specific and long-acting renin inhibitor in the marmoset. *Hypertension* **1985**, *7*, 797–803.
- (104) Wood, J. M.; Schnell, C. R.; Cumin, F.; Menard, J.; Webb, R. L. Aliskiren, a novel, orally effective renin inhibitor, lowers blood pressure in marmosets and spontaneously hypertensive rats. *J. Hypertens.* **2005**, *23*, 417–426.
- (105) Fossa, A. A.; DePasquale, M. J.; Ringer, L. J.; Winslow, R. L. Synergistic effect on reduction in blood pressure with coadministration of a renin inhibitor or an angiotensin-converting enzyme inhibitor with an angiotensin II receptor antagonist. *Drug Dev. Res.* **1994**, *33*, 422–428.
- (106) Ohkubo, H.; Kawakami, H.; Kakehi, Y.; Takumi, T.; Arai, H.; Yokota, Y.; Iwai, M.; Tanabe, Y.; Masu, M.; Hata, J.; Iwao, H.; Okamoto, H.; Yokoyama, M.; Nomura, T.; Katsuki, M.; Nakanishi, S. Generation of transgenic mice with elevated blood pressure by introduction of the rat renin and angiotensinogen genes. *Proc. Natl. Acad. Sci. U.S.A.* **1990**, *87*, 5153–5157.
- (107) Bohlender, J.; Fukamizu, A.; Lippoldt, A.; Nomura, T.; Dietz, R.; Menard, J.; Murakami, K.; Luft, F. C.; Ganten, D. High human renin hypertension in transgenic rats. *Hypertension* **1997**, *29*, 428–434.
- (108) Shimokama, T.; Haraoka, S.; Horiguchi, H.; Sugiyama, F.; Murakami, K.; Watanabe, T. The Tsukuba hypertensive mouse (transgenic mouse carrying human genes for both renin and angiotensinogen) as a model of human malignant hypertension: development of lesions and morphometric analysis. *Virchows Arch* **1998**, *432*, 169–175.
- (109) Dechend, R.; Shagdarsuren, E.; Gratzke, P.; Fiebeler, A.; Pilz, B.; Meiners, S.; Derer, W.; Feldman, D. L.; Webb, R. L.; Müller, D. N. Low dose inhibitor and low dose AT1 receptor blocker therapy ameliorate target organ change in rats harbouring renin and angiotensinogen genes. *J. Renin–Angiotensin–Aldosterone Syst.* **2007**, *8*, 81–84.
- (110) Feldman, D. L.; Jin, L.; Xuan, H.; Contrepas, A.; Zhou, Y.; Webb, R. L.; Müller, D. N.; Feldt, S.; Cumin, F.; Maniara, W.; Persohn, E.; Schuetz, H.; Danser, A. H. J.; Nguyen, G. Effects of aliskiren on blood pressure, albuminuria, and (pro)renin receptor expression in diabetic TG(mRen-2)27 rats. *Hypertension* **2008**, *52*, 130–136.
- (111) Kelly, D. J.; Zhang, Y.; Moe, G.; Naik, G.; Gilbert, R. E. Aliskiren, a novel renin inhibitor, is renoprotective in a model of advanced diabetic nephropathy in rats. *Diabetologia* **2007**, *50*, 2398–2404.
- (112) Lastra, G.; Habibi, J.; Whaley-Connell, A. T.; Manrique, C.; Hayden, M. R.; Rehmer, J.; Patel, K.; Ferrario, C.; Sowers, J. R. Direct renin inhibition improves systemic insulin resistance and skeletal muscle glucose transport in a transgenic rodent model



- of tissue renin overexpression. *Endocrinology* **2009**, *150*, 2561–2568.
- (113) Habibi, J.; Whaley-Connell, A.; Hayden, M. R.; DeMarco, V. G.; Schneider, R.; Sowers, S. D.; Karuparthi, P.; Ferrario, C. M.; Sowers, J. R. Renin inhibition attenuates insulin resistance, oxidative stress, and pancreatic remodeling in the transgenic Ren2 rat. *Endocrinology* **2008**, *149*, 5643–5653.
- (114) Whaley-Connell, A.; Habibi, J.; Cooper, S. A.; DeMarco, V. G.; Hayden, M. R.; Stump, C. S.; Link, D.; Ferrario, C. M.; Sowers, J. R. Effect of renin inhibition and AT1R blockade on myocardial remodeling in the transgenic Ren2 rat. *Am. J. Physiol.: Endocrinol. Metab.* **2008**, *295*, E103–E109.
- (115) Müller, D. N.; Luft, F. C. Direct renin inhibition with aliskiren in hypertension and target organ damage. *Clin. J. Am. Soc. Nephrol.* **2006**, *1*, 221–228.
- (116) Lu, H.; Rateri, D. L.; Feldman, D. L.; Charnigo, R. J.; Fukamizu, A.; Ishida, J.; Oesterling, E. G.; Cassis, L. A.; Daugherty, A. Renin inhibition reduces hypercholesterolemia-induced atherosclerosis in mice. *J. Clin. Invest.* **2008**, *118*, 984–993.
- (117) Nussberger, J.; Aubert, J. F.; Bouzourene, K.; Pellegrin, M.; Haypz, D.; Mazzolai, L. Renin inhibition by aliskiren prevents atherosclerosis progression. *Hypertension* **2008**, *51*, 1306–1311.
- (118) Imanishi, T.; Tsujioka, H.; Ikejima, H.; Kuroi, A.; Takarada, S.; Kitabata, H.; Tanimoto, T.; Muragaki, Y.; Mochizuki, S.; Goto, M.; Yoshida, K.; Akasaka, T. Renin inhibitor aliskiren improves impaired nitric oxide bioavailability and protects against atherosclerotic changes. *Hypertension* **2008**, *52*, 563–572.
- (119) Luft, F. C. Renin inhibition and atherosclerosis. *Nephrol., Dial., Transplant.* **2008**, *23*, 2474–2476.
- (120) Kumar, R.; Singh, V. P.; Baker, K. M. The intracellular renin–angiotensin system: a new paradigm. *Trends Endocrinol. Metab.* **2007**, *18*, 208–214.
- (121) Cook, J. L.; Zhang, Z.; Re, R. N. In vitro evidence for an intracellular site of angiotensin action. *Circ. Res.* **2001**, *89*, 1138–1146.
- (122) Singh, V. P.; Baker, K. M.; Kumar, R. Activation of the intracellular renin–angiotensin system in cardiac fibroblasts by high glucose: role in extracellular matrix production. *Am. J. Physiol.: Heart Circ. Physiol.* **2008**, *294*, H1675–H1684.
- (123) Singh, V. P.; Le, B.; Khode, R.; Baker, K. M.; Kumar, R. Intracellular angiotensin II production in diabetic rats is correlated with cardiomyocyte apoptosis, oxidative stress, and cardiac fibrosis. *Diabetes* **2008**, *57*, 3297–3306.
- (124) Navar, L. G.; Langford, H. G. Effects of Angiotensin on the Renal Circulation. In *Angiotensin*; Page, I. H., Bumpus, F. M., Eds.; Springer-Verlag: New York, 1974; pp 455–474.
- (125) Johnston, C. I. Angiotensin Converting Enzyme Inhibitors. In *Handbook of Hypertension. Clinical Pharmacology of Antihypertensive Drugs*; Doyle, A. E., Ed.; Elsevier: Amsterdam, 1984; Vol. 5, pp 272–311.
- (126) Zimmerman, B. G. Blocking and agonistic actions of angiotensin antagonists in normotensive and hypertensive dogs. *Cardiovasc. Med. N.Y.* **1979**, *4*, 231–241.
- (127) Neisius, D.; Wood, J. M.; Hofbauer, K. G. Renal vasodilatation after inhibition of renin or converting enzyme in marmoset. *Am. J. Physiol.* **1986**, *251*, H897–H902.
- (128) Verburg, K. M.; Kleinert, H. D.; Chekal, M. A.; Kadam, J. R. C.; Young, G. A. Renal hemodynamic and excretory responses to renin inhibition induced by A-64662. *J. Pharmacol. Exp. Ther.* **1990**, *252*, 449–455.
- (129) (a) Fischli, W.; Clozel, J. P.; El Amrani, K.; Wostl, W.; Neidhart, W.; Stadler, H.; Branca, Z. Ro 42-5892 is a potent orally active renin inhibitor in primates. *Hypertension* **1991**, *18*, 22–31. (b) Fischli, W.; Clozel, J. P.; Breu, V.; Buchmann, S.; Mathews, S.; Stadler, H.; Vieira, E.; Wostl, W. Ciprokren (Ro 44-9375): a renin inhibitor with increasing effects on chronic treatment. *Hypertension* **1994**, *24*, 163–169.
- (130) Clozel, J. P.; Fischli, W. Comparative effects of three different potent renin inhibitors in primates. *Hypertension* **1993**, *22*, 9–17.
- (131) Richter, W. F.; Whitby, B. R.; Chou, R. C. Distribution of remikiren, a potent orally active inhibitor of human renin, in laboratory animals. *Xenobiotica* **1996**, *26*, 243–254.
- (132) El Amrani, A. K.; Menard, J.; Gonzales, M. F.; Michel, J. B. Effects of blocking the angiotensin II receptor, converting enzyme, and renin activity on the renal hemodynamics of normotensive guinea pigs. *J. Cardiovasc. Pharmacol.* **1993**, *22*, 231–239.
- (133) Cordero, P.; Fisher, N. D.; Moore, T. J.; Gleason, R.; Williams, G. H.; Hollenberg, N. K. Renal and endocrine responses to a renin inhibitor, enalkiren, in normal humans. *Hypertension* **1991**, *17*, 510–516.
- (134) Fisher, N. D. L.; Allan, D.; Kifor, I.; Gaboury, C. L.; Williams, G. H.; Moore, T. J.; Hollenberg, N. K. Responses to converting enzyme and renin inhibition. *Hypertension* **1994**, *23*, 44–51.
- (135) Fisher, N. D. L.; Hollenberg, N. Renal vascular responses to renin inhibition with zankiren in men. *Clin. Pharmacol. Ther.* **1995**, *57*, 342–348.
- (136) Fisher, N. D. L.; Danser, A. H. J.; Nussberger, J.; Dole, W. P.; Hollenberg, N. K. Renal and hormonal responses to direct renin inhibition with aliskiren in healthy humans. *Circulation* **2008**, *117*, 3199–3205.
- (137) Feldman, D. L.; Persohn, E.; Schuetz, H.; Jin, L.; Miserendino-Moltini, R.; Xuan, H.; Zhuang, S.; Zhou, W. Renal localization of the renin inhibitor aliskiren. *J. Clin. Hypertens.* **2006**, *8*, A80–A81.
- (138) Krop, M.; Garrelds, I. M.; de Bruin, J. A.; van Gool, J. M. G.; Fisher, N. D. L.; Hollenberg, N. K.; Danser, A. H. J. Aliskiren accumulates in renin secretory granules and binds plasma prorenin. *Hypertension* **2008**, *52*, 1076–1083.
- (139) Feldt, S.; Maschke, U.; Dechend, R.; Luft, F. C.; Müller, D. N. The putative (pro)renin receptor blocker HRP fails to prevent (pro)renin signaling. *J. Am. Soc. Nephrol.* **2008**, *19*, 743–748.
- (140) Durvasula, R. V.; Shankland, S. J. Activation of a local renin angiotensin system in podocytes by glucose. *Am. J. Physiol.: Renal Physiol.* **2008**, *294*, F830–F839.
- (141) Parving, H. H.; Persson, F.; Lewis, J. B.; Lewis, E. J.; Hollenberg, N. K. Aliskiren combined with losartan in type 2 diabetes and nephropathy. *N. Engl. J. Med.* **2008**, *358*, 2433–2446.
- (142) Hsueh, W. A.; Carlson, E. J.; Dzau, V. J. Characterization of inactive renin from human kidney and plasma: evidence of a renal source of circulating inactive renin. *J. Clin. Invest.* **1983**, *71*, 506–517.
- (143) Reudelhuber, T. L.; Mercure, C.; Ramla, D.; Methot, D.; Postonvd, A. Y. Molecular Mechanisms of Processing and Sorting in Renin Secretion. In *Hypertension: Pathophysiology, Diagnosis and Management*; Laragh, J. H., Brenner, B. M., Eds.; Raven Press: New York, 1995; pp 1621–1636.
- (144) Nielsen, A. H.; Poulsen, K. Is prorenin of physiological and clinical significance? *J. Hypertens.* **1988**, *6*, 949–958.
- (145) Luetscher, J. A.; Draemer, F. B.; Wilson, D. M.; Schwartz, H. C.; Bryer-Ash, M. Increased plasma inactive renin in diabetes mellitus. *N. Engl. J. Med.* **1985**, *312*, 1412–1417.
- (146) Sealey, J. E.; Catanzaro, D. F.; Lavin, T. N.; Gahnm, F.; Pitarresi, T.; Hu, L. F.; Laragh, J. H. Specific prorenin/renin binding (ProBP): identification and characterization of a novel membrane site. *Am. J. Hypertens.* **1996**, *9*, 491–502.
- (147) Campbell, D. J.; Valentijn, A. J. Identification of vascular renin-binding proteins by chemical cross-linking: inhibition of binding of renin by renin inhibitors. *J. Hypertens.* **1994**, *12*, 879–890.
- (148) Nguyen, G.; Delarue, F.; Berrou, J.; Rondeau, E.; Sraer, J. D. Specific receptor binding of renin on human mesangial cells in culture increases plasminogen activator inhibitor-1 antigen. *Kidney Int.* **1996**, *50*, 1897–1903.
- (149) (a) Saris, J. J.; Derckx, F. H. M.; Lamers, J. M. J.; Saxena, P. R.; Schalekamp, M. A. D. H.; Danser, A. H. J. Cardiomyocytes bind and activate native human prorenin: role of soluble mannose 6-phosphate receptors. *Hypertension* **2001**, *37*, 710–715. (b) Saris, J. J.; van den Eijnden, M. M. E. D.; Lamers, J. M. J.; Saxena, P. R.; Schalekamp, M. A. D. H.; Danser, A. H. J. Prorenin-induced myocyte proliferation: no role for intracellular angiotensin II. *Hypertension* **2002**, *39*, 573–577.
- (150) Nguyen, G.; Delarue, F.; Burcklé, C.; Bouzahir, L.; Giller, T.; Sraer, J. D. Pivotal role for the renin/prorenin receptor in angiotensin II production and cellular responses to renin. *J. Clin. Invest.* **2002**, *109*, 1417–1427.
- (151) Zhang, J.; Noble, N. A.; Border, W. A.; Owens, R. T.; Huang, Y. Receptor-dependent prorenin activation and induction of PAI-1 expression in vascular smooth muscle cells. *Am. J. Physiol.: Endocrinol. Metab.* **2008**, *295*, E810–E819.
- (152) Huang, Y.; Vongamorntham, S.; Kasting, J.; McQuillan, D.; Owens, R. T.; Yu, L.; Noble, N. A.; Border, W. Renin increases mesangial cell transforming growth factor- $\beta$ 1 and matrix proteins through receptor-mediated, angiotensin II-independent mechanisms. *Kidney Int.* **2006**, *69*, 105–113.
- (153) Suzuki, F.; Hayakawa, M.; Nakagawa, T.; Nasir, U. M.; Ebihara, A.; Iwasawa, A.; Ishida, Y.; Nakamura, Y.; Murakami, K. Human prorenin has “gate and handle” regions for its non-proteolytic activation. *J. Biol. Chem.* **2003**, *278*, 22217–22222.
- (154) Batenburg, W. W.; Krop, M.; Garrelds, I. M.; de Vries, R.; de Bruin, R. J. A.; Burckle, C. A.; Müller, D. N.; Bader, M.; Nguyen, G.; Danser, A. H. J. Prorenin is the endogenous agonist of the (pro)renin receptor. Binding kinetics of renin and prorenin in rat vascular smooth muscle cells overexpressing the human (pro)renin receptor. *J. Hypertens.* **2007**, *25*, 2241–2453.
- (155) Gratzke, P.; Boschmann, M.; Dechend, F.; Qadi, F.; Malchow, J.; Graeske, S.; Engeli, S.; Janke, J.; Springer, J.; Contrepas, A.;

- Plehm, R.; Klaus, S.; Nguyen, G.; Luft, F. C.; Müller, D. N. Energy metabolism in human renin-gene transgenic rats: Does renin contribute to obesity? *Hypertension* **2009**, *53*, 516–523.
- (156) Uehara, S.; Tsuchida, M.; Kanno, T.; Sasaki, M.; Nishikibe, M.; Fukamizu, A. Late-onset obesity in mice transgenic for the human renin gene. *Int. J. Mol. Med.* **2003**, *11*, 723–727.
- (157) Burckle, C. A.; Danser, A. H. J.; Müller, D. N.; Garrelds, I. M.; Gasc, J. M.; Popova, E.; Plehm, R.; Peters, J.; Bader, M.; Nguyen, G. Elevated blood pressure and heart rate in human renin receptor transgenic rats. *Hypertension* **2006**, *47*, 552–556.
- (158) Ichihara, A.; Sakoda, M.; Kurauchi-Mito, A.; Kaneshiro, Y.; Itoh, H. Renin, prorenin and the kidney: a new chapter in an old saga. *J. Nephrol.* **2009**, *22*, 306–311.
- (159) Feldt, S.; Batenburg, W. W.; Mazak, I.; Maschke, U.; Wellner, M.; Kvakan, H.; Dechend, R.; Febel, A.; Burckle, C.; Contrepas, A.; Danser, A. H. J.; Bader, M.; Nguyen, G.; Luft, F. C.; Müller, D. N. Prorenin and renin-induced extracellular signal-regulated kinase 1/2 activation in monocytes is not blocked by aliskiren or the handle-region peptide. *Hypertension* **2008**, *51*, 682–688.
- (160) Mercure, C.; Prescott, G.; Lacombe, M. J.; Silversides, D. W.; Reudelhuber, T. L. Chronic increases in circulating prorenin are not associated with renal or cardiac pathologies. *Hypertension* **2009**, *53*, 1062–1069.
- (161) Peters, B.; Grisk, O.; Becher, B.; Wanka, H.; Kuttler, B.; Ludemann, J.; Lorenz, G.; Rettig, R.; Mullins, J. J.; Peters, J. Dose-dependent titration of prorenin and blood pressure in Cyp11a1ren-2 transgenic rats: absence of prorenin-induced glomerulosclerosis. *J. Hypertens.* **2008**, *26*, 102–109.
- (162) Batenburg, W. W.; de Bruin, R. J. A.; van Gool, J. M. G.; Müller, D. N.; Bader, M.; Nguyen, G.; Danser, A. H. J. Aliskiren-binding increases the half life of renin and prorenin in rat aortic vascular smooth muscle cells. *Arterioscler., Thromb., Vasc. Biol.* **2008**, *28*, 1151–1157.
- (163) Siragy, H.; Huang, J.; Lieb, D. C. The development of the direct renin inhibitor aliskiren: treating hypertension and beyond. *Expert Opin. Emerging Drugs* **2008**, *13*, 417–430.
- (164) Vaidyanathan, S.; Jarugula, V.; Dieterich, H. A.; Howard, D.; Dole, W. P. Clinical pharmacokinetics and pharmacodynamics of aliskiren. *Clin. Pharm.* **2008**, *47*, 515–531.
- (165) Fisher, N. D.; Hollenberg, N. K. Is there a future for renin inhibitors? *Expert Opin. Invest. Drugs* **2001**, *10*, 417–426.
- (166) Vaidyanathan, S.; Jermany, J.; Yeh, C. M.; Bizot, M.-N.; Camisasca, R. Aliskiren, a novel orally effective renin inhibitor, exhibits similar pharmacokinetics and pharmacodynamics in Japanese and Caucasian subjects. *Br. J. Clin. Pharmacol.* **2006**, *62*, 690–698.
- (167) Waldmeier, F.; Glaenzel, U.; Wirz, B.; Oberer, L.; Schmid, D.; Seiberling, M.; Valencia, J.; Riviere, G. J.; End, P.; Vaidyanathan, S. Absorption, distribution, metabolism, and elimination of the direct renin inhibitor aliskiren in healthy volunteers. *Drug Metab. Dispos.* **2007**, *35*, 1418–1428.
- (168) Nussberger, J.; Wuerzner, G.; Jensen, C.; Brunner, H. R. Angiotensin II suppression in humans by the orally active renin inhibitor aliskiren (SPP100). *Hypertension* **2002**, *39*, e1–e8.
- (169) Stanton, A.; Jensen, C.; Nussberger, J.; O'Brien, E. Blood pressure lowering in essential hypertension with an oral renin inhibitor, aliskiren. *Hypertension* **2003**, *42*, 1137–1143.
- (170) Gradman, A. H.; Schmieder, R. E.; Lins, R. L.; Nussberger, J.; Chiang, Y.; Bedigian, M. P. Aliskiren, a novel orally effective renin inhibitor, provides dose-dependent antihypertensive efficacy and placebo-like tolerability in hypertensive patients. *Circulation* **2005**, *111*, 1012–1018.
- (171) Andersen, K.; Weinberger, M. H.; Egan, B.; Constance, C. M.; Ali, M. A.; Jin, J.; Keefe, D. L. Comparative efficacy and safety of aliskiren, an oral direct renin inhibitor, and ramipril in hypertension: a 6-month, randomized, double-blind trial. *J. Hypertens.* **2008**, *26*, 589–599.
- (172) Oh, B. H.; Mitchell, J.; Herron, J. R.; Chung, J.; Khan, M.; Keefe, D. L. Aliskiren, an oral renin inhibitor, provides dose-dependent efficacy and sustained 24-h blood pressure control in patients with hypertension. *J. Am. Coll. Cardiol.* **2007**, *49*, 1157–1163.
- (173) Nussberger, J.; Gradman, A. H.; Schmieder, R. E.; Lins, R. L.; Chiang, Y.; Prescott, M. F. Plasma renin and the antihypertensive effect of the orally active renin inhibitor aliskiren in clinical hypertension. *Int. J. Clin. Pract.* **2007**, *61*, 1461–1468.
- (174) Vergaro, G.; Fontana, M.; Poletti, R.; Giannoni, A.; Iervasi, A. L.; Masi, L.; Mammì, C.; Gabutti, A.; Passino, C.; Emdin, M. Plasma renin activity is an independent prognostic factor in chronic heart failure. *Eur. Heart J.* **2008**, *29* (Suppl.), 393 (Abstract 2493).
- (175) Chobanian, A. V.; Bakris, G. L.; Black, H. R.; Cushman, W. C.; Green, L. A.; Izzo, J. L. Seventh report of the Joint National Committee on Prevention, Detection, Evaluation, and Treatment of High Blood Pressure. *Hypertension* **2003**, *42*, 1206–1252.
- (176) Villamil, A.; Chrysant, S. G.; Calhoun, D.; Schober, B.; Hsu, H.; Matrisciano-Dimichino, L.; Zhang, J. Renin inhibition with aliskiren provides additive antihypertensive efficacy when used in combination with hydrochlorothiazide. *J. Hypertens.* **2007**, *25*, 217–226.
- (177) O'Brien, E.; Barton, J.; Nussberger, J.; Mulcahy, D.; Jensen, C.; Dicker, P.; Stanton, A. Aliskiren reduces blood pressure and suppresses plasma renin activity in combination with a thiazide diuretic, an angiotensin converting enzyme inhibitor, or an angiotensin receptor blocker. *Hypertension* **2007**, *49*, 276–284.
- (178) Oparil, S.; Yarrows, S. A.; Patel, S.; Fang, H.; Zhang, J.; Satlin, A. Efficacy and safety of combined use of aliskiren and valsartan in patients with hypertension: a randomized, double-blind trial. *Lancet* **2007**, *370*, 221–229.
- (179) Drummond, W.; Munger, M. A.; Essop, R.; Maboudian, M.; Khan, M.; Keefe, D. L. Antihypertensive efficacy of the oral direct renin inhibitor aliskiren as add-on therapy in patients not responding to amlodipine monotherapy. *J. Clin. Hypertens. (Greenwich)* **2007**, *9*, 742–750.
- (180) Solomon, S. D.; Appelbau, E.; Manning, W. J.; Verma, A.; Berglund, T.; Lukashevich, V.; Papst, C. C.; Smith, B. A.; Dahlöf, B. Effect of the direct renin inhibitor aliskiren, the angiotensin receptor blocker losartan, or both on left ventricular mass in patients with hypertension and left ventricular hypertrophy. *Circulation* **2009**, *119*, 530–537.
- (181) McMurray, J. J. V.; Pitt, B.; Latini, R.; Maggioni, A. P.; Solomon, S. D.; Keefe, D. L.; Ford, J.; Verma, A.; Lewsey, J. Effects of the oral direct renin inhibitor aliskiren in patients with symptomatic heart failure. *Circ.: Heart Fail.* **2008**, *1*, 17–24.
- (182) (a) Dembowsky, K. Human Phase 0 Microdosing Studies. Practical Examples Using Renin Inhibitors. Evolution 2007, Monaco, October 1, 2007. [http://www.xceleron.com/metadot/index.pl?id=3081&isa=DBRow&op=show&dbview\\_id=3047#](http://www.xceleron.com/metadot/index.pl?id=3081&isa=DBRow&op=show&dbview_id=3047#) (accessed December 21, 2009). (b) Speedel Annual General Meeting, April 15, 2008. [http://www.speedel.com/assets/AGM\\_2008\\_presentation\\_2.pdf](http://www.speedel.com/assets/AGM_2008_presentation_2.pdf) (accessed December 21, 2009).
- (183) Vitae Pharmaceuticals Press Release, September 21, 2009: Vitae Initiates Phase I Trial of Novel Renin Inhibitor. In *Genetic Engineering & Biotechnology News*, September 21, 2009. <http://www.genengnews.com/news/bnitem.aspx?name=63361020> (accessed December 21, 2009).
- (184) (a) Actelion Annual Report 2008. [http://www1.actelion.com/documents/corporate/annual\\_reports/AR\\_Actelion\\_InDetail\\_E.pdf](http://www1.actelion.com/documents/corporate/annual_reports/AR_Actelion_InDetail_E.pdf) (accessed December 21, 2009). (b) *A Study To Determine the Effectiveness and Tolerability of MK8141 in Patients with High Blood Pressure*; U.S. National Institutes of Health: Bethesda, MD, October 5, 2007; <http://clinicaltrials.gov/ct2/show/study/NCT00543413>. Accessed December 21, 2009.
- (185) Parving, H. H.; Brenner, B. M.; McMurray, J. J. V.; de Zeeuw, D.; Haffner, S. M.; Solomon, S. D.; Chaturvedi, N.; Ghadanfar, M.; Weissbach, N.; Xiang, Z.; Armbrrecht, J.; Pfeffer, M. A. Aliskiren trial in type 2 diabetes using cardio-renal endpoints (ALTITUDE): rationale and study design. *Nephrol., Dial., Transplant.* **2009**, *24*, 1663–1671.